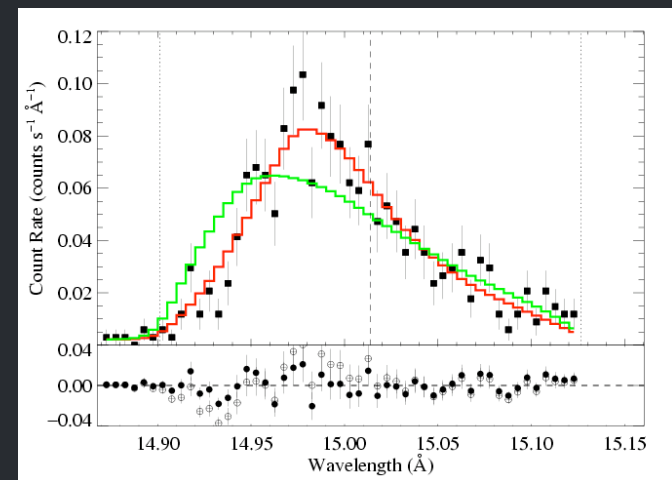
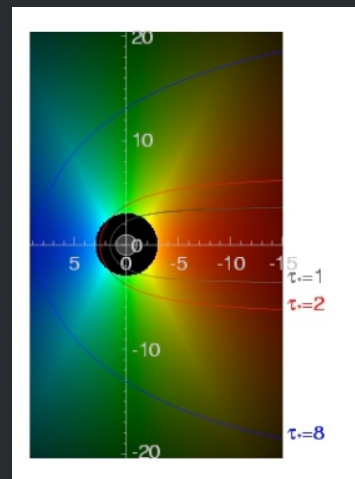
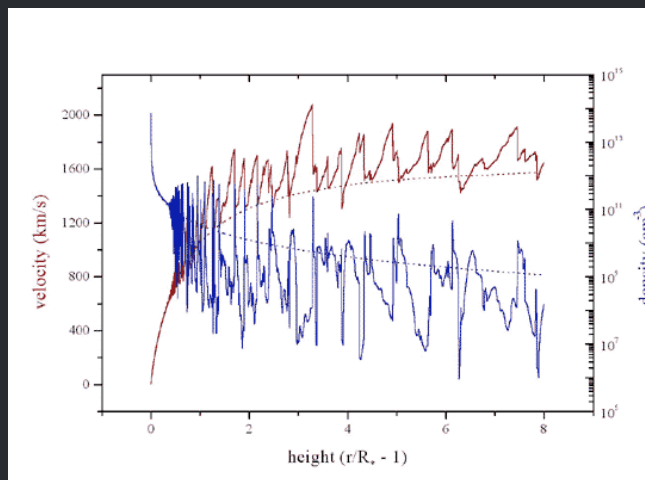


X-ray Spectral Diagnostics of Activity in O and Early-B Stars

wind shocks and mass-loss rates

David Cohen
Swarthmore College



Scope

X-ray emission from normal, effectively single and non-magnetic O and early-B stars

What does it tell us about high-energy process and about the winds on these stars?

Goal

To go from the observed X-ray spectra to a physical picture:

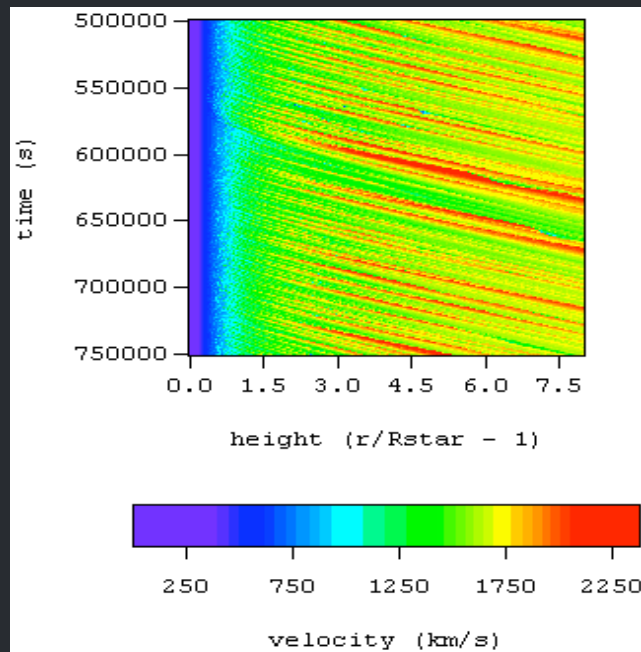
1. Kinematics and spatial distribution of the $> 1,000,000$ K plasma
2. Column-density information that can be used to measure the mass-loss rate of these winds

aside

The X-rays are quite time-steady, but the underlying processes are highly dynamic – *activity*

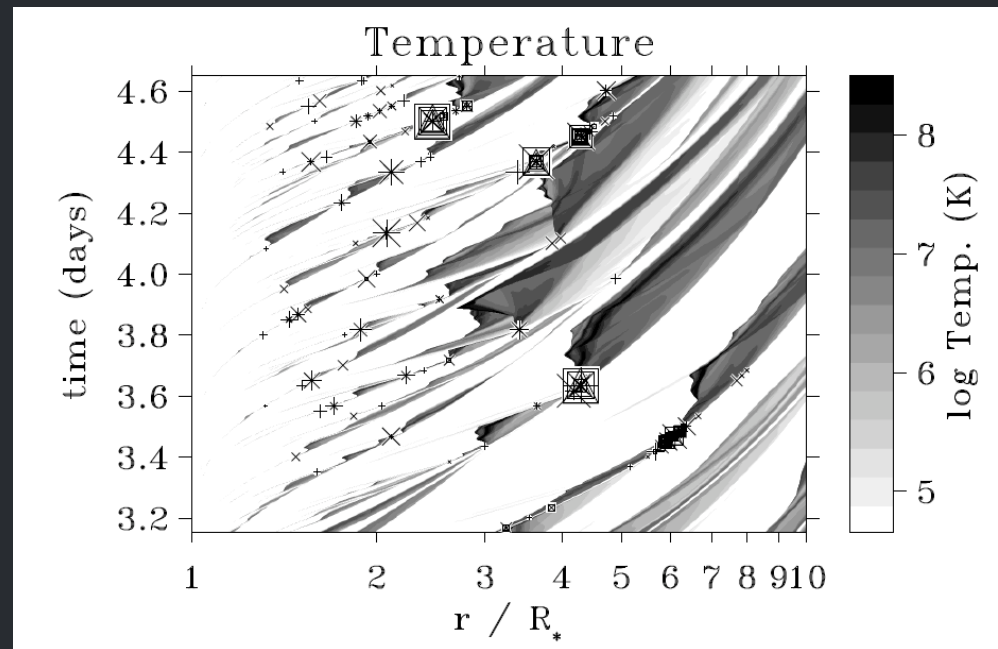
Theory & numerical simulations

Self-excited instability



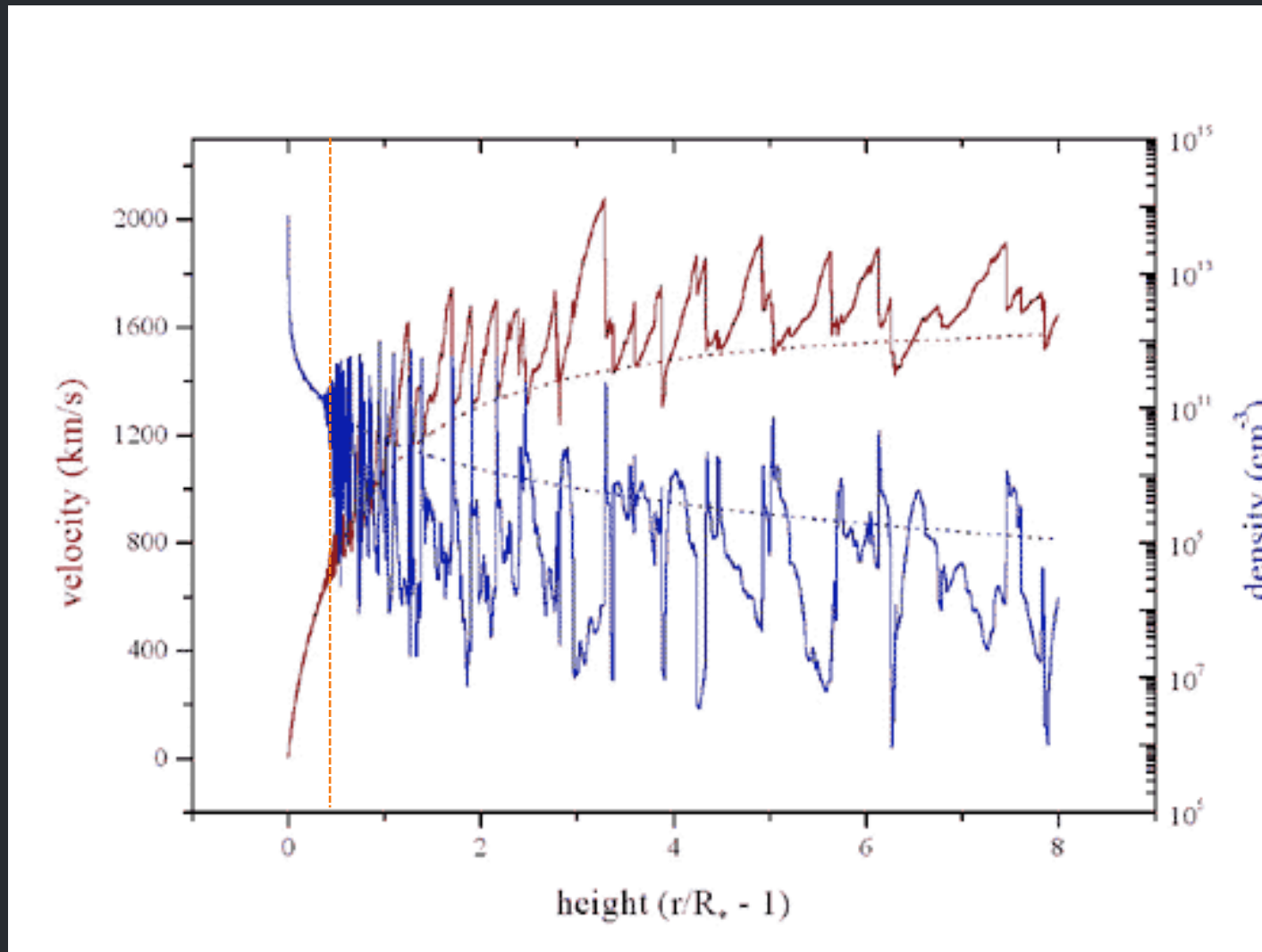
Owocki, Cooper, Cohen 1999

Excited by turbulence imposed at the wind base



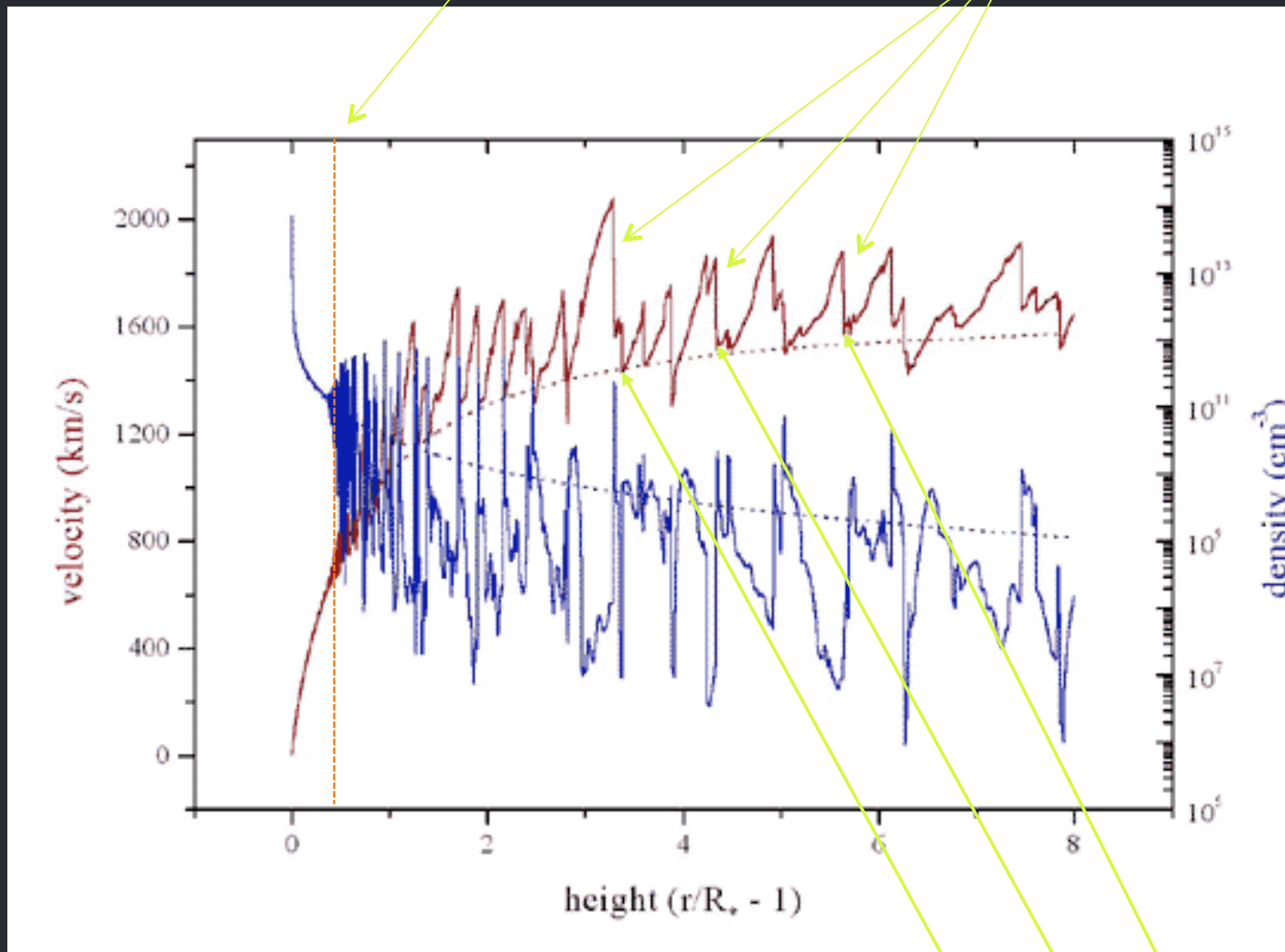
Feldmeier, Puls, Pauldrach 1997

Numerous shock structures, distributed above $\sim 1.5 R_*$



shock onset at $r \sim 1.5 R_{\text{star}}$

$V_{\text{shock}} \sim 300 \text{ km/s} :$
 $T \sim 10^6 \text{ K}$



Shocked wind plasma is decelerated back down to the local CAK wind velocity

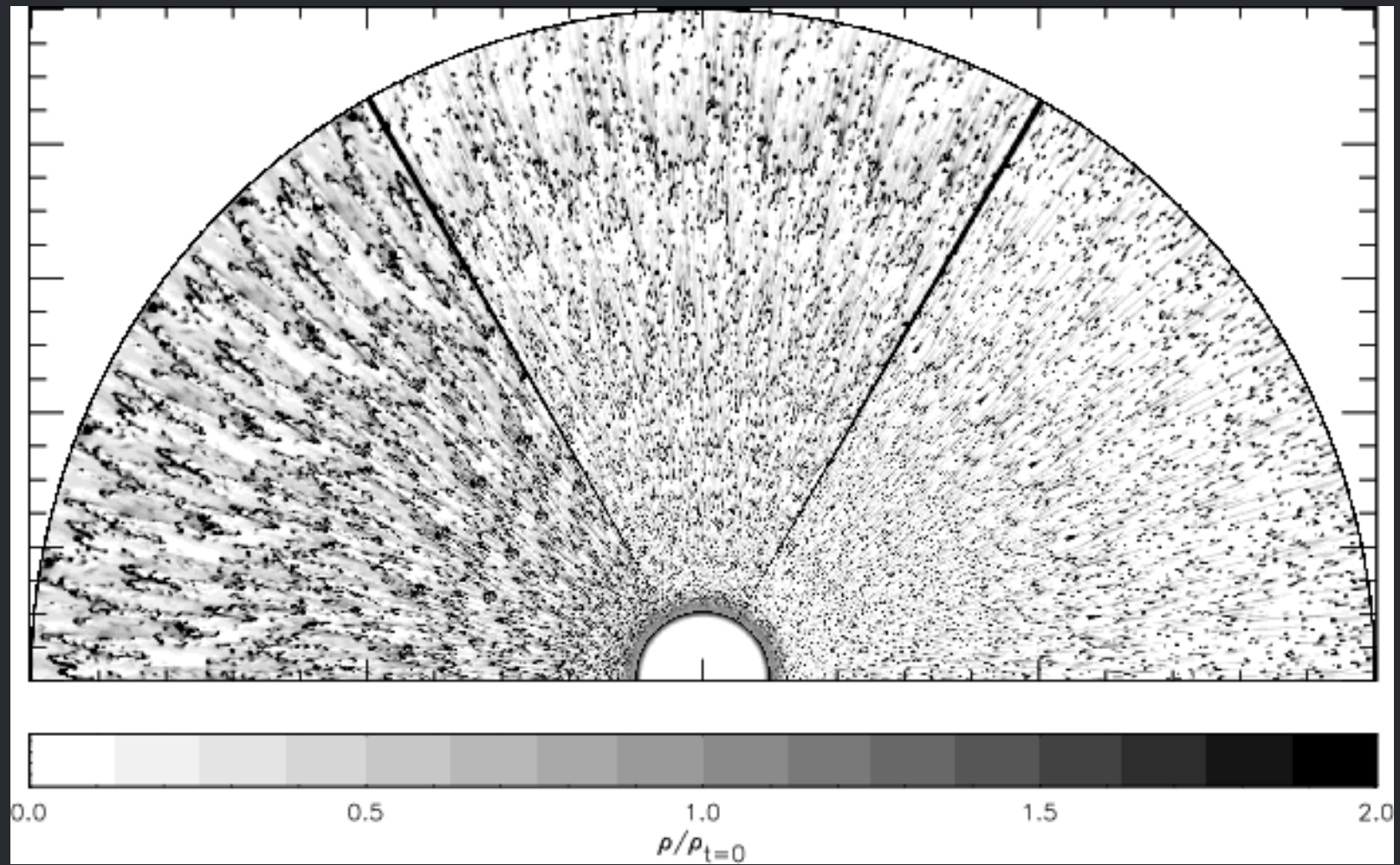
The paradigm

Shock-heated, X-ray emitting plasma is distributed throughout the wind, above some onset radius (R_o)

The bulk of the wind ($\sim 99\%$) is unshocked, cool ($T < T_{\text{eff}}$) and X-ray absorbing (τ_*)

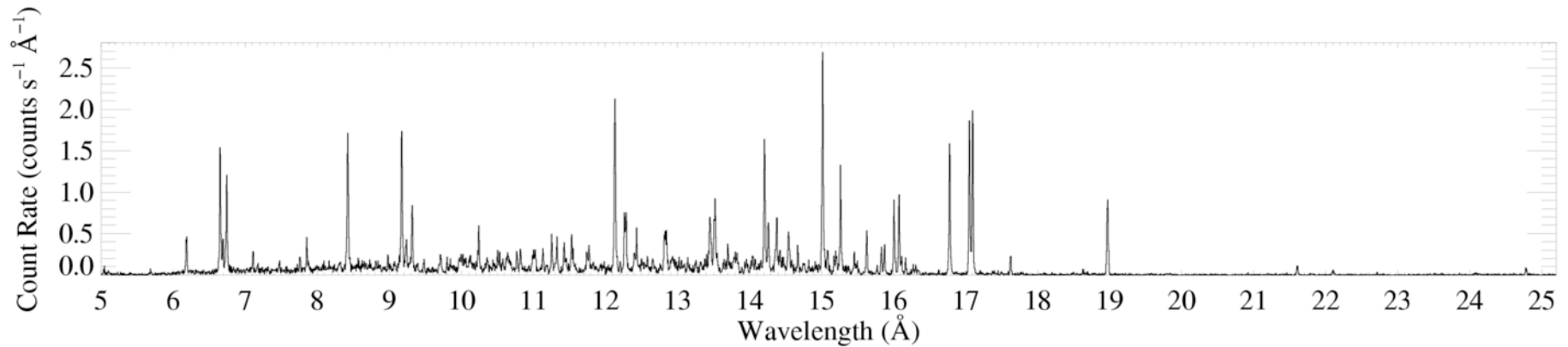
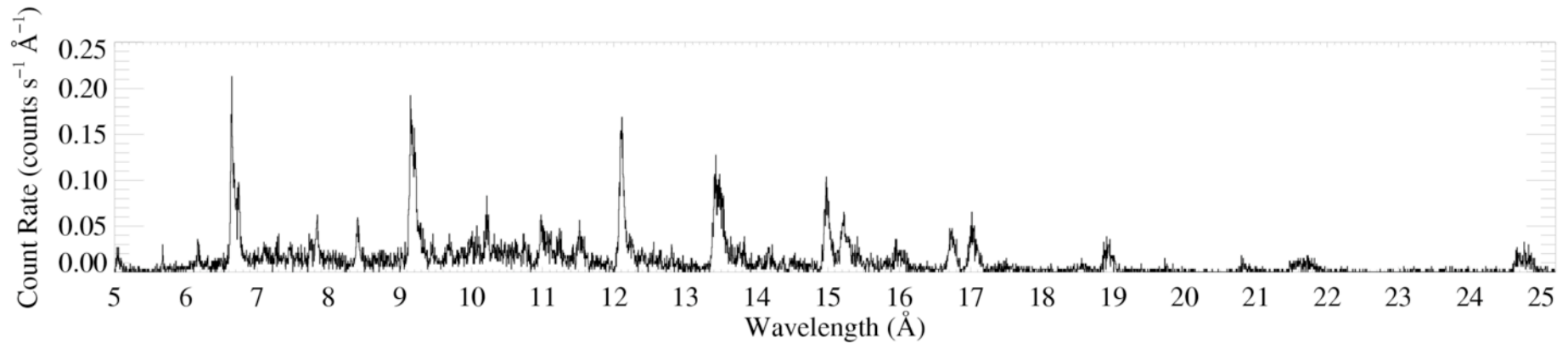
There are different types of specific models within this paradigm, and many open questions

More realistic 2-D simulations: R-T like break-up;
structure on quite *small scales*



Morphology

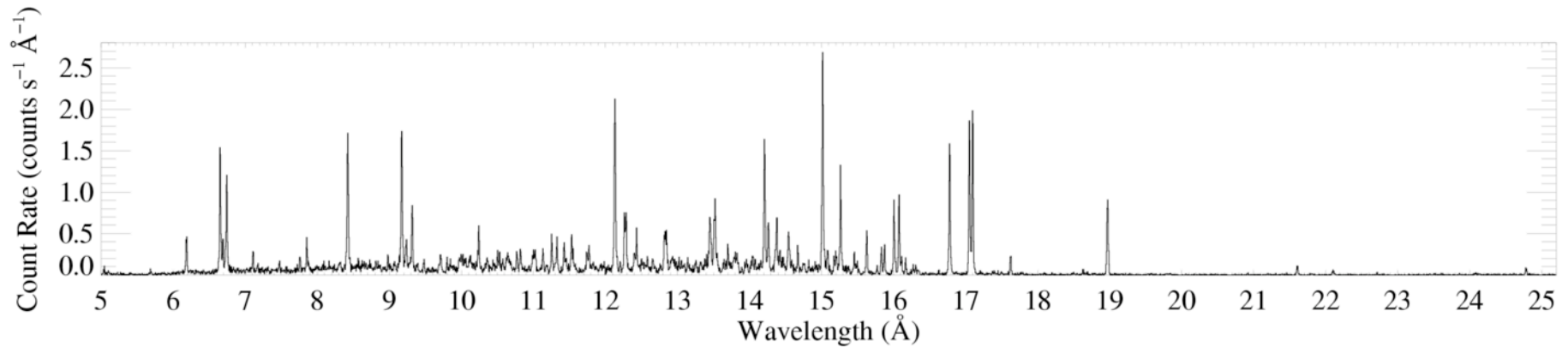
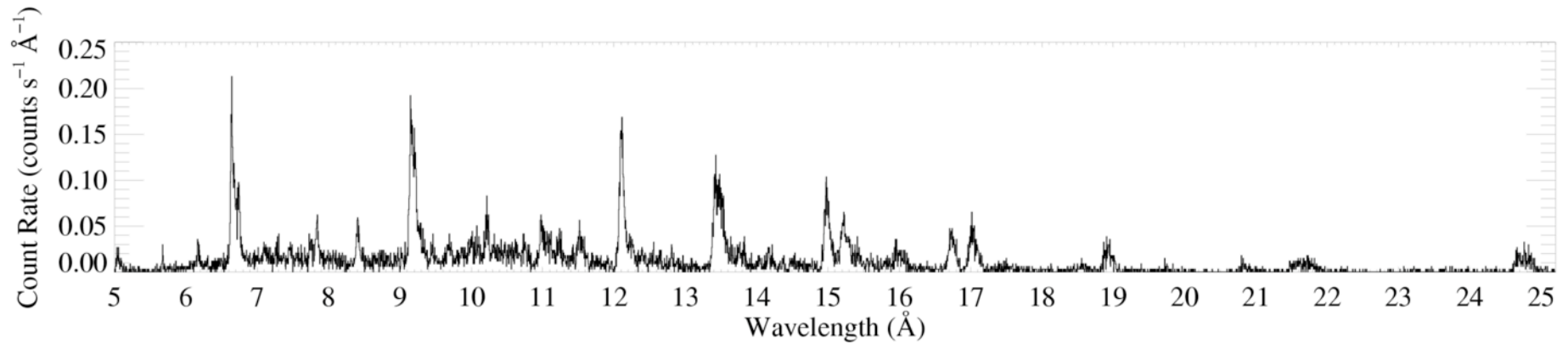
ζ Pup (O₄ If)



Capella (G5 III) – coronal source
– for comparison

Chandra HETGS ($R < 1000$)

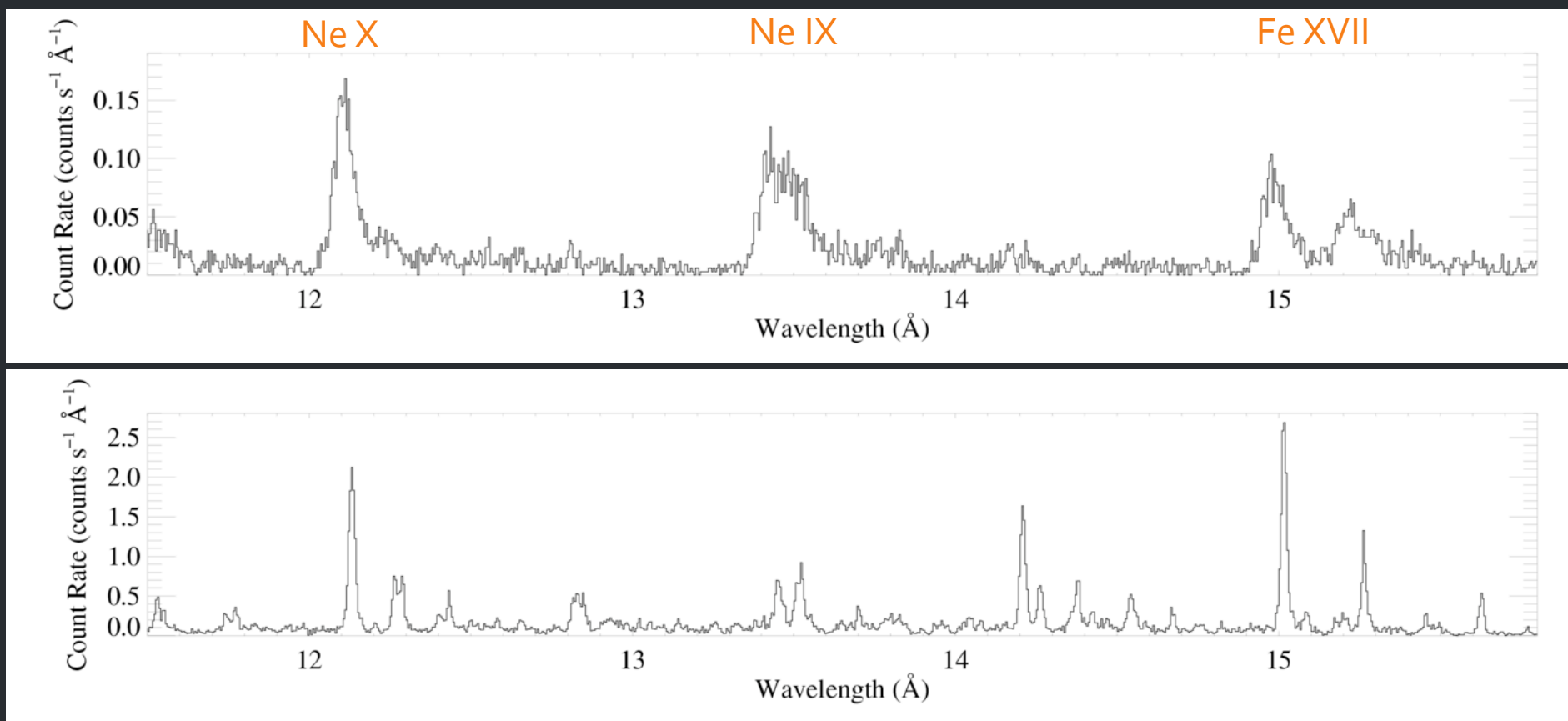
ζ Pup (O₄ If)



Capella (G5 III) – coronal source
– for comparison

Morphology – line widths

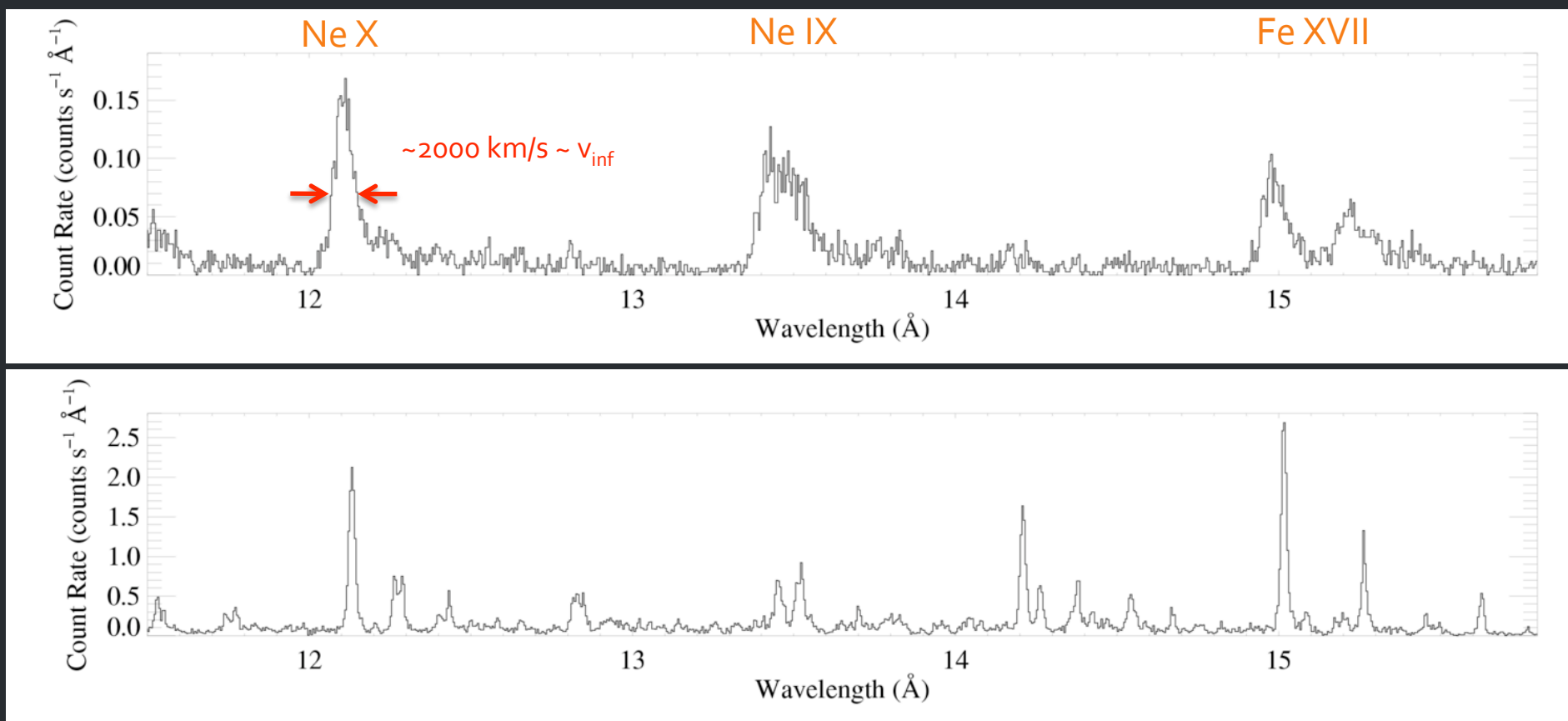
ζ Pup (O₄ If)



Capella (G5 III) – coronal source
– for comparison

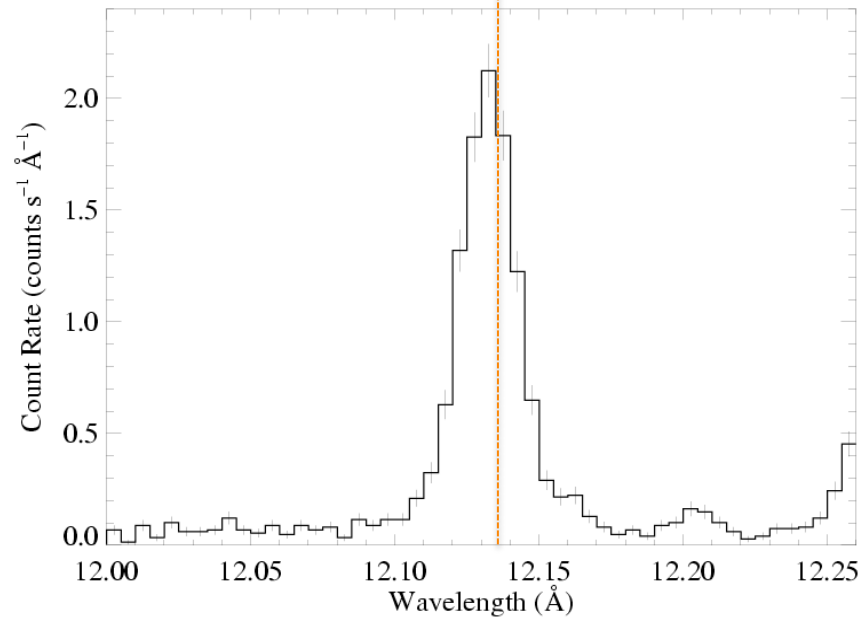
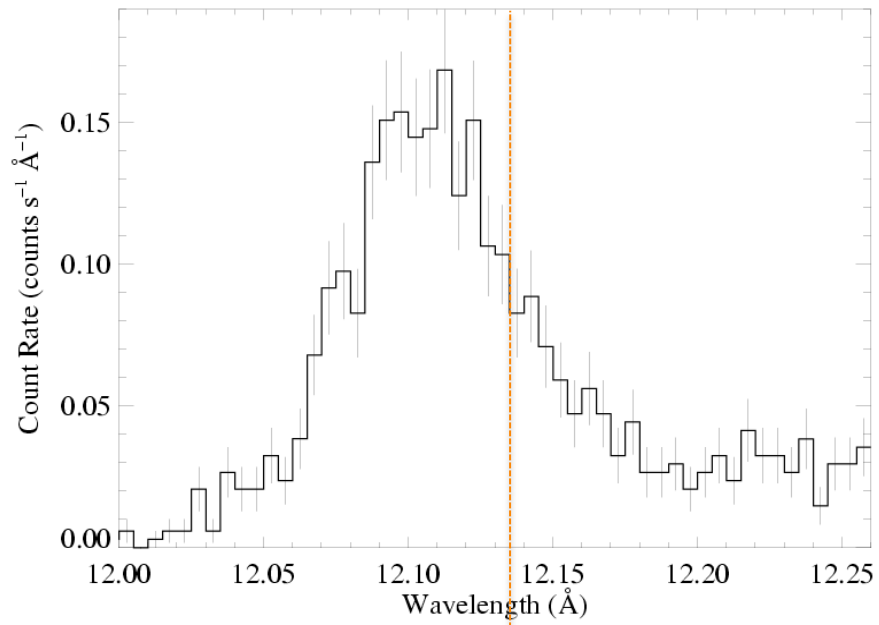
Morphology – line widths

ζ Pup (O₄ If)



Capella (G5 III) – coronal source
– for comparison

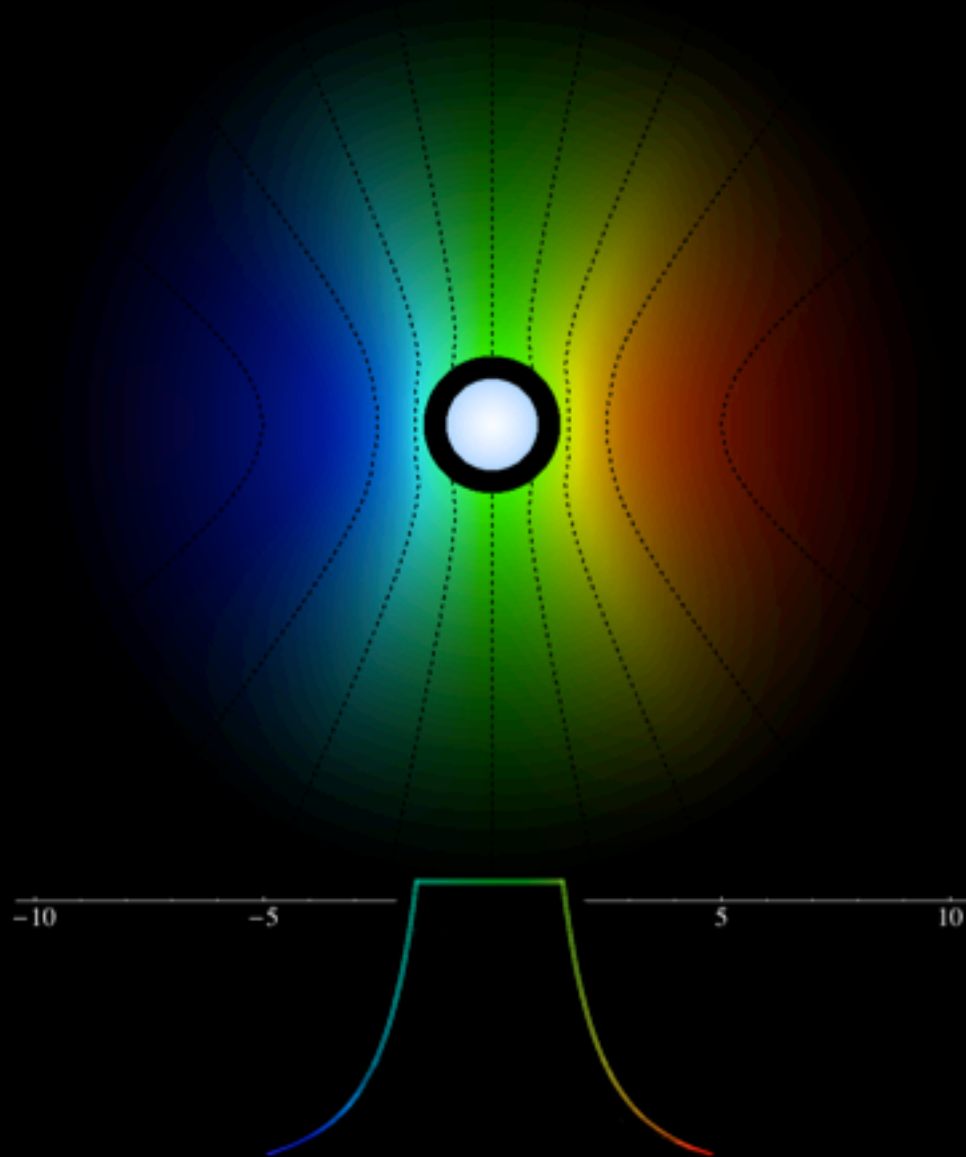
ζ Pup (O4 If)



Capella (G5 III) – *unresolved*

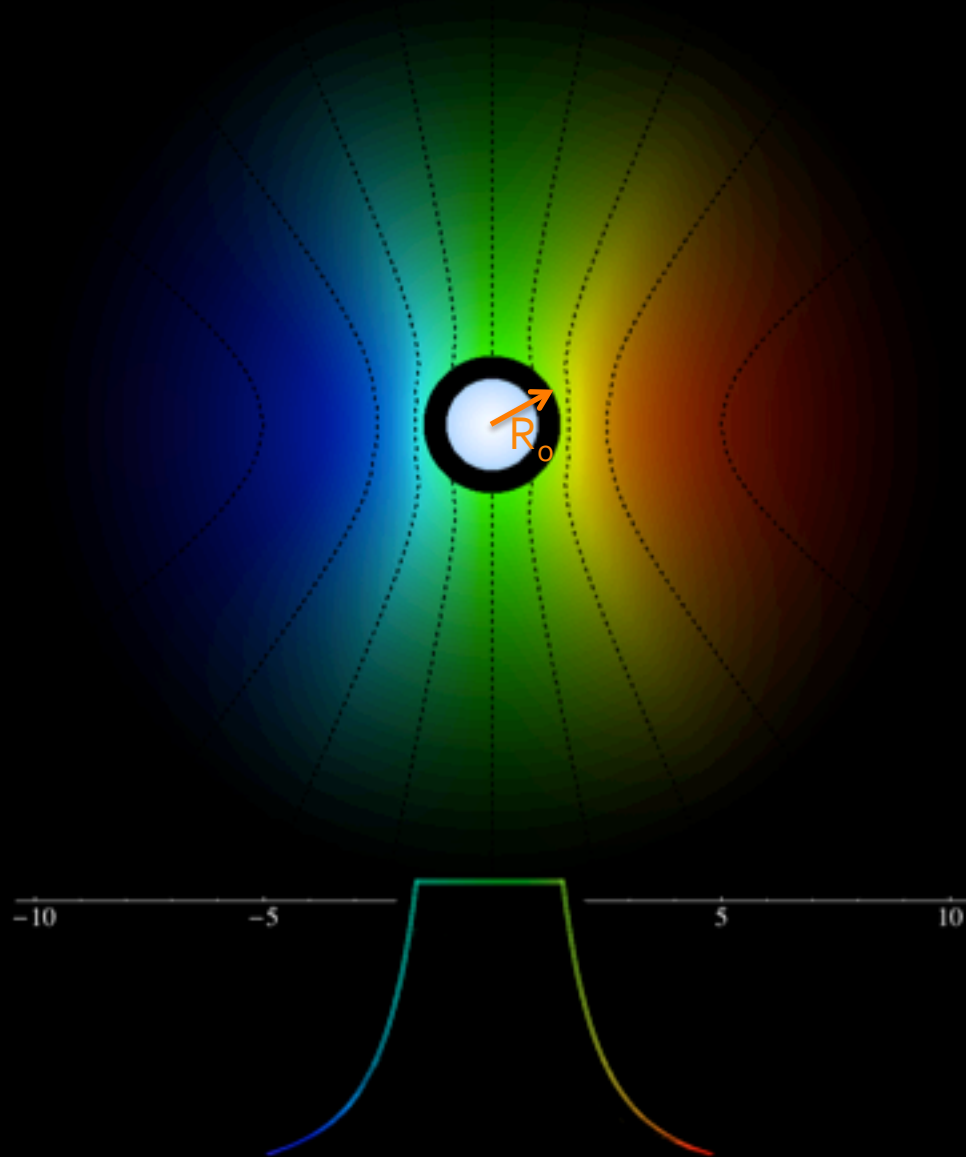
Line Asymmetry

A



Line Asymmetry

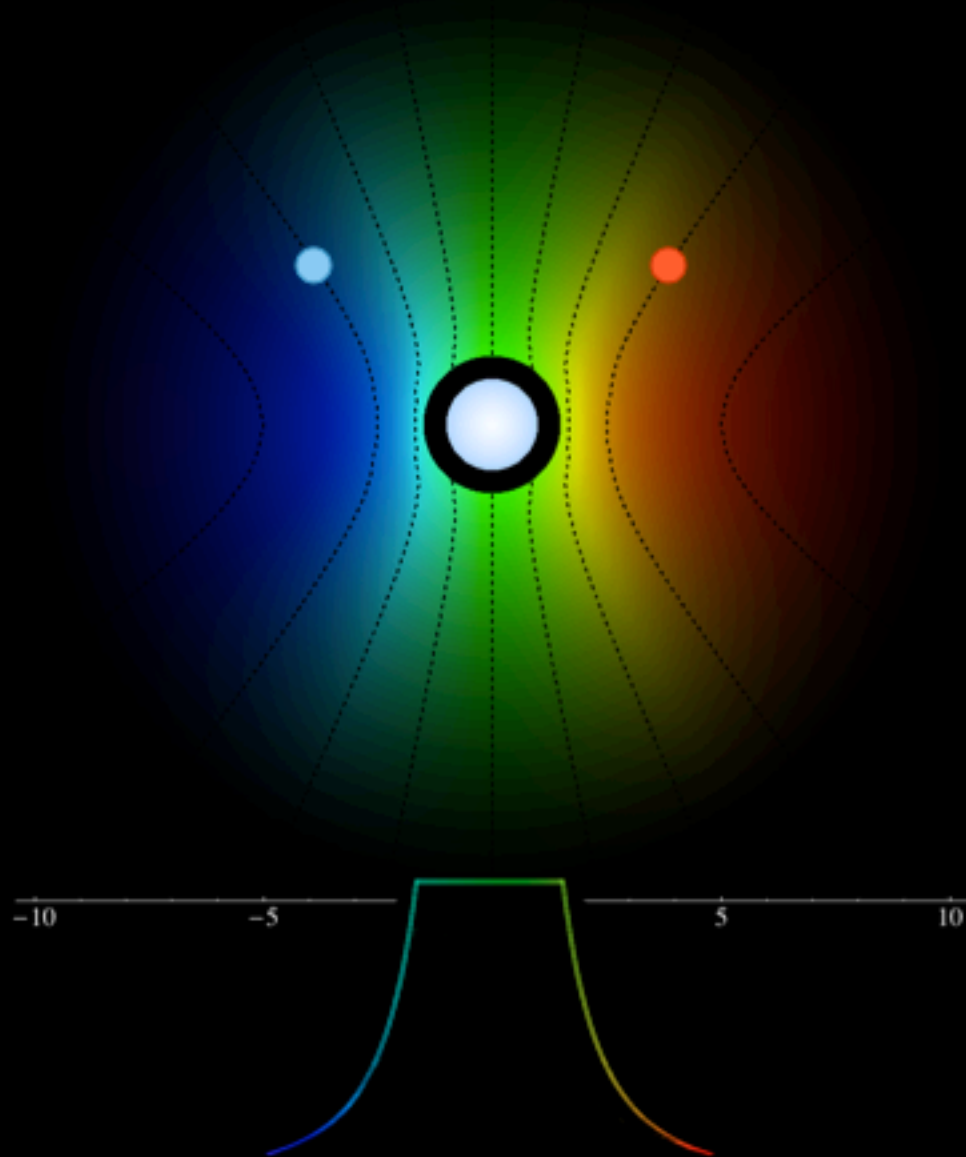
A



Profile shape
assumes beta
velocity law and
onset radius, R_0

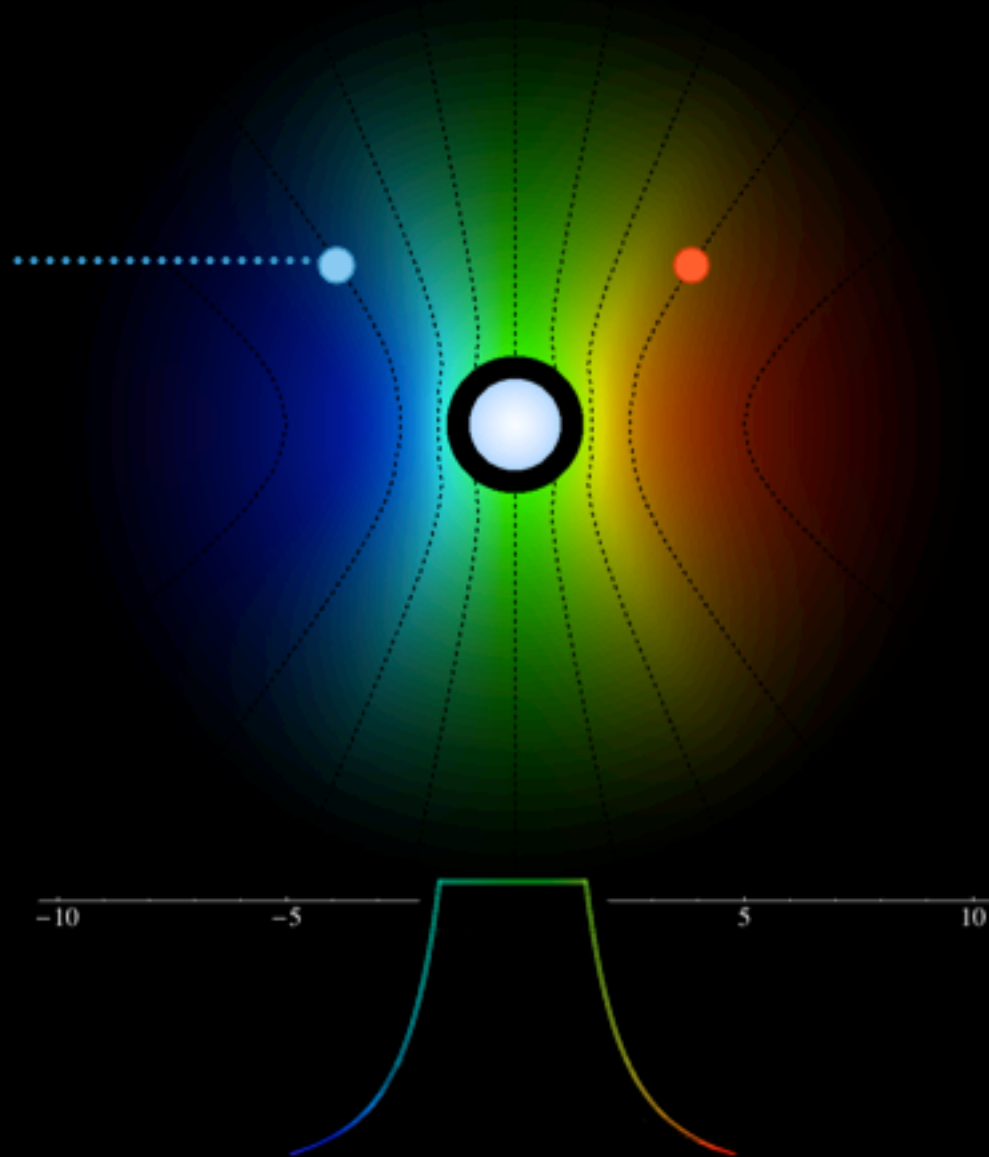
Line Asymmetry

A



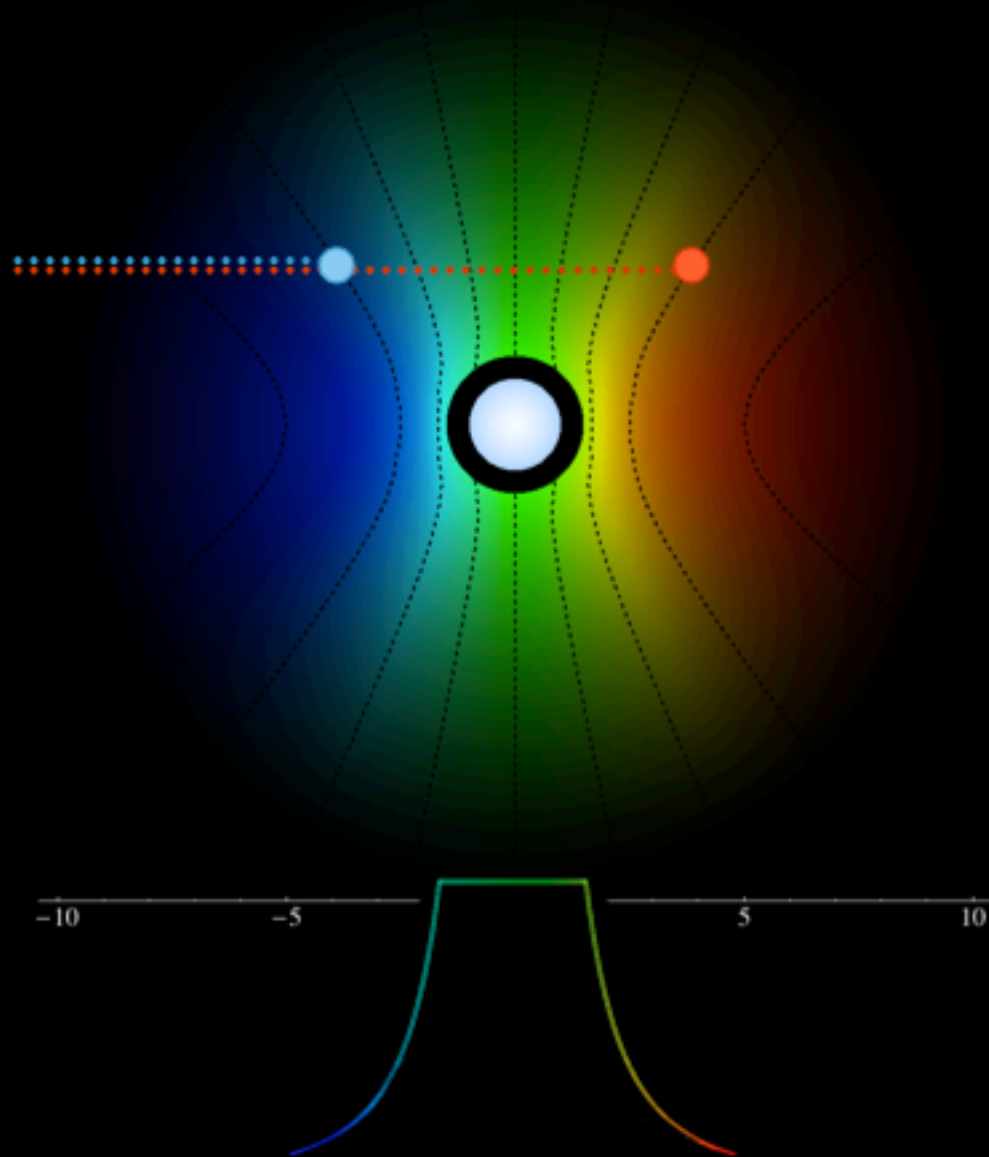
Line Asymmetry

A



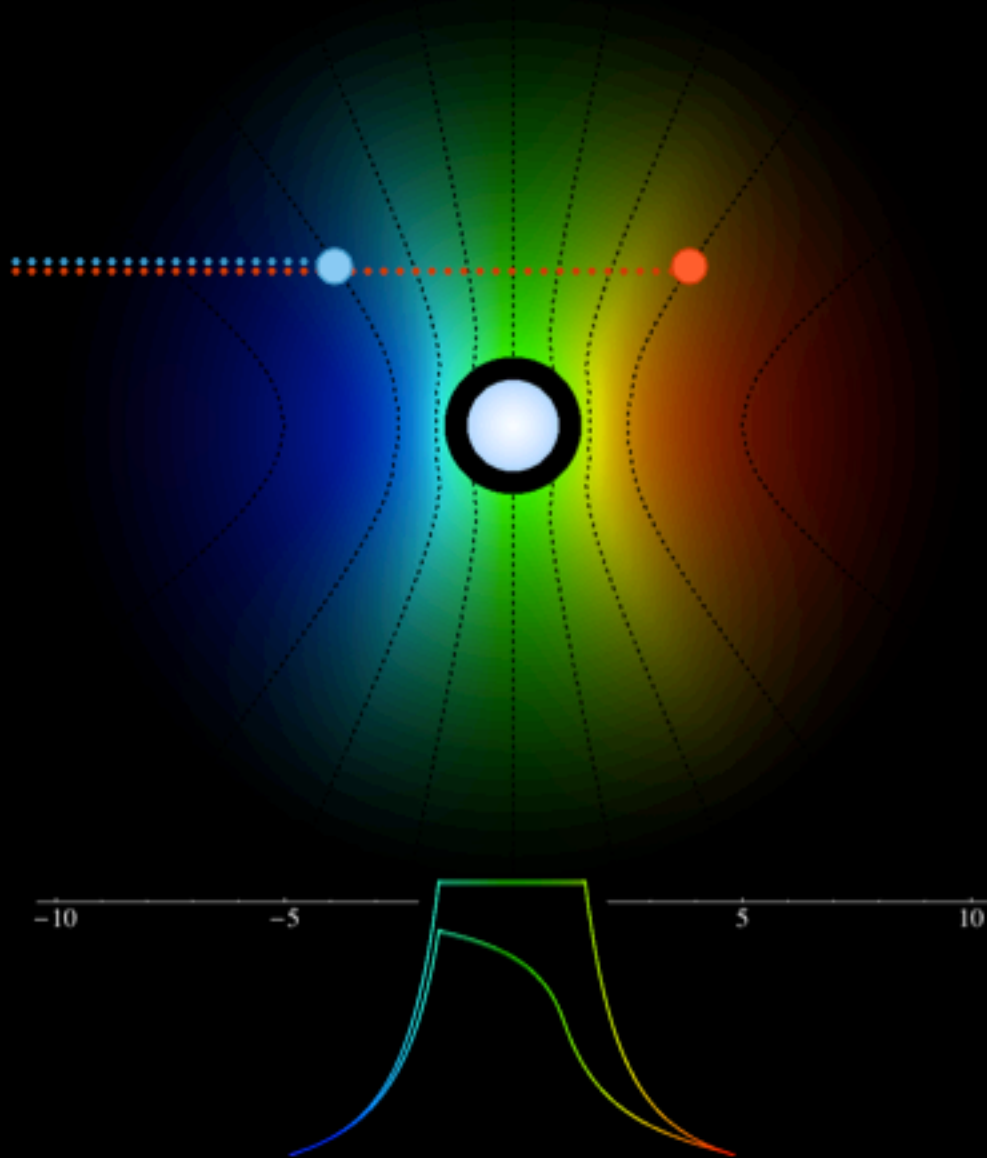
Line Asymmetry

A



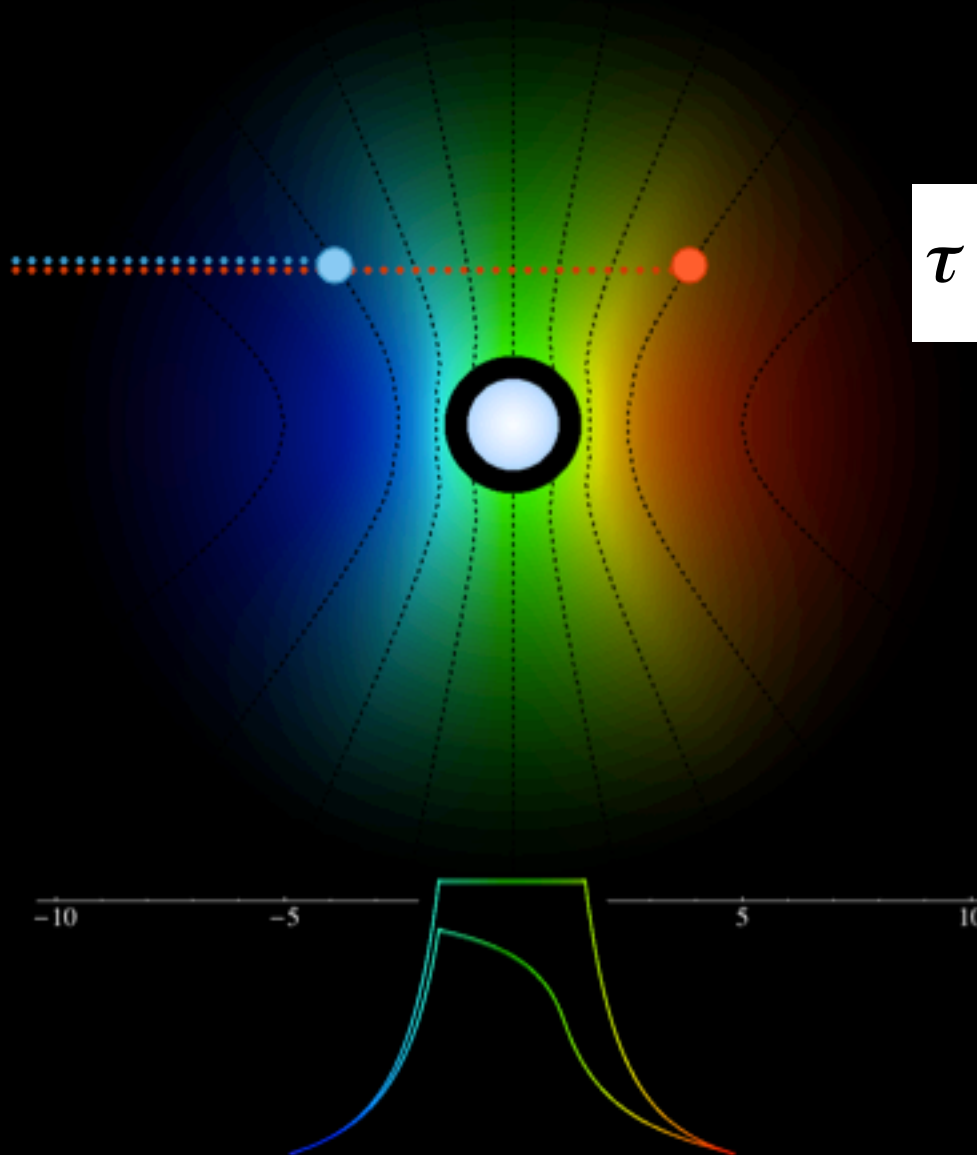
Line Asymmetry

A



Line Asymmetry

A



$$\tau = \tau_* \int_z^{\infty} \frac{R_* dz'}{r'^2 (1 - R_*/r')^\beta}$$

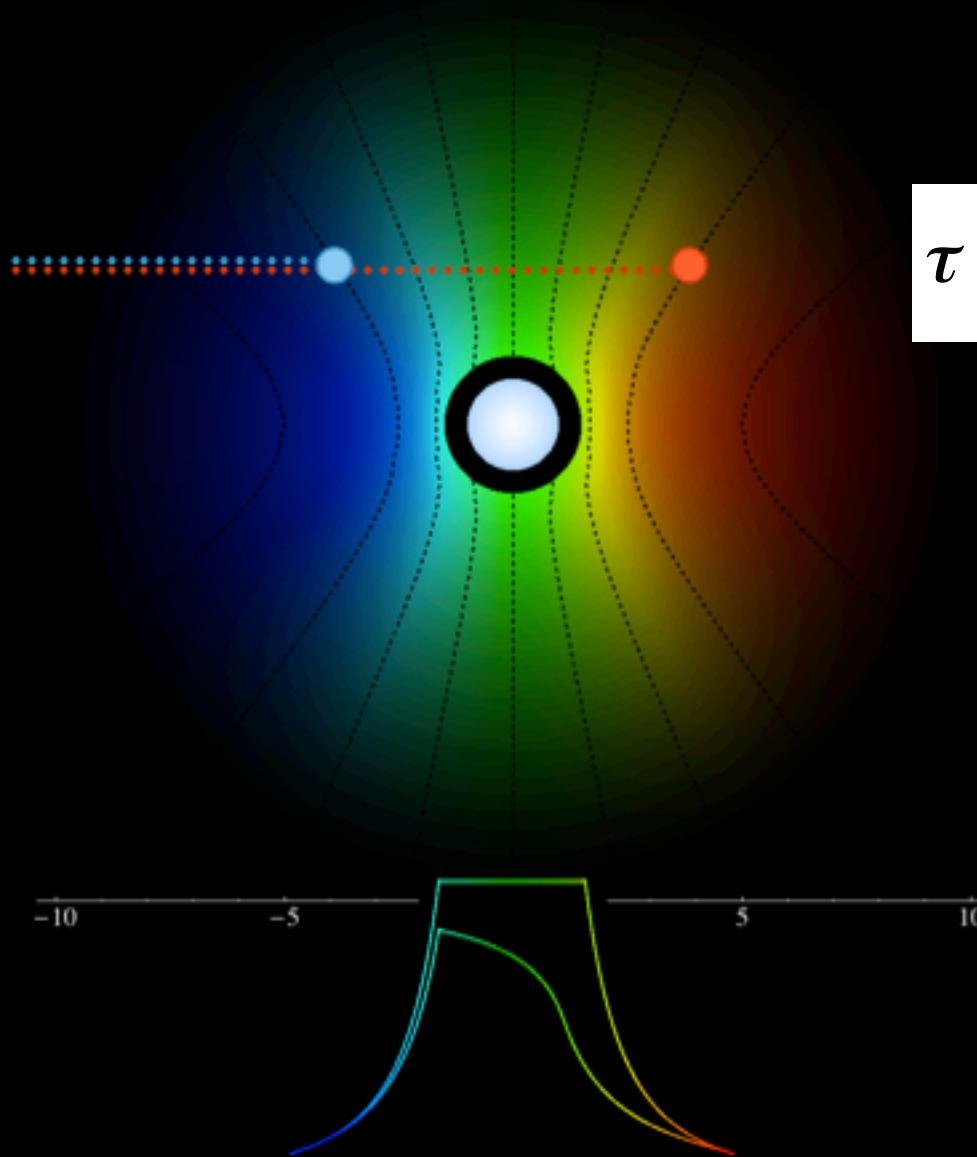
Line Asymmetry

Universal property of the wind

$$\tau = \tau_* \int_z^\infty \frac{R_* dz'}{r'^2 (1 - R_*/r')^\beta}$$

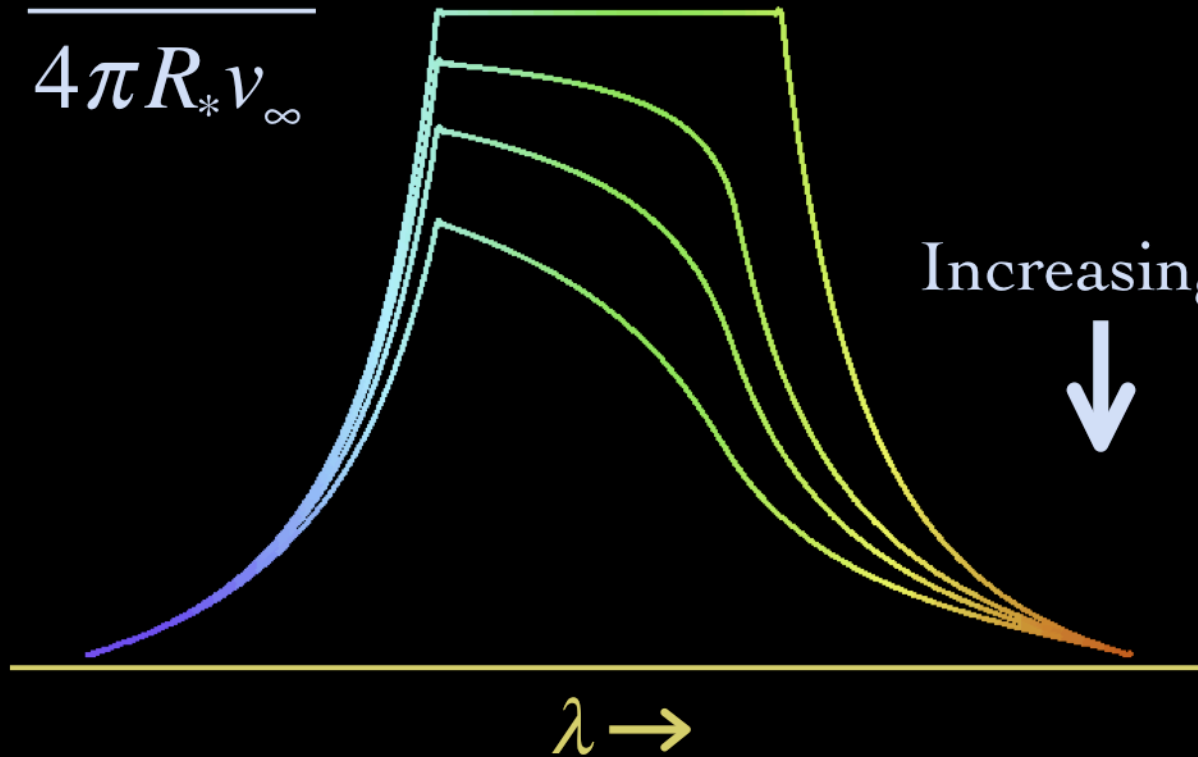
z different for each point

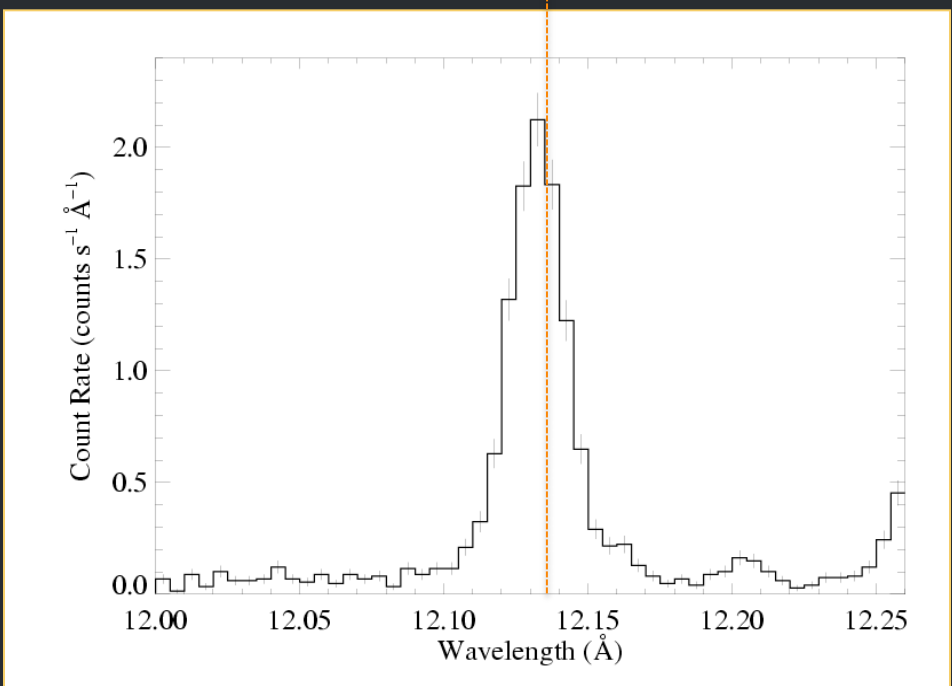
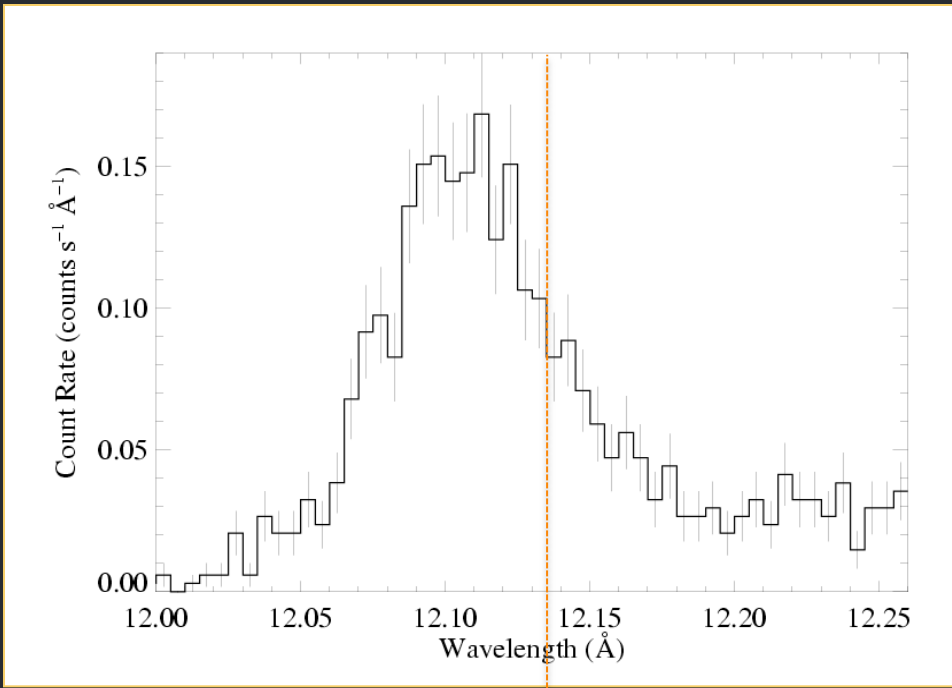
A



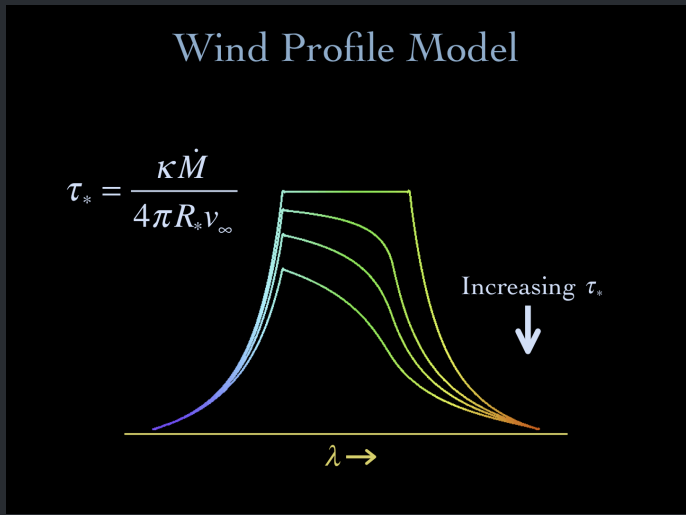
Wind Profile Model

$$\tau_* = \frac{\kappa \dot{M}}{4\pi R_* v_\infty}$$



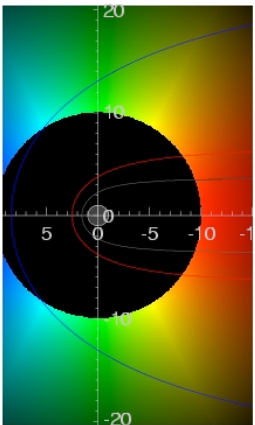
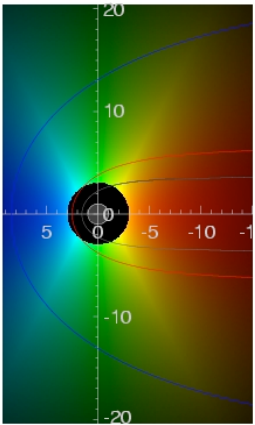
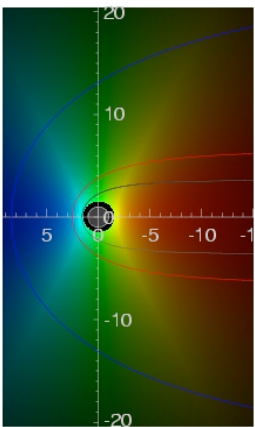


ξ Pup (O4 If)

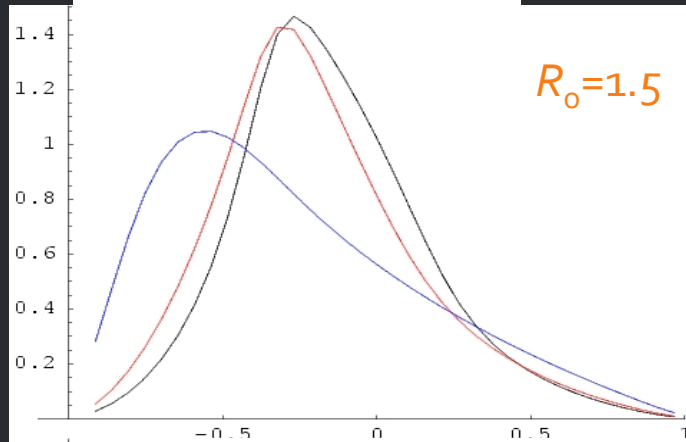


Capella (G5 III) – *unresolved*

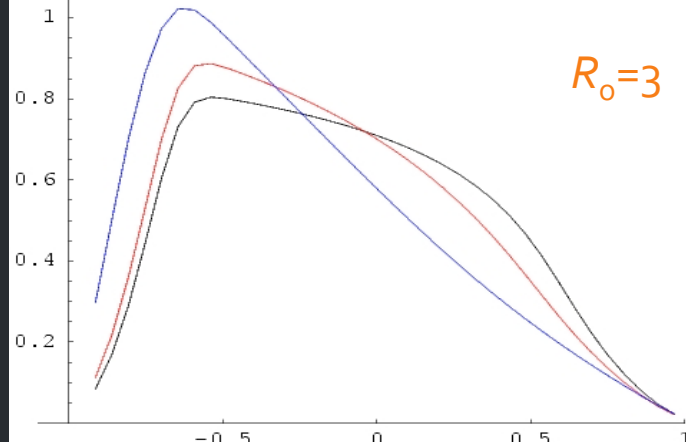
$\tau = 1$ contours



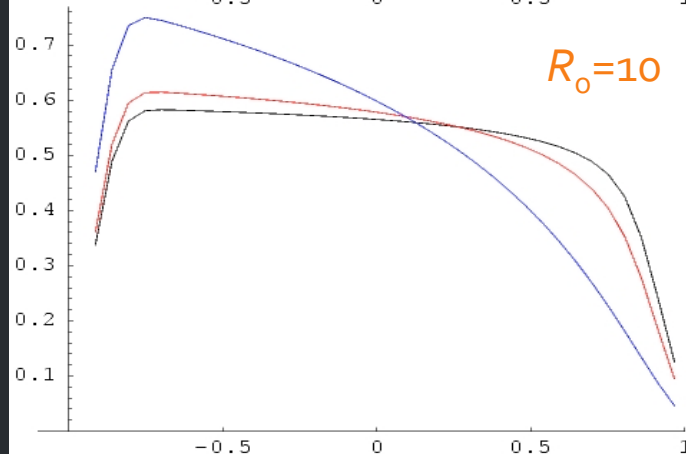
$\tau_* = 1, 2, 8$



$R_0 = 1.5$



$R_0 = 3$



$R_0 = 10$

key parameters: R_0 & τ_*

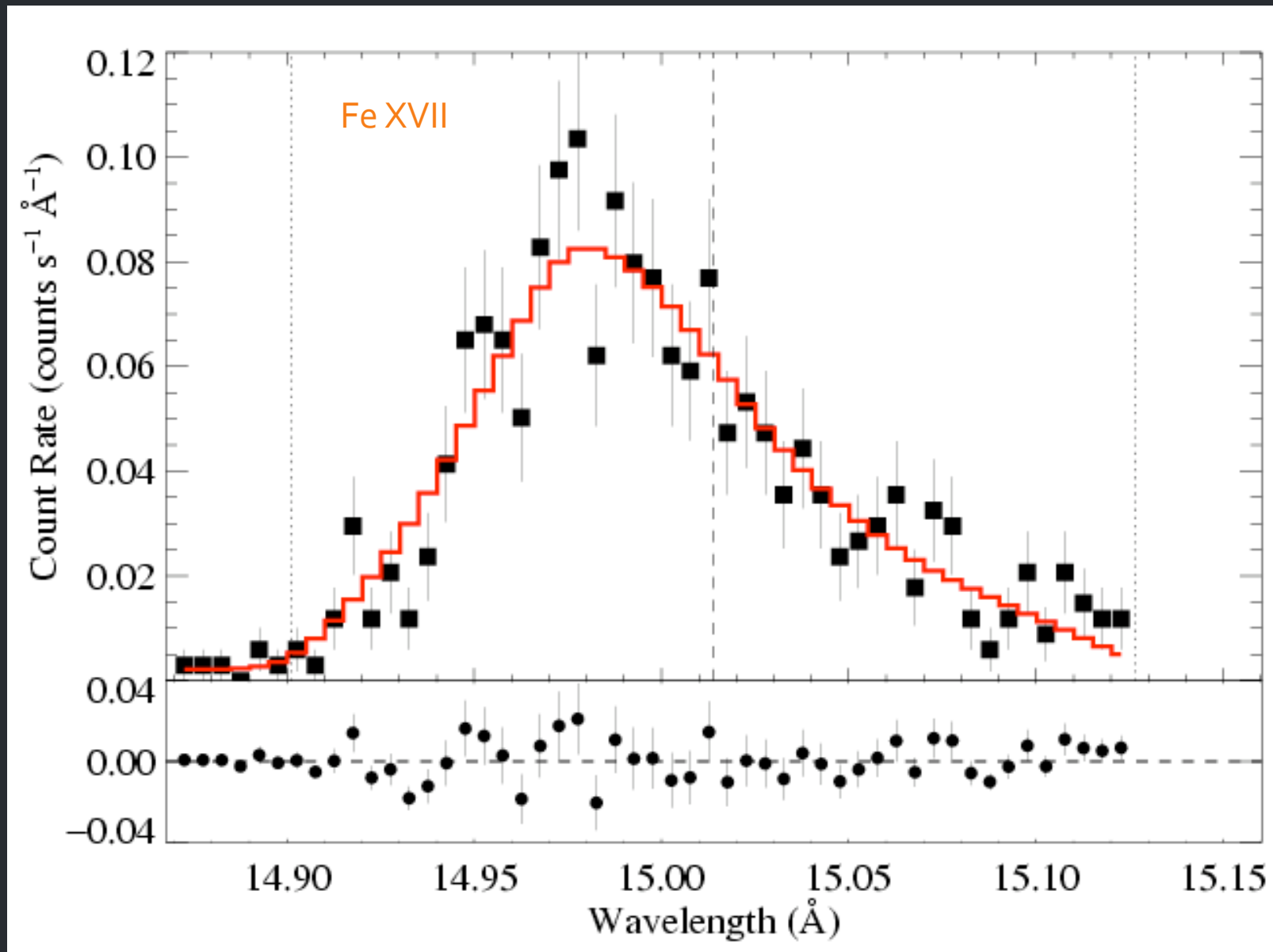
$$j \sim \rho^2 \text{ for } r/R_* > R_0$$

$$= 0 \text{ otherwise}$$

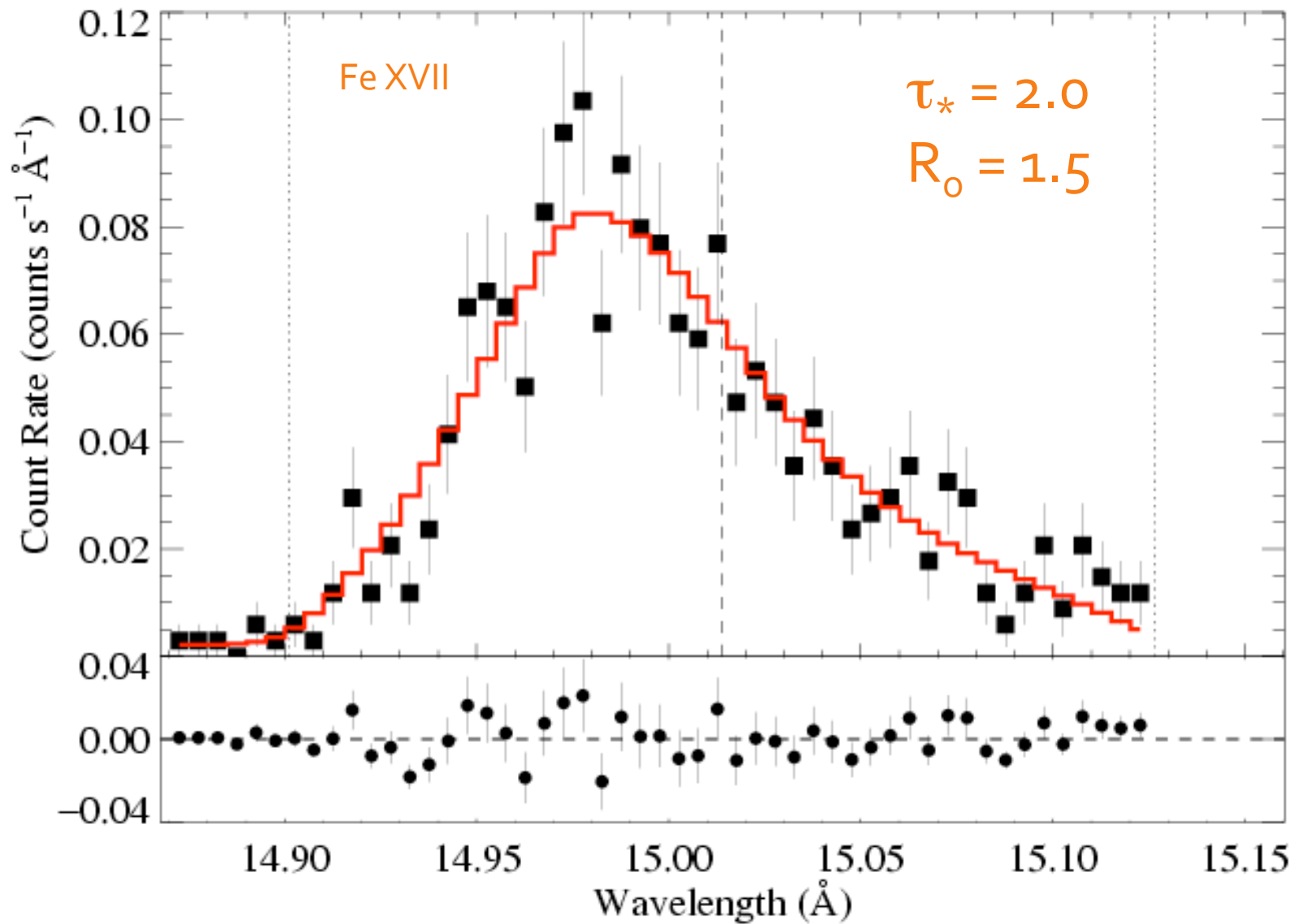
$$\tau = \tau_* \int_z^\infty \frac{R_* dz'}{r'^2 (1 - R_*/r')^\beta}$$

$$\tau_* \equiv \frac{\kappa \dot{M}}{4\pi R_* v_\infty}$$

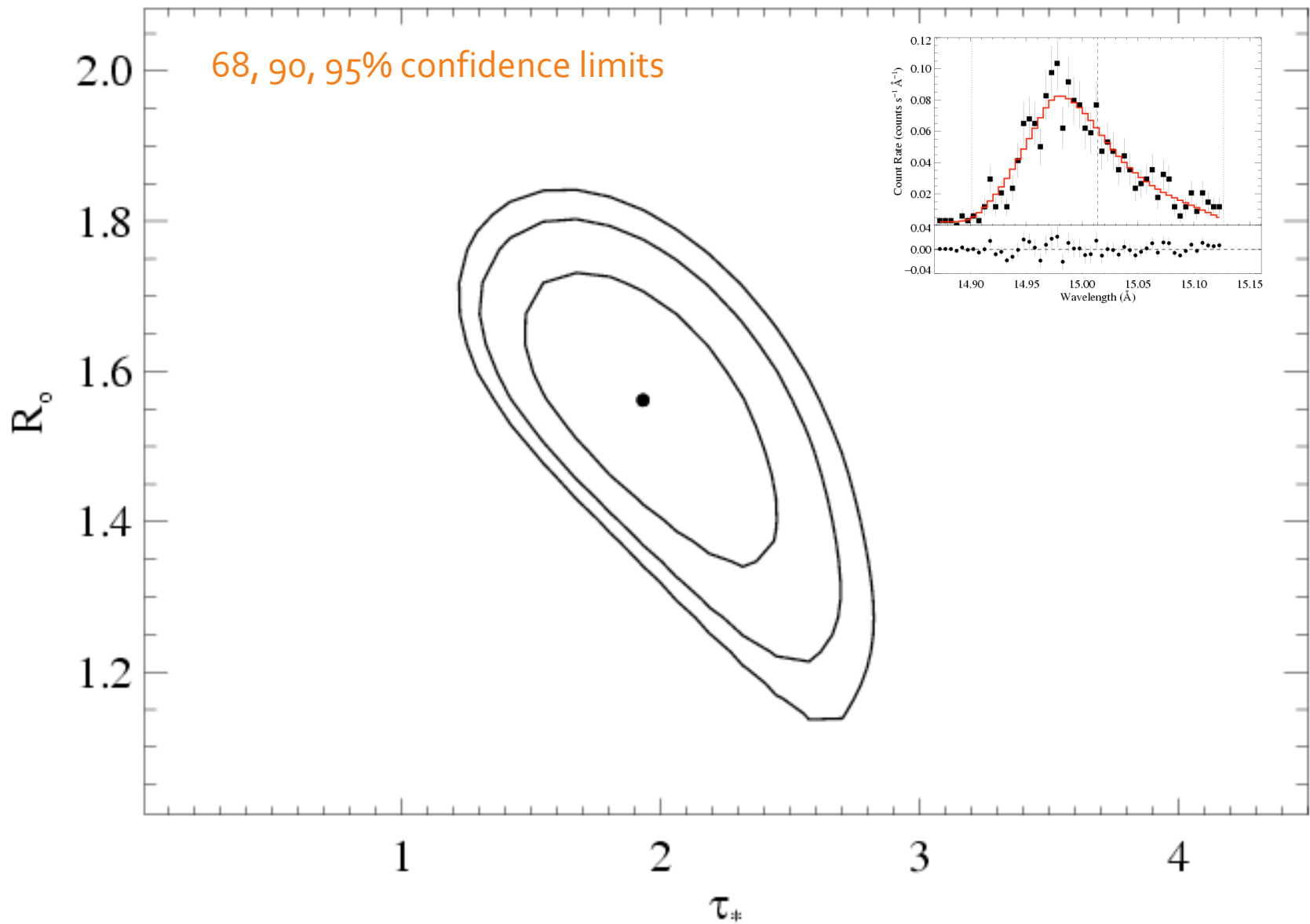
We fit these x-ray line profile models to each line in the *Chandra* data



And find a best-fit τ_* and R_o ...

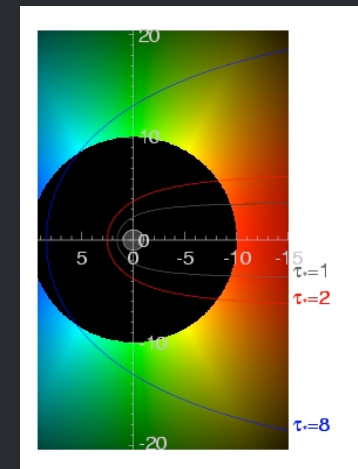
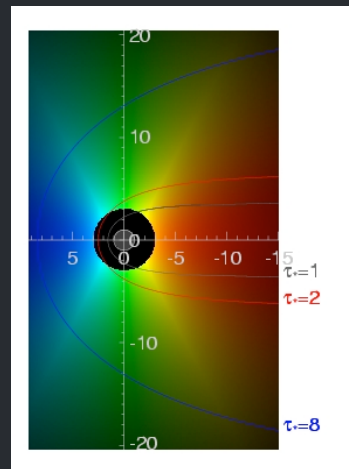
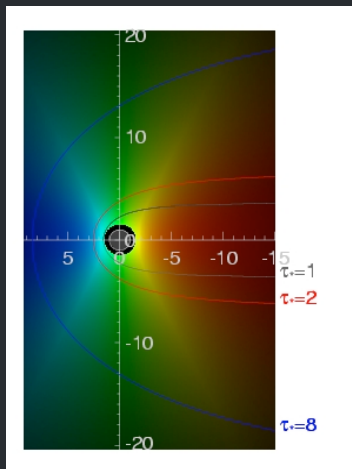


...and place confidence limits on these fitted parameter values

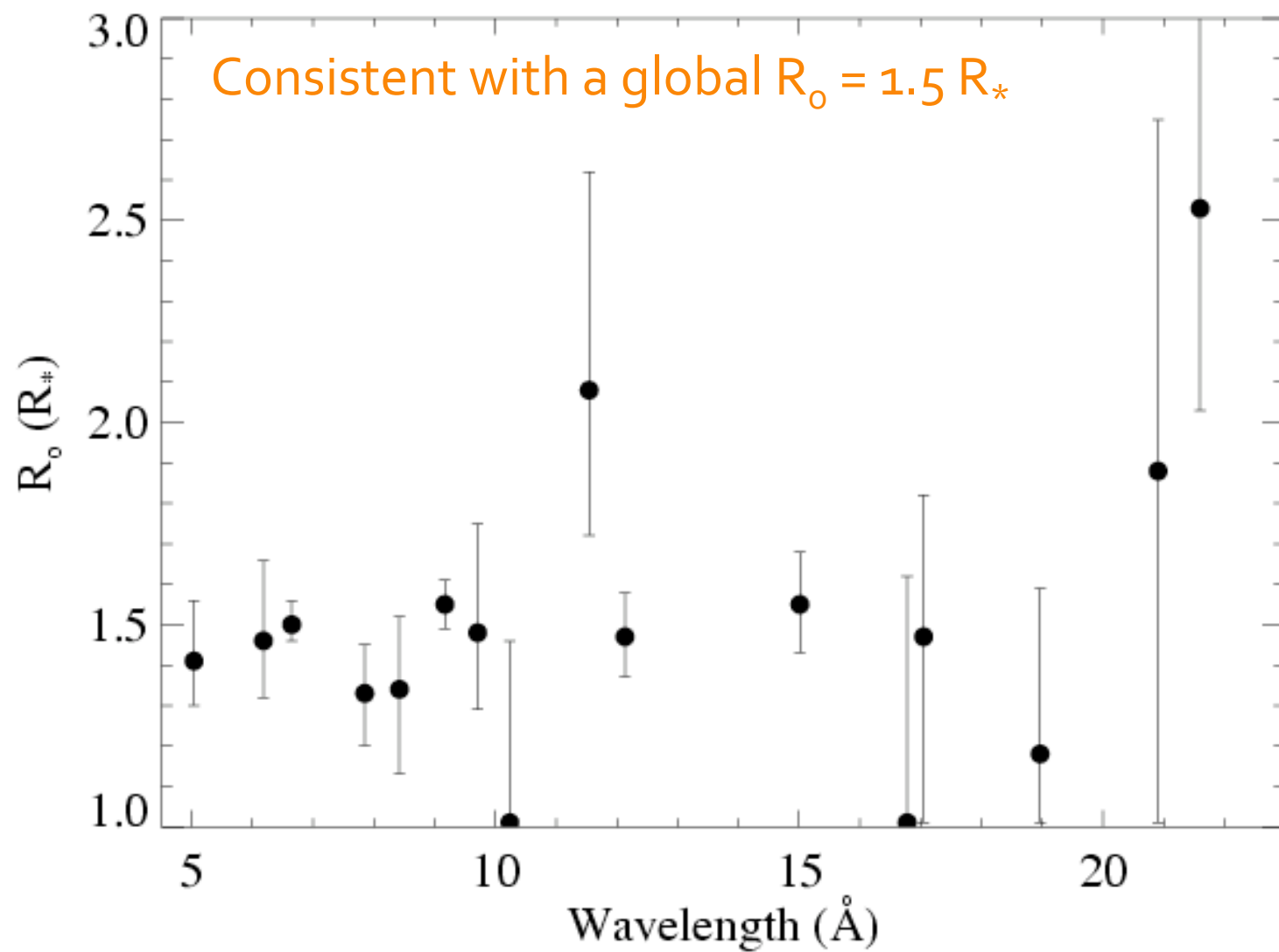


Let's focus on the R_0 parameter first

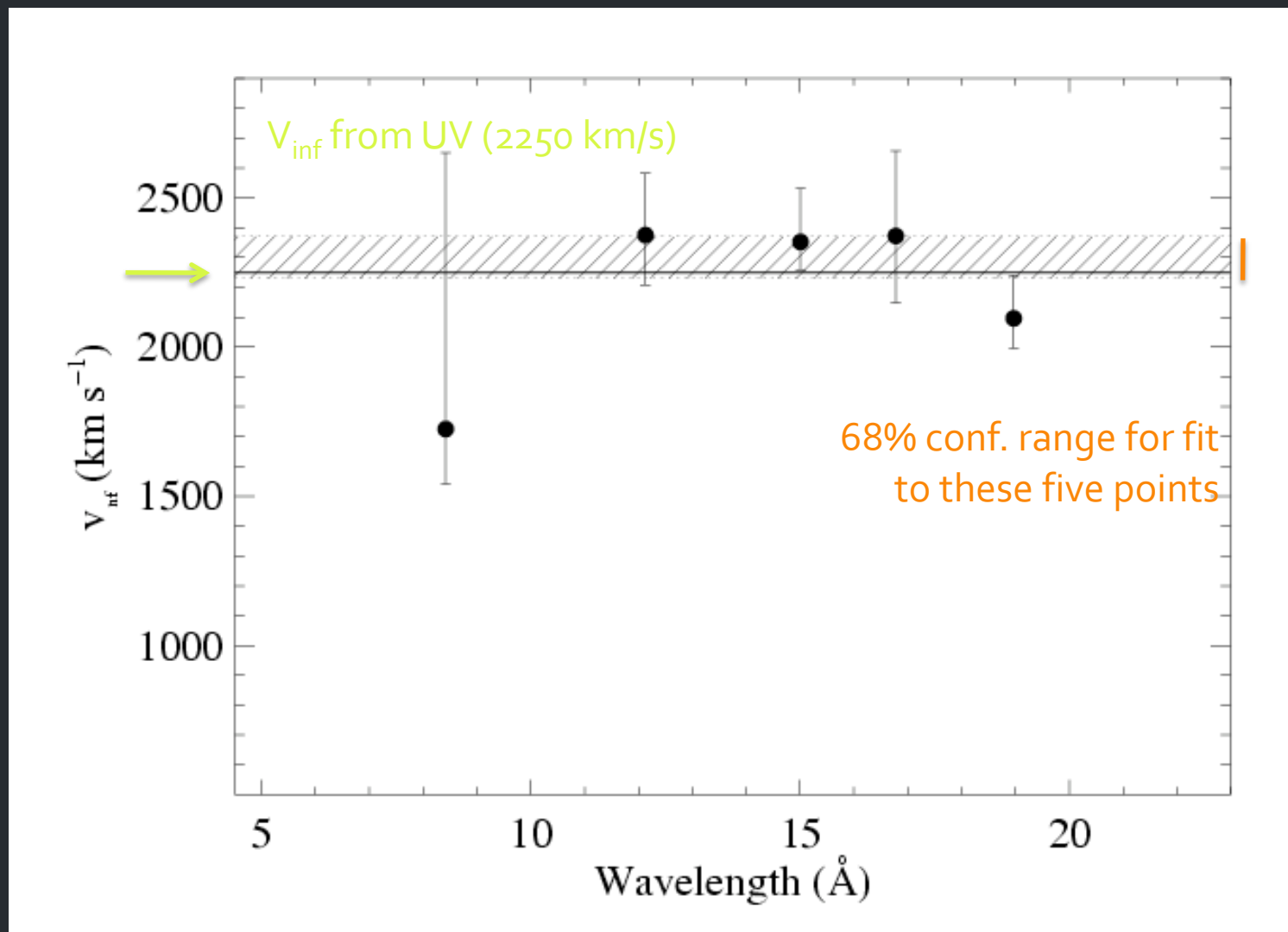
Note that for $\beta = 1$,
 $v = 1/3 v_{\text{inf}}$ at $1.5 R_*$
 $v = 1/2 v_{\text{inf}}$ at $2 R_*$



Distribution of R_o values in the Chandra spectrum of ζ Pup



V_{inf} can be constrained by the line fitting too



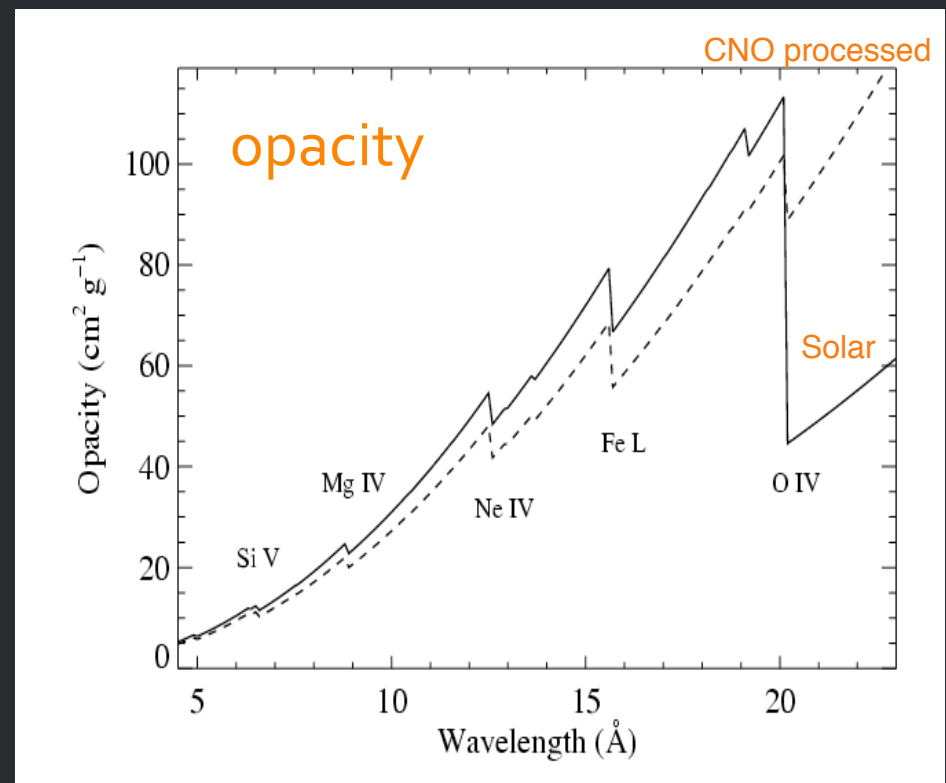
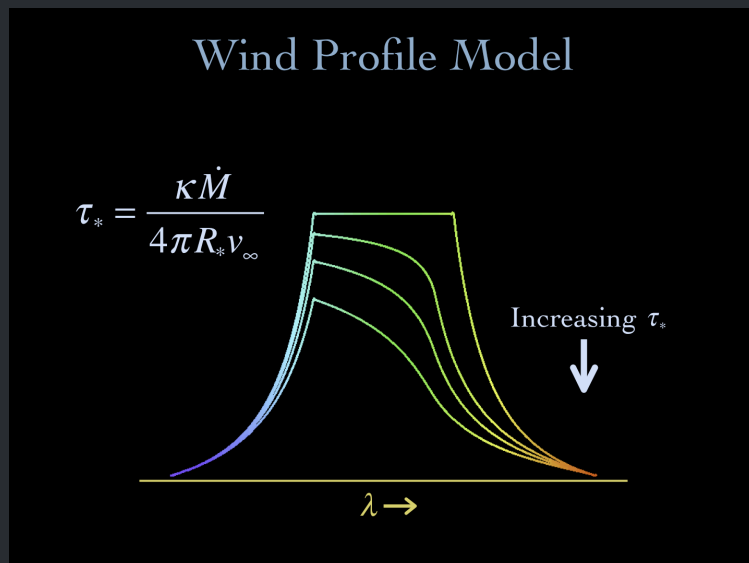
Kinematics conclusions

Line widths and shapes are *consistent* with :

1. X-ray onset radius of $\sim 1.5 R_*$
2. Same β , v_{inf} as the bulk, cold wind

Wind Absorption

Next, we see how absorption in the bulk, cool, partially ionized wind component affects the observed X-rays



opacity of the cold wind

wind mass-loss rate

$$\dot{M} = 4\pi r^2 v \rho$$

τ_* is the key parameter
describing the
absorption

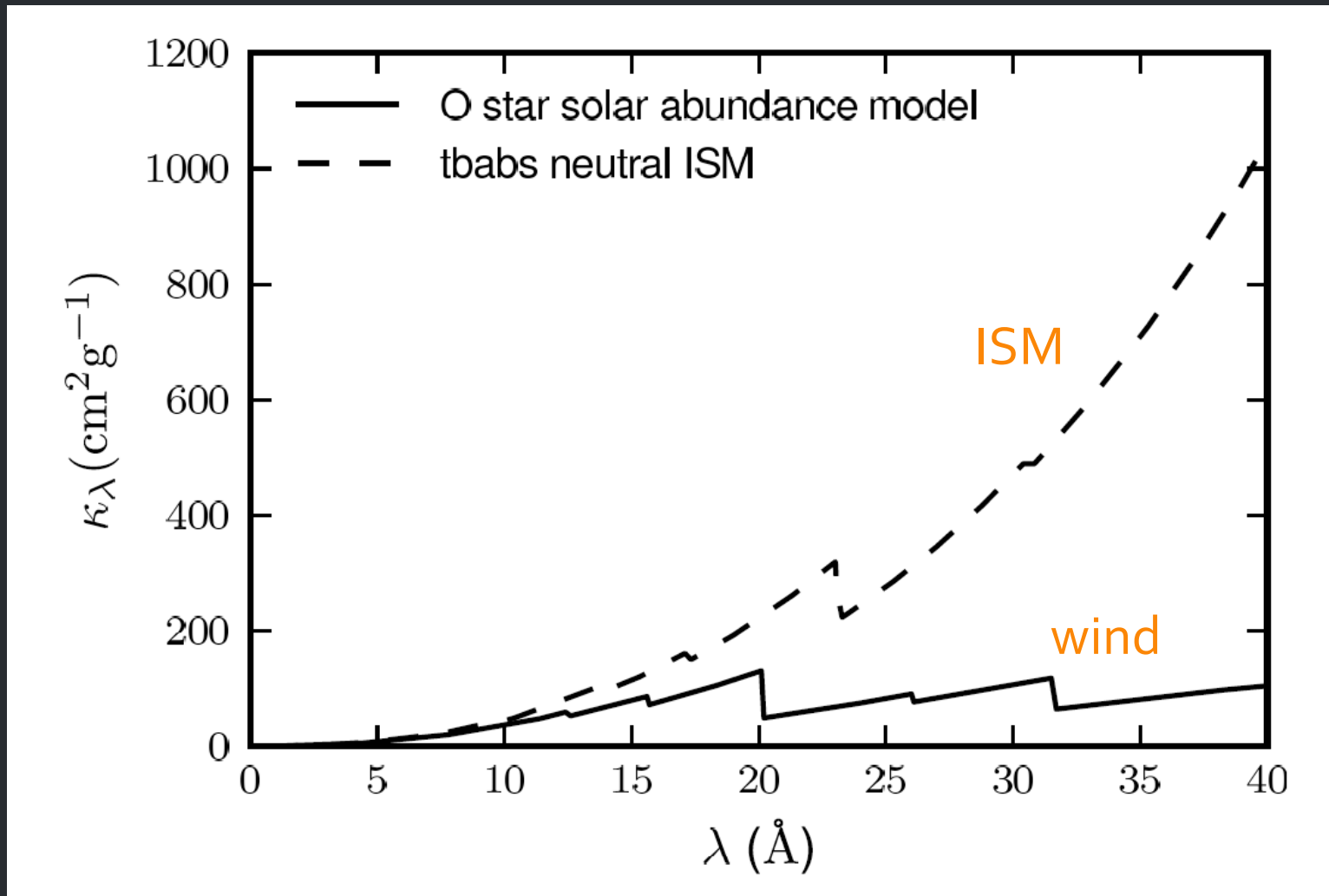
$$\tau_* \equiv \frac{\kappa \dot{M}}{4\pi R_* v_\infty}$$

radius of the star

wind terminal velocity

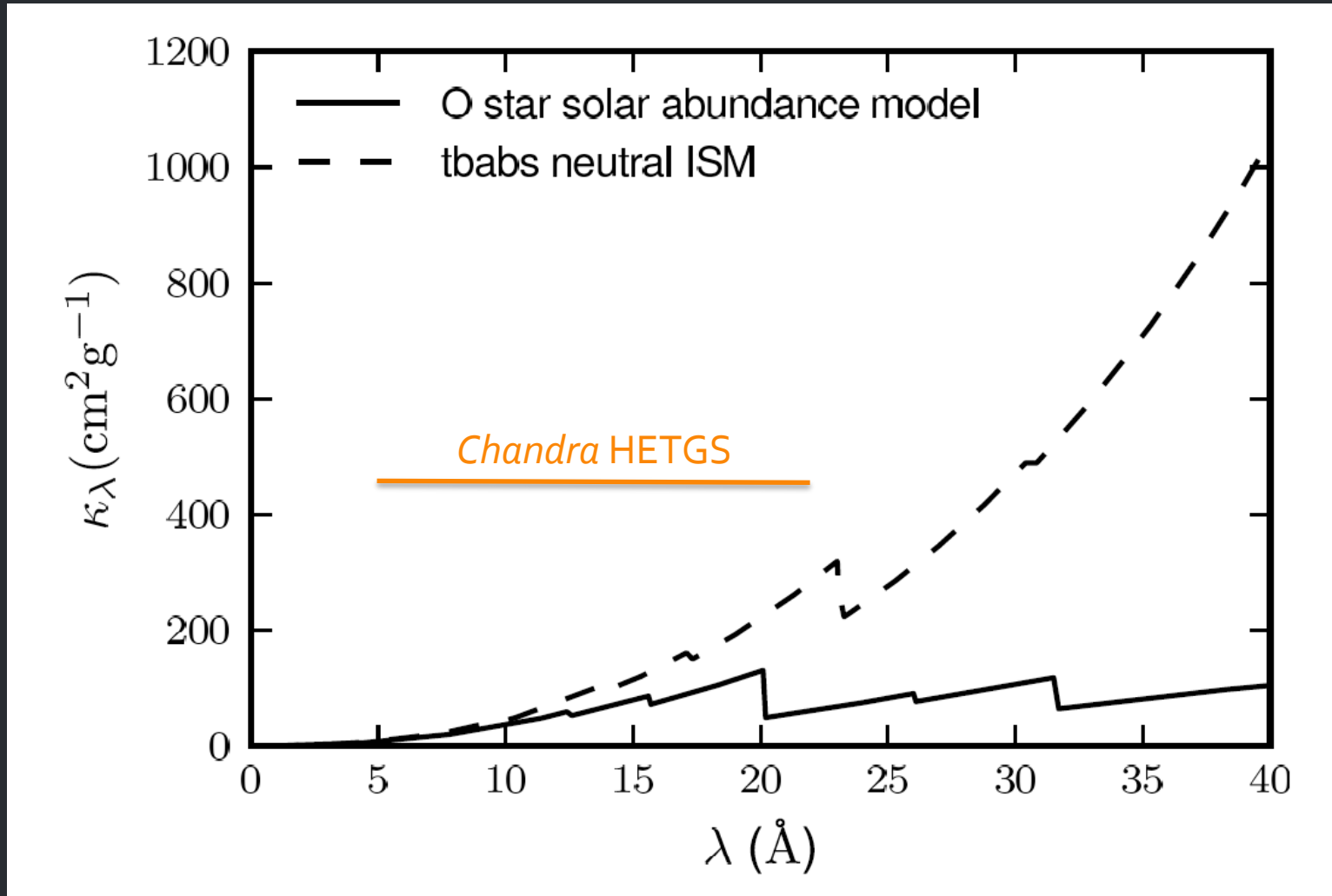
Wind opacity

X-ray bandpass



Wind opacity

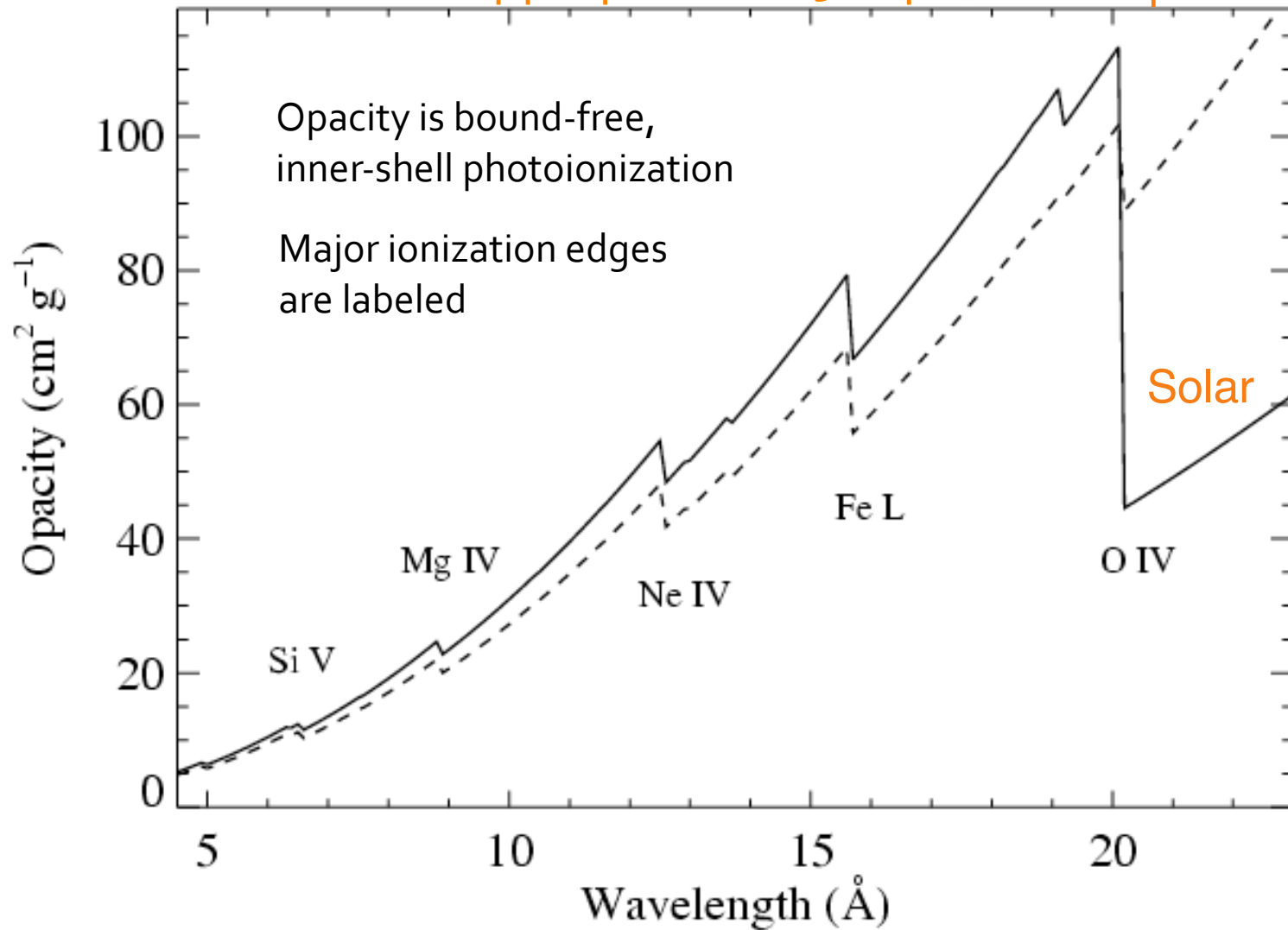
X-ray bandpass



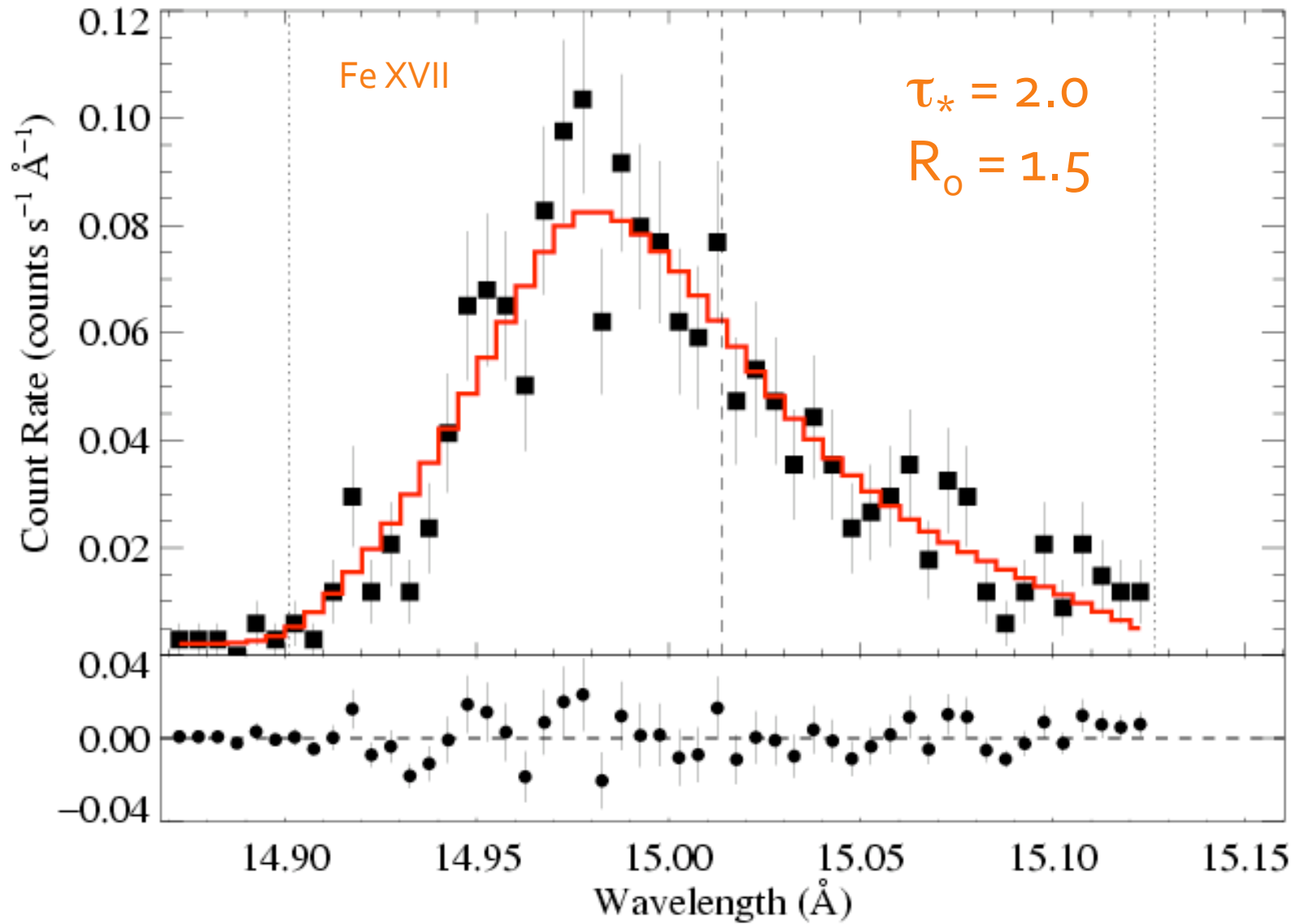
X-ray opacity

Zoom in

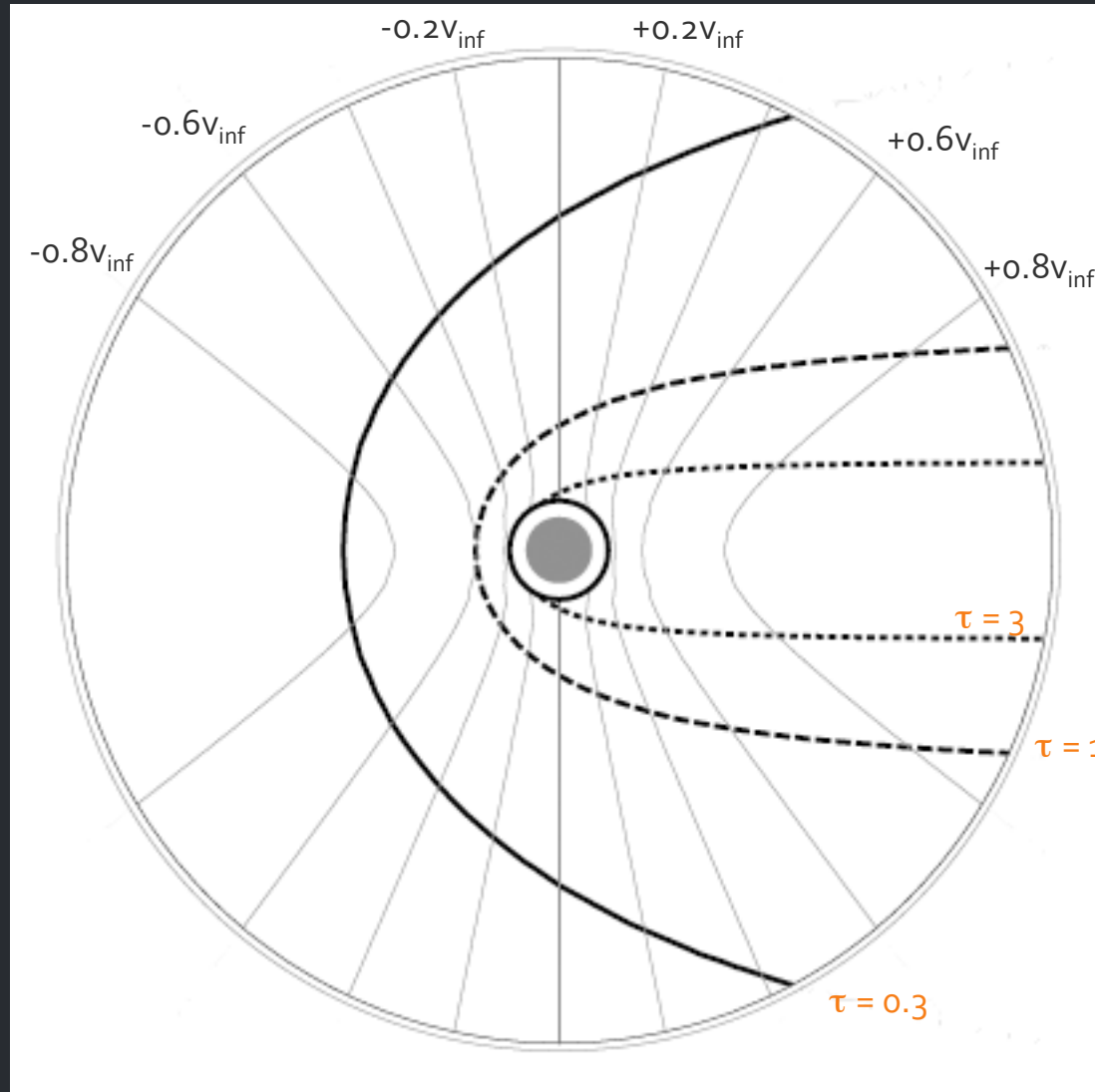
appropriate to ζ Pup \leftarrow CNO processed



This is the same Fe XVII line we saw a minute ago



$\tau_* = 2$ in this wind



observer
on left

optical depth
contours

Other lines?

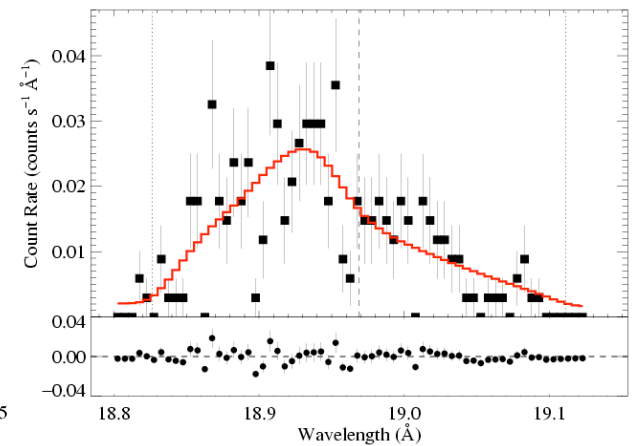
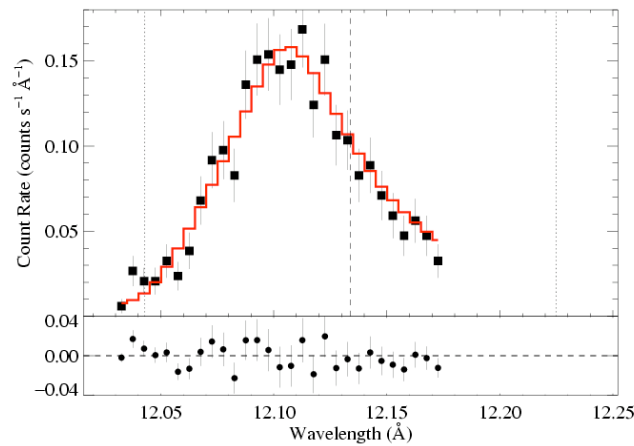
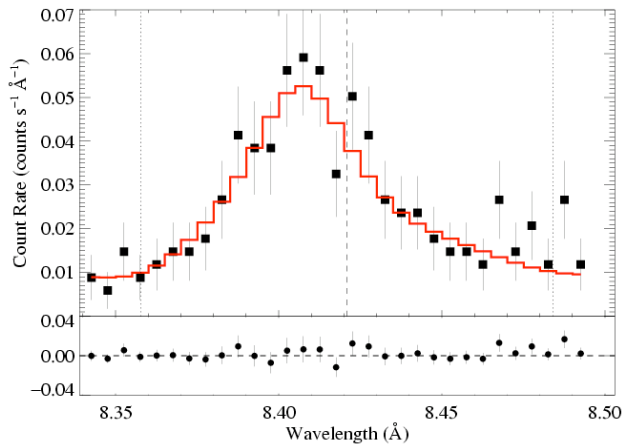
Different κ – and thus τ_* – at each wavelength

ζ Pup: three emission lines

Mg Ly α : 8.42 Å

Ne Ly α : 12.13 Å

O Ly α : 18.97 Å



$$\tau_* = 1$$

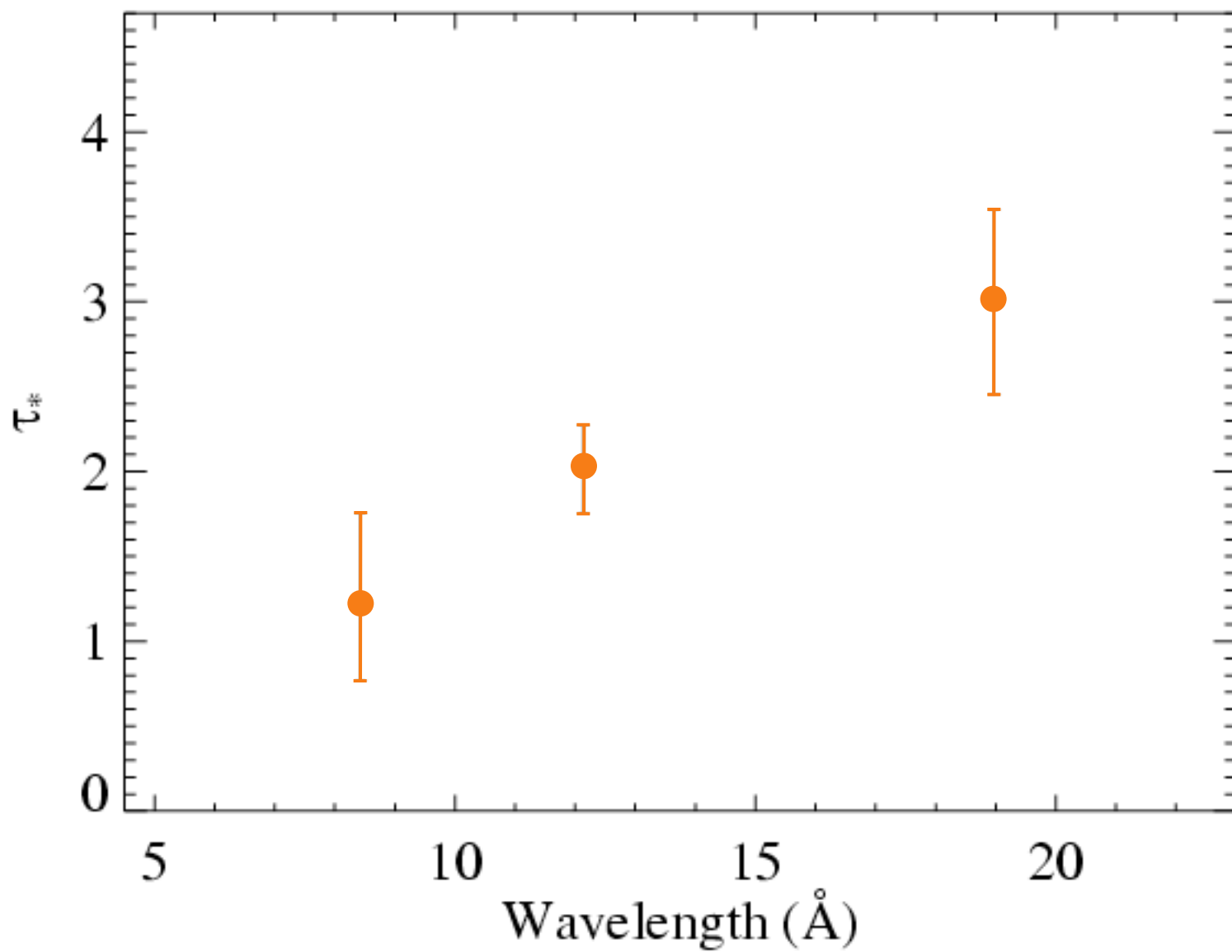
$$\tau_* = 2$$

$$\tau_* = 3$$

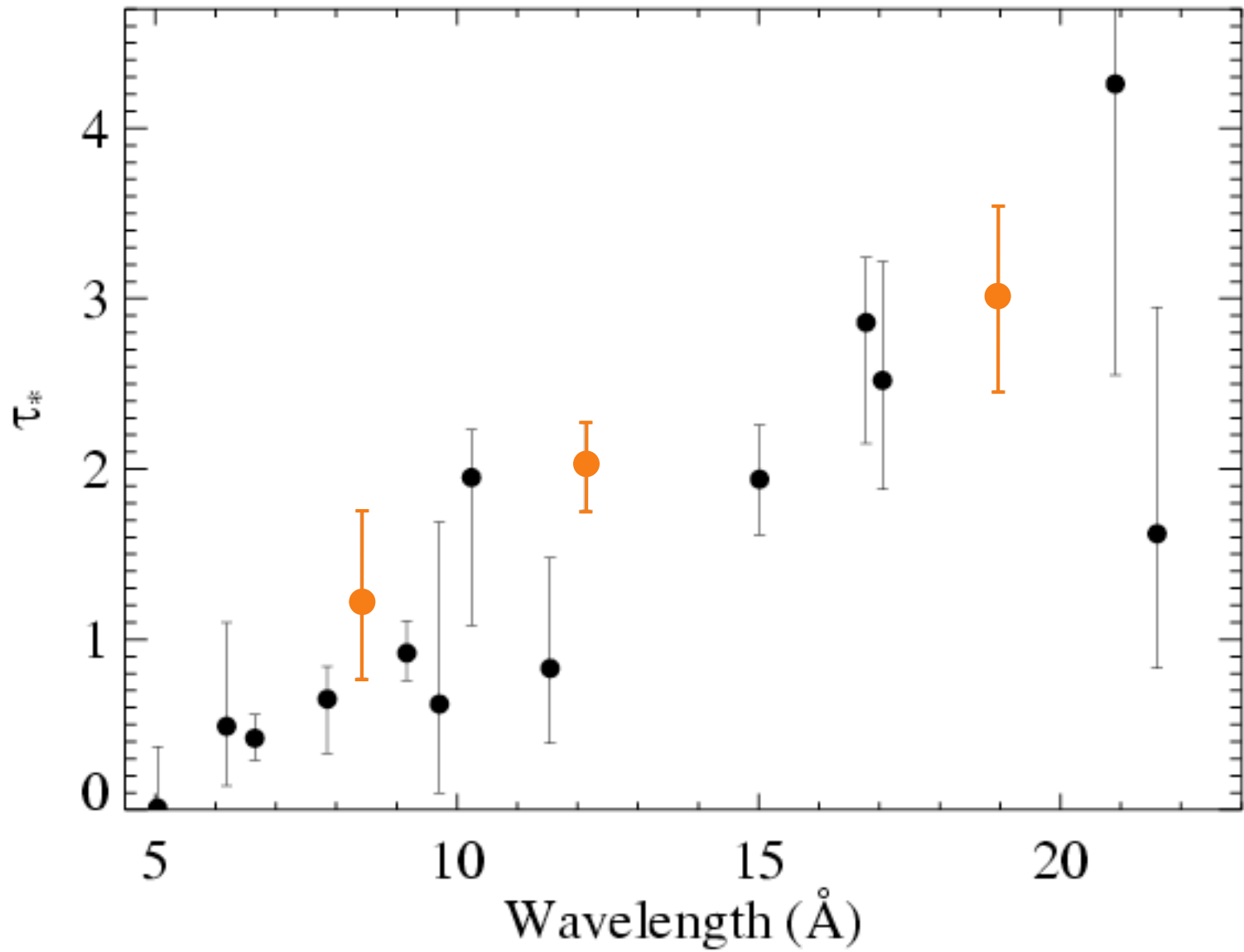
Recall:

$$\tau_* \equiv \frac{\kappa \dot{M}}{4\pi R_* v_\infty}$$

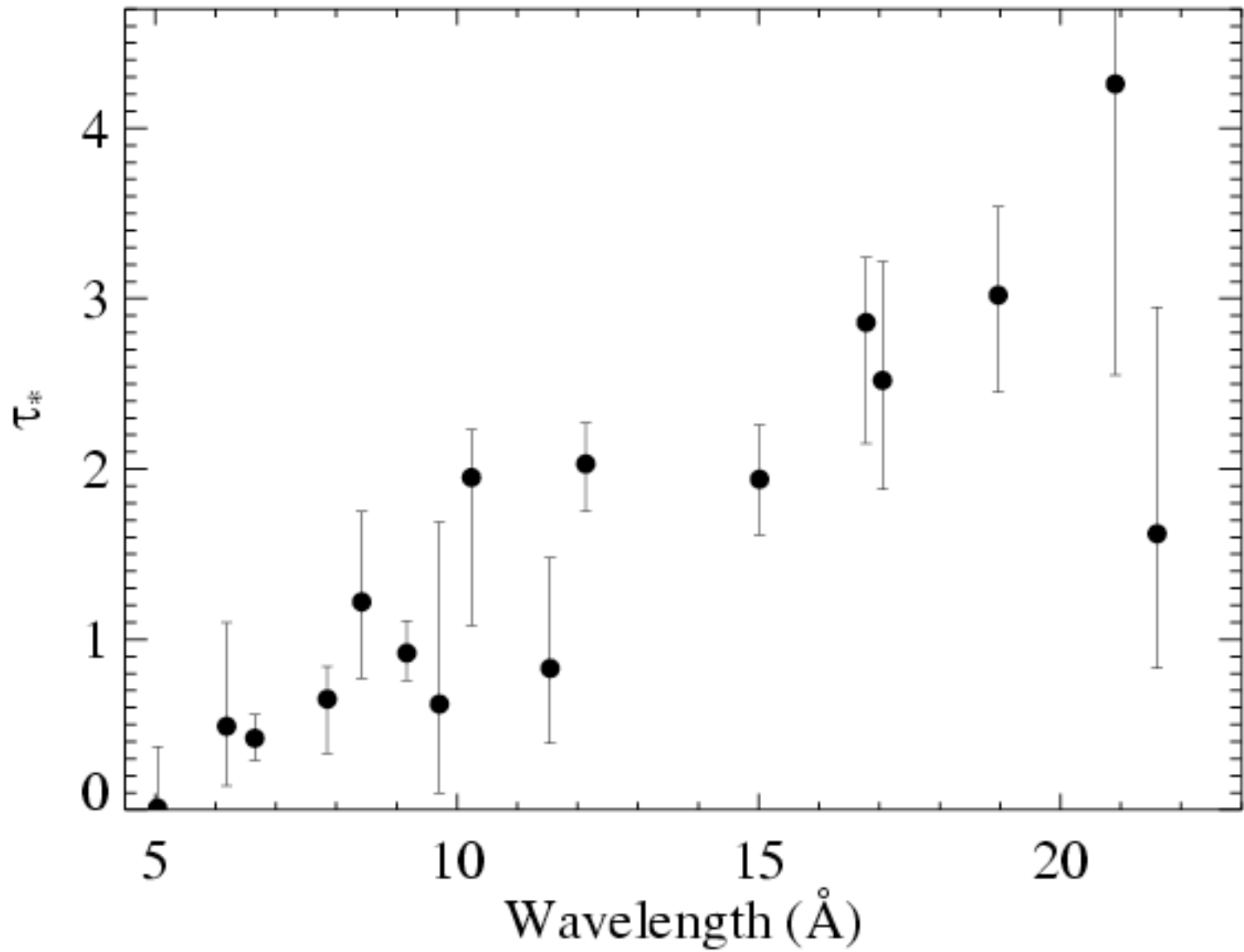
Results from the 3 line fits shown previously



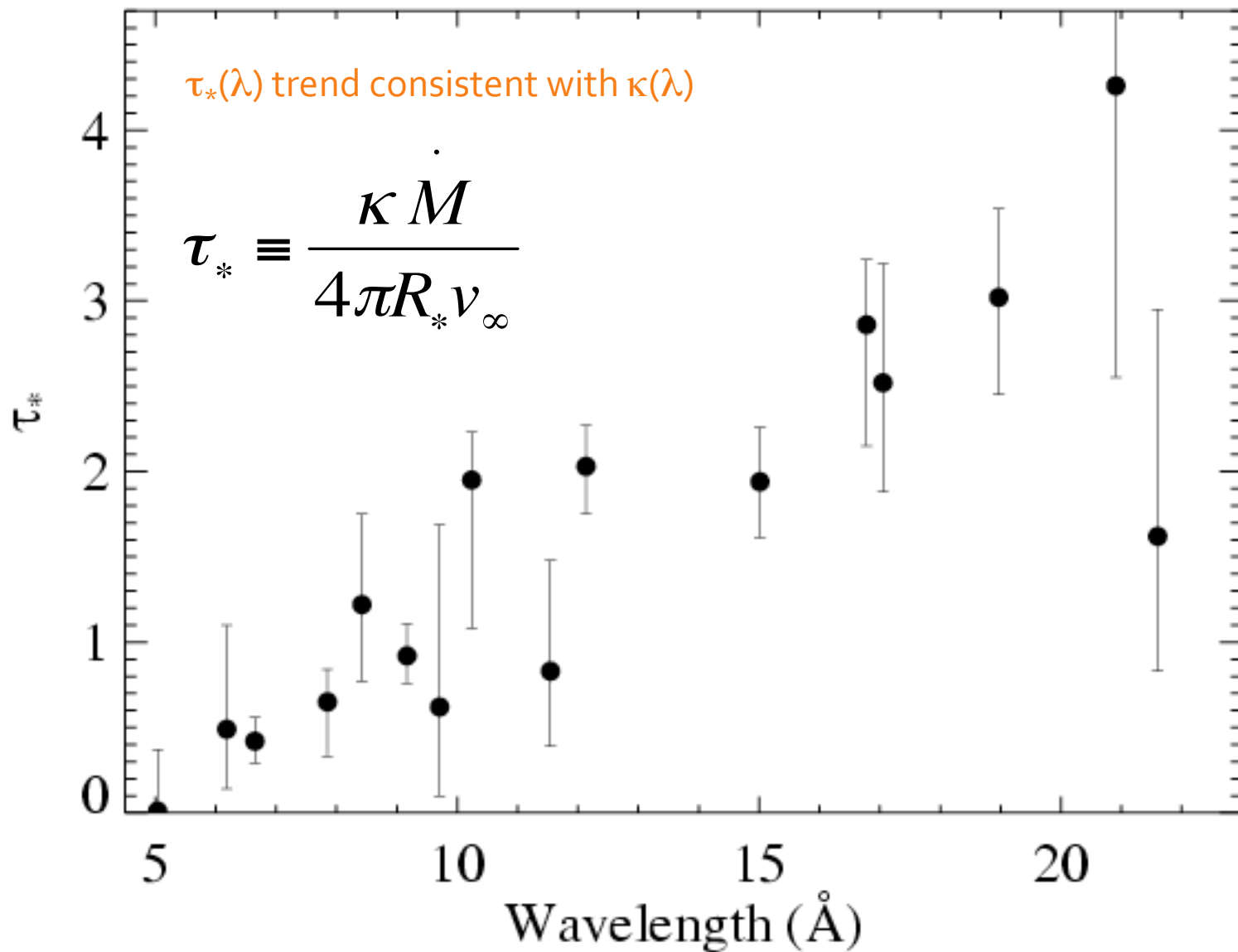
Fits to 16 lines in the *Chandra* spectrum of ζ Pup



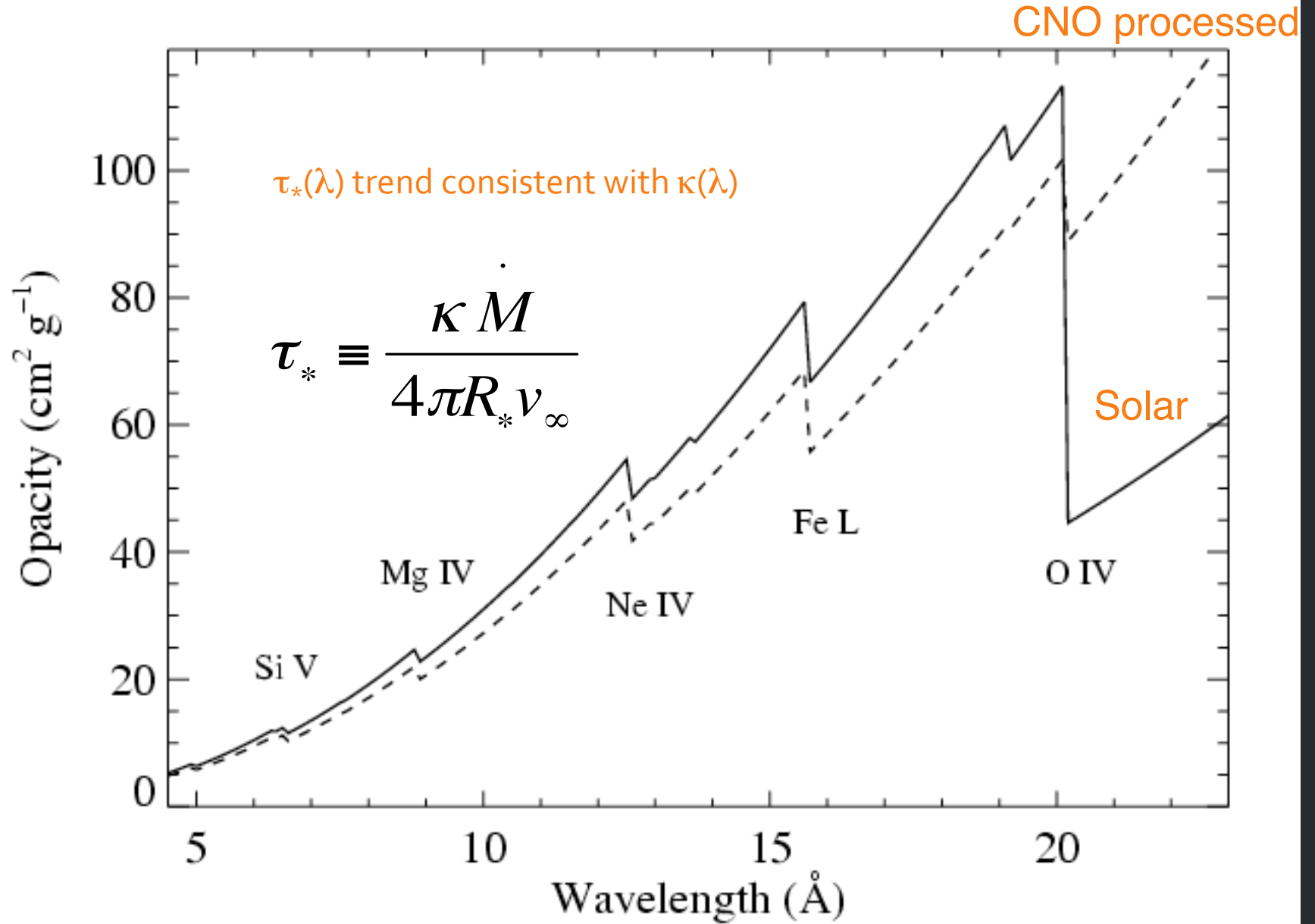
Fits to 16 lines in the *Chandra* spectrum of ζ Pup



Fits to 16 lines in the *Chandra* spectrum of ζ Pup

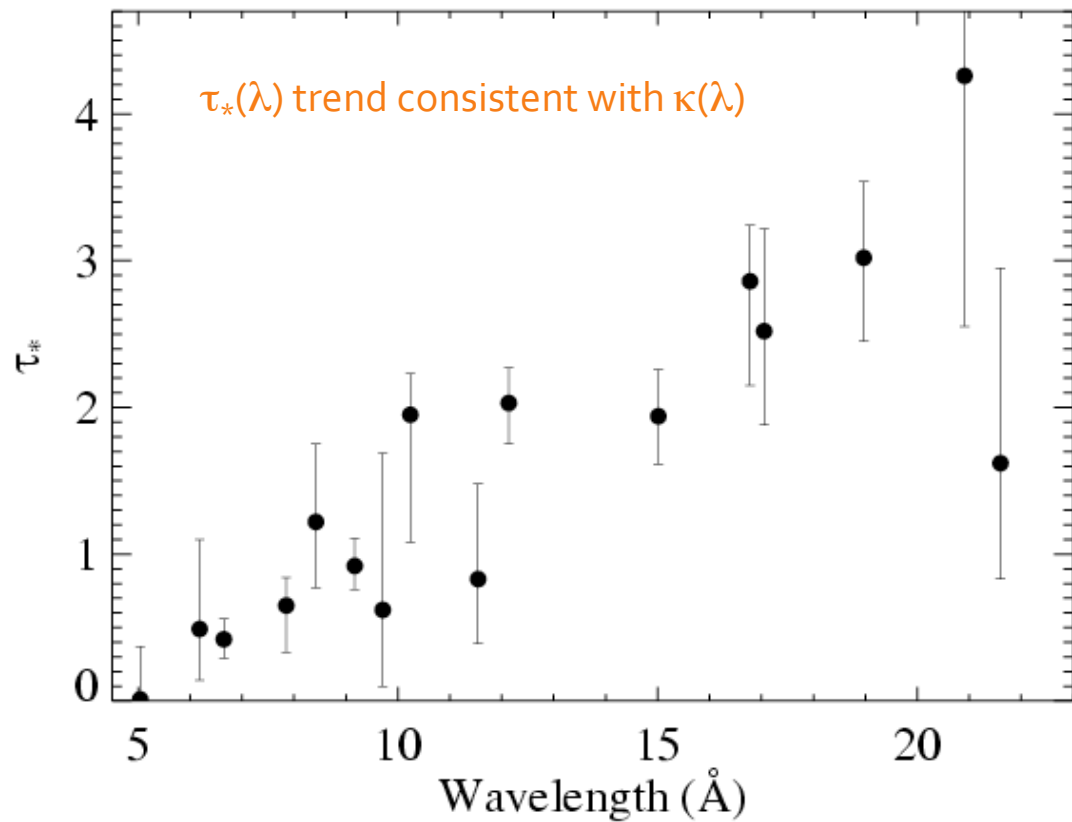


Fits to 16 lines in the *Chandra* spectrum of ζ Pup



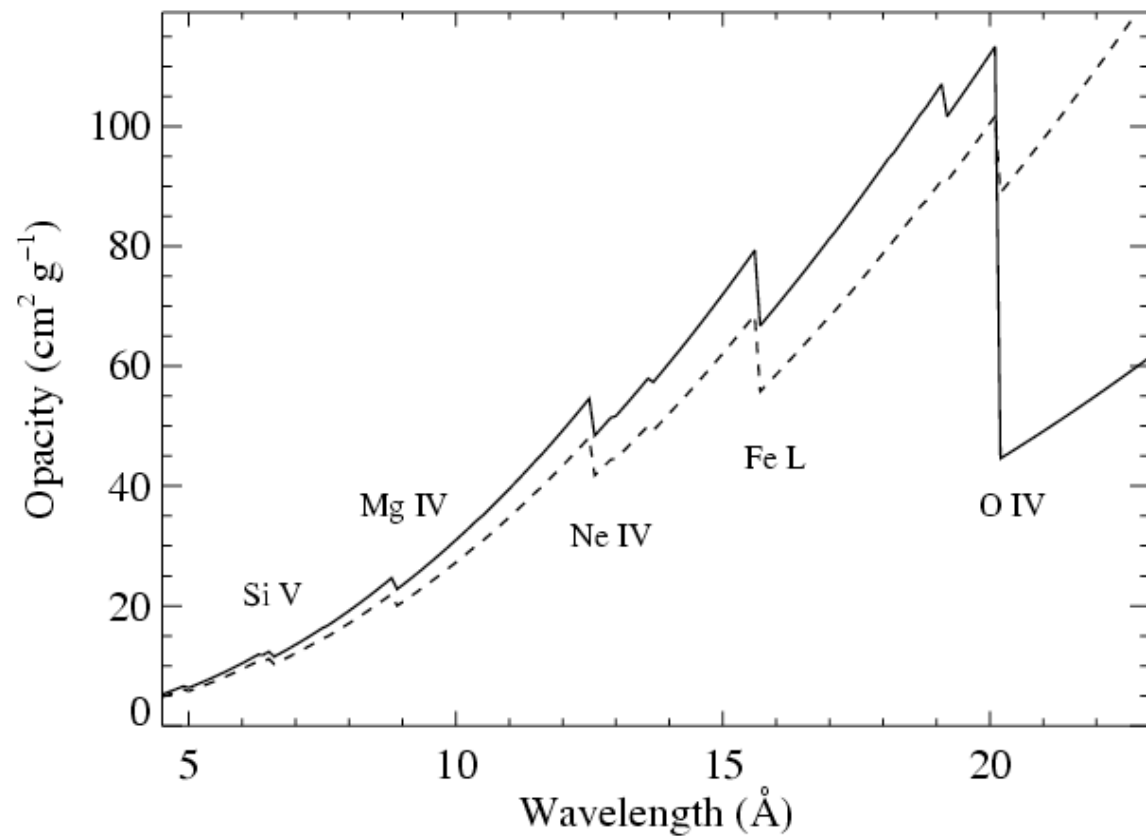
$$\tau_* \equiv \frac{\kappa \dot{M}}{4\pi R_* v_\infty}$$

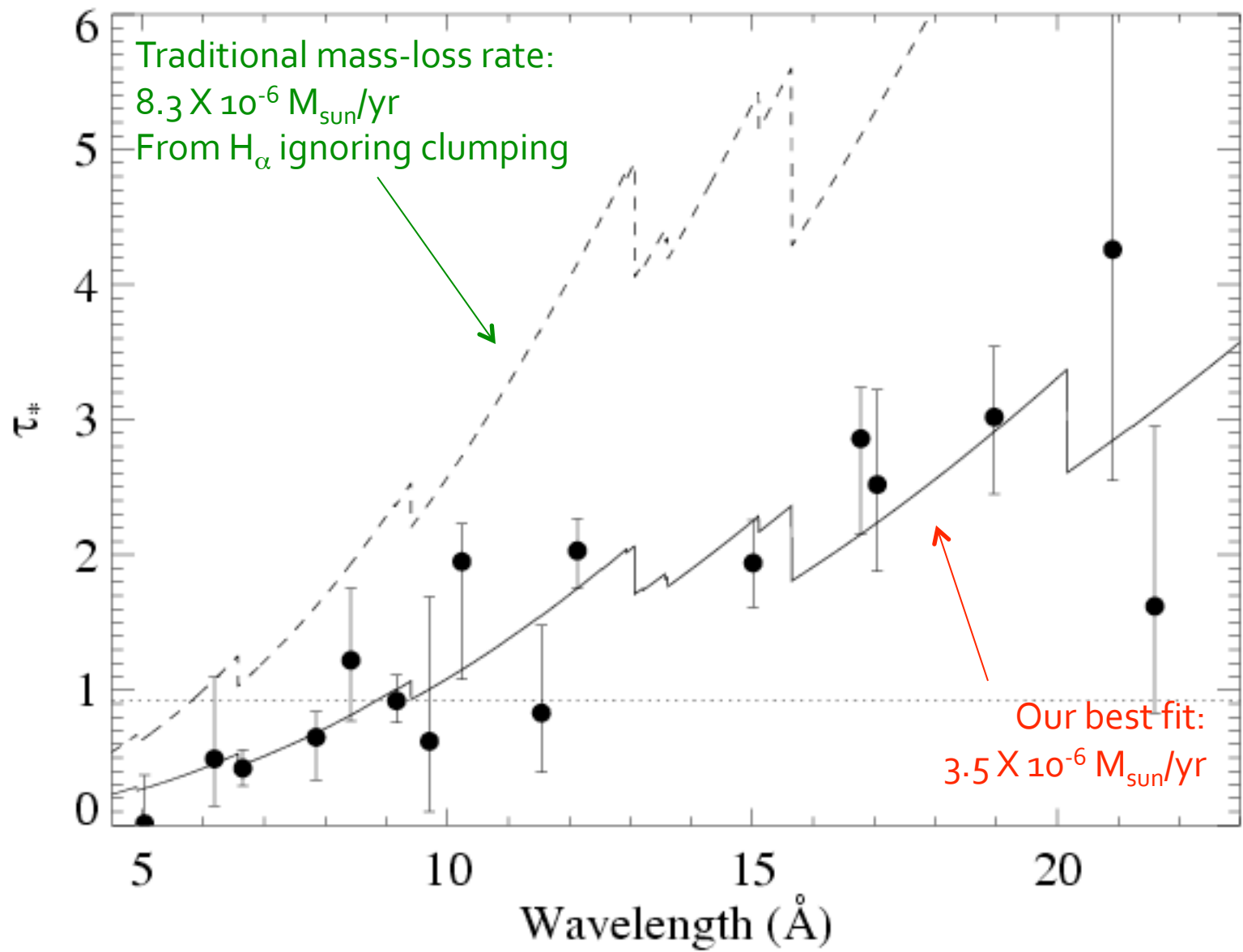
• \dot{M} becomes the free parameter of the fit to the $\tau_*(\lambda)$ trend

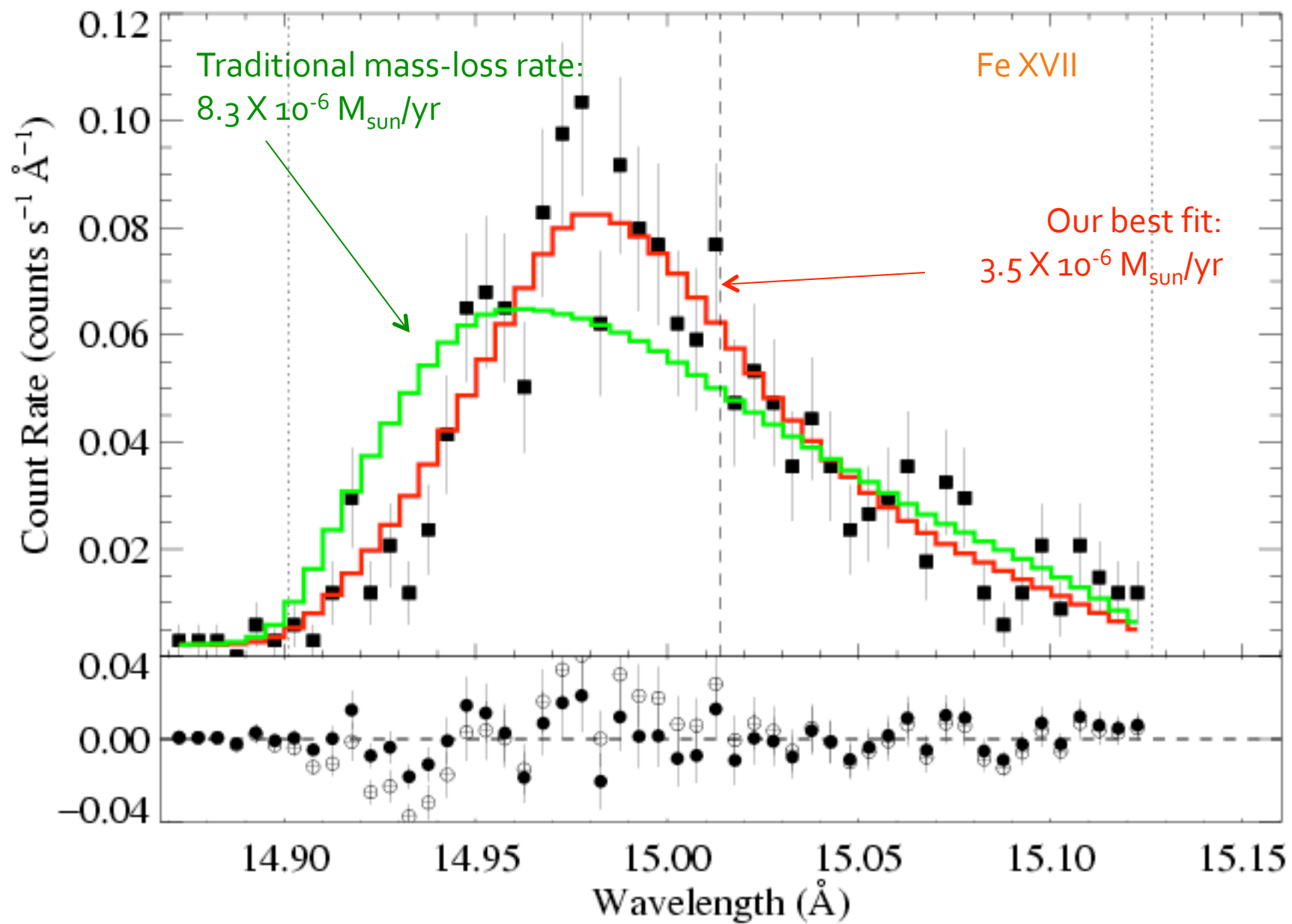


$$\tau_* \equiv \frac{\kappa \dot{M}}{4\pi R_* v_\infty}$$

• \dot{M} becomes the free parameter of the fit to the $\tau_*(\lambda)$ trend







Mass-loss rate conclusions

The trend of τ_* value with λ is *consistent* with :

Mass-loss rate of $3.5 \times 10^{-6} M_{\text{sun}}/\text{yr}$

Factor of ~ 3 reduction w.r.t. unclumped H-alpha

Note: this mass-loss rate diagnostic is a column density diagnostic; it is not a density squared diagnostic and so is *not sensitive to clumping* (as long as individual clumps are not optically thick).

Bright OB stars in the Galaxy

III. Constraints on the radial stratification of the **clumping** factor in hot star winds from a combined H_{α} , IR and radio analysis[★]

J. Puls¹, N. Markova², S. Scuderi³, C. Stanghellini⁴, O. G. Taranova⁵, A. W. Burnley⁶ and I. D. Howarth⁶

¹ Universitäts-Sternwarte München, Scheinerstr. 1, D-81679 München, Germany, e-mail: uh101aw@usm.uni-muenchen.de

² Institute of Astronomy, Bulgarian National Astronomical Observatory, P.O. Box 136, 4700 Smoljan, Bulgaria, e-mail: nmarkova@astro.bas.bg

³ INAF - Osservatorio Astrofisico di Catania, Via S. Sofia 78, I-95123 Catania, Italy, e-mail: scuderi@oact.inaf.it

⁴ INAF - Istituto di Radioastronomia, Via P. Gobetti 101, I-40129 Bologna, Italy, e-mail: c.stanghellini@ira.inaf.it

⁵ Sternberg Astronomical Institute, Universitetski pr. 13, Moscow, 119992, Russia, e-mail: taranova@sai.msu.ru

⁶ Department of Physics and Astronomy, University College London, Gower Street, London WC1E 6BT, UK, e-mail: awxb@star.ucl.ac.uk, idh@star.ucl.ac.uk

Received; accepted

Abstract. Recent results strongly challenge the canonical picture of massive star winds: various evidence indicates that currently accepted mass-loss rates, \dot{M} , may need to be revised downwards, by factors extending to one magnitude or even more. This is because the most commonly used mass-loss diagnostics are affected by “clumping” (small-scale density inhomogeneities), influencing our interpretation of observed spectra and fluxes.

Such downward revisions would have dramatic consequences for the evolution of, and feedback from, massive stars, and thus robust determinations of the clumping properties and mass-loss rates are urgently needed. We present a first attempt concerning this objective, by means of constraining the radial stratification of the so-called clumping factor.

To this end, we have analyzed a sample of 19 Galactic O-type supergiants/giants, by combining our own and archival data for H_{α} , IR, mm and radio fluxes, and using approximate methods, calibrated to more sophisticated models. Clumping has been included into our analysis in the “conventional” way, by assuming the inter-clump matter to be void. Because (almost) all our diagnostics depends on the square of density, we cannot derive absolute clumping factors, but only factors normalized to a certain minimum.

This minimum was usually found to be located in the outermost, radio-emitting region, i.e., the radio mass-loss rates are the lowest ones, compared to \dot{M} derived from H_{α} and the IR. The radio rates agree well with those predicted by theory, but are only upper limits, due to unknown clumping in the outer wind. H_{α} turned out to be a useful tool to derive the clumping properties inside $r < 3 \dots 5 R_{*}$. Our most important result concerns a (physical) difference between denser and thinner winds: for denser winds, the innermost region is more strongly clumped than the outermost one (with a normalized clumping factor of 4.1 ± 1.4), whereas thinner winds have similar clumping properties in the inner and outer regions.

Our findings are compared with theoretical predictions, and the implications are discussed in detail, by assuming different scenarios regarding the still unknown clumping properties of the outer wind.

Implications for broadband X-rays

Si XIV

Mg XII

Ne X

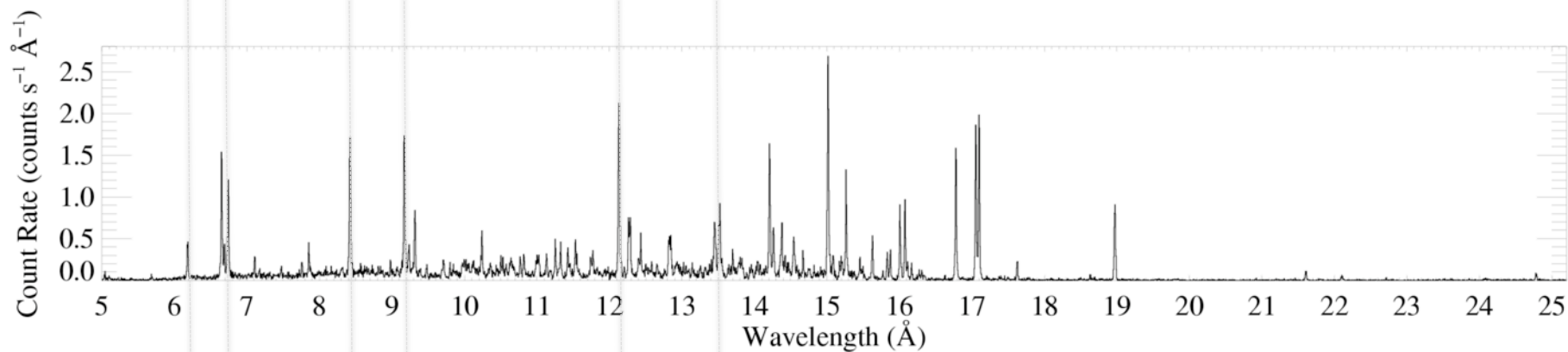
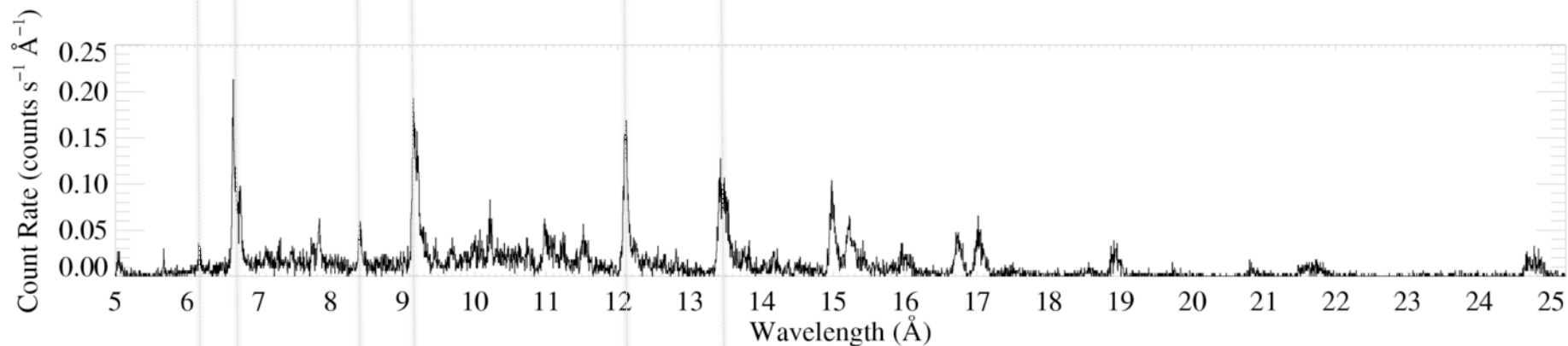
H-like vs. He-like

Si XIII

Mg XI

Ne IX

ζ Pup (O4 If)



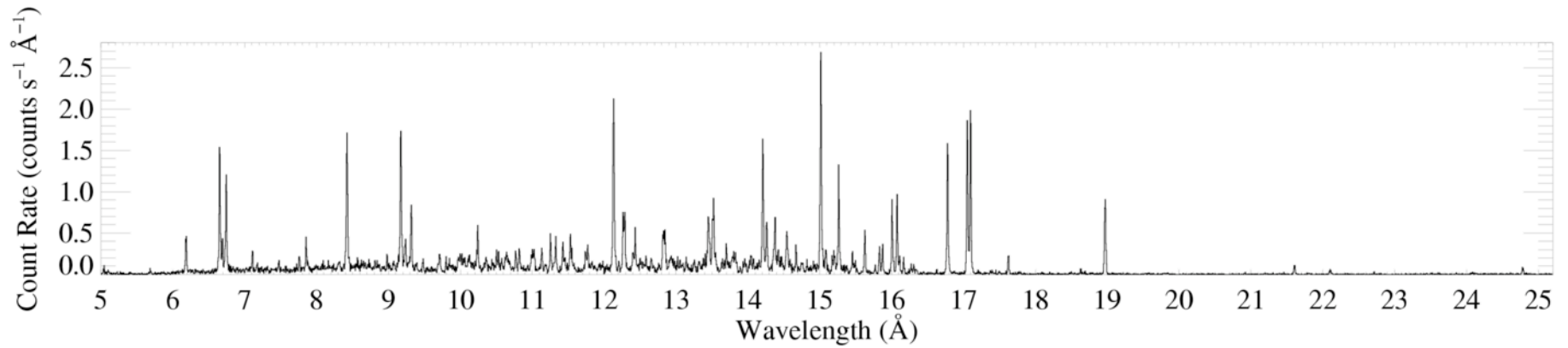
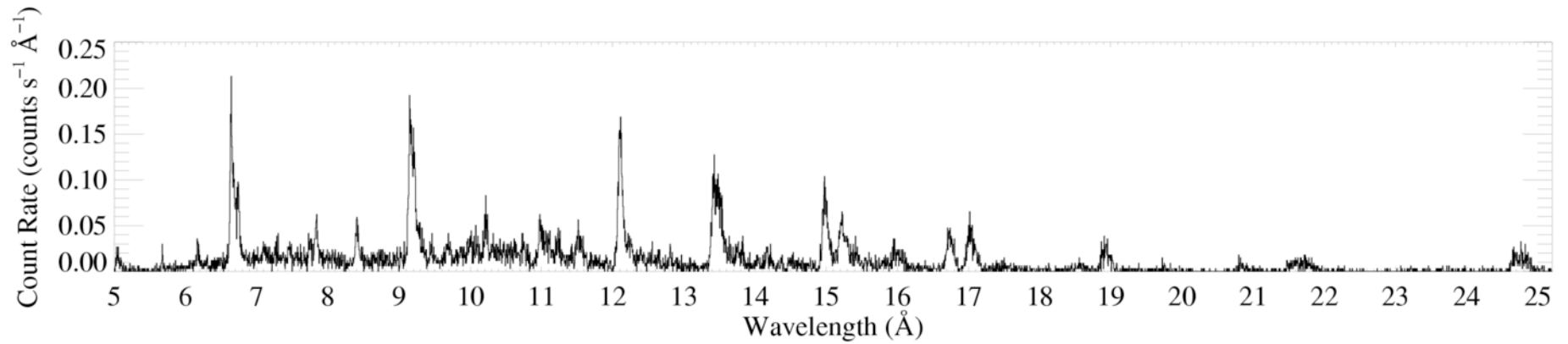
Capella (G5 III) – coronal source
– for comparison

Mg XII

Mg XI

H-like vs. He-like

ζ Pup (O4 If)

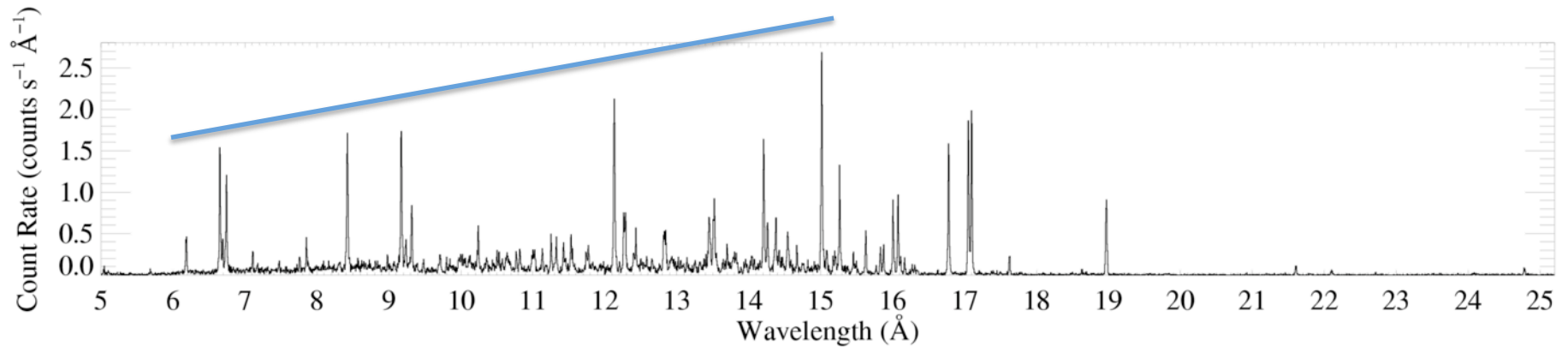
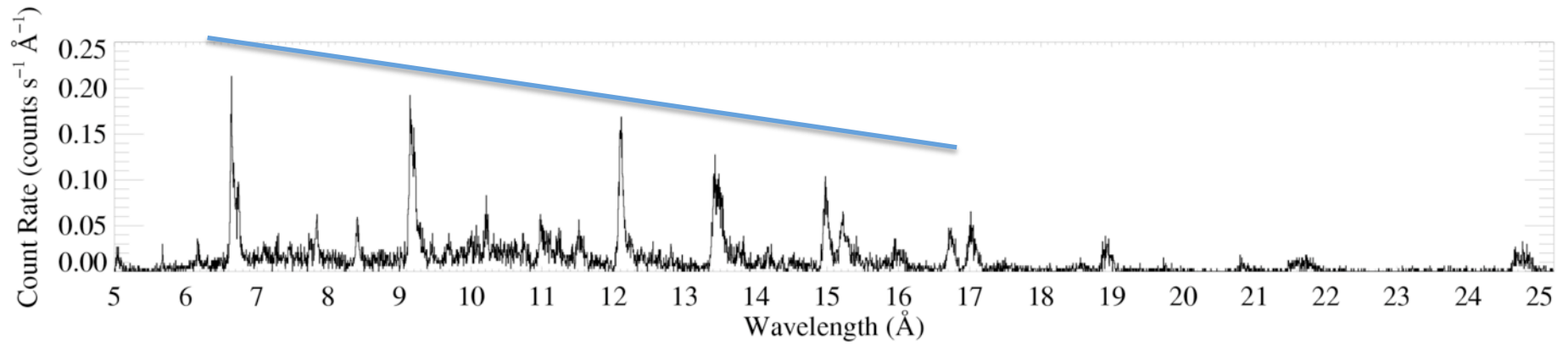


Capella (G5 III) – coronal source
– for comparison

Mg XII
Mg XI

H-like vs. He-like

ζ Pup (O4 If)

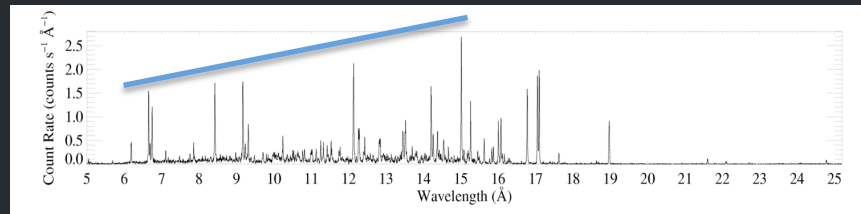
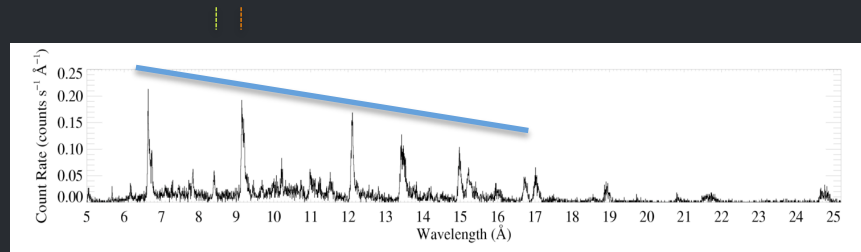


Capella (G5 III) – coronal source
– for comparison

Spectral energy distribution trends

The O star has a *harder spectrum*, but apparently *cooler plasma*

*This is explained
by wind
absorption*



Wind absorption model

Note that a realistic model of the radiation transport and of the opacity is required to properly account for broadband absorption effects

See Leutenegger et al. 2010 for simple method to incorporate these effects into data analysis

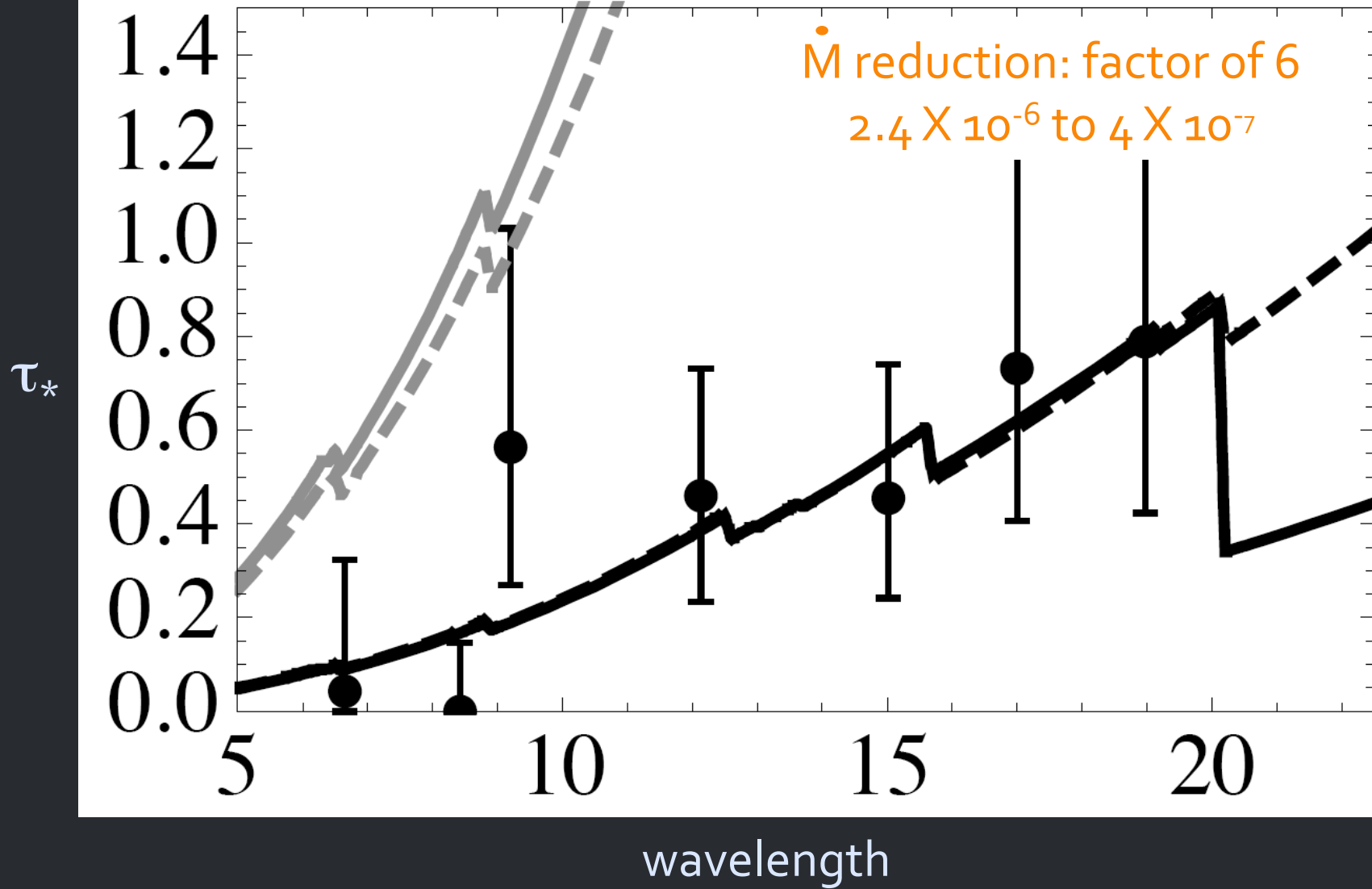
Other stars?

9 Sgr (O₄ V)

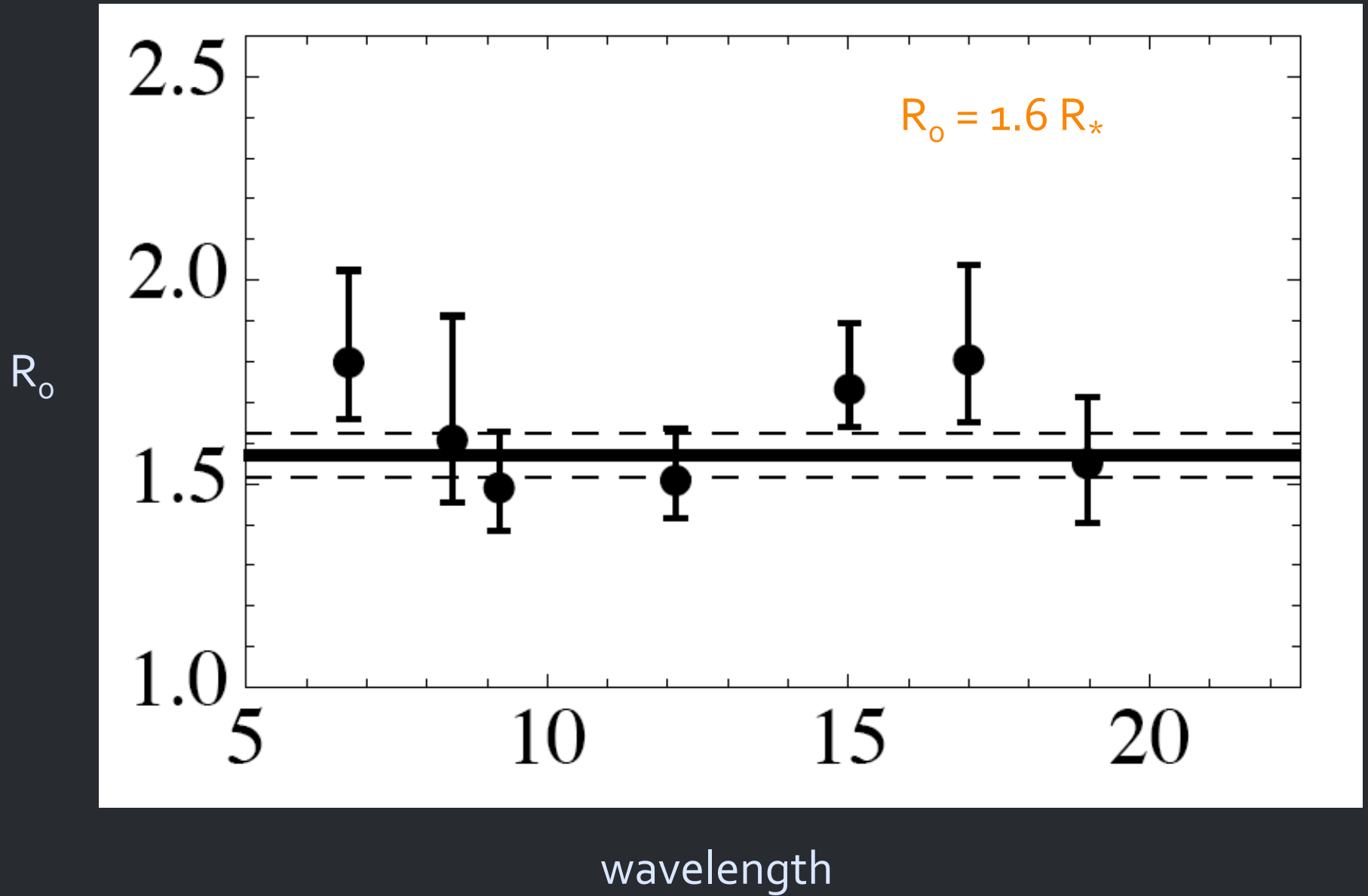


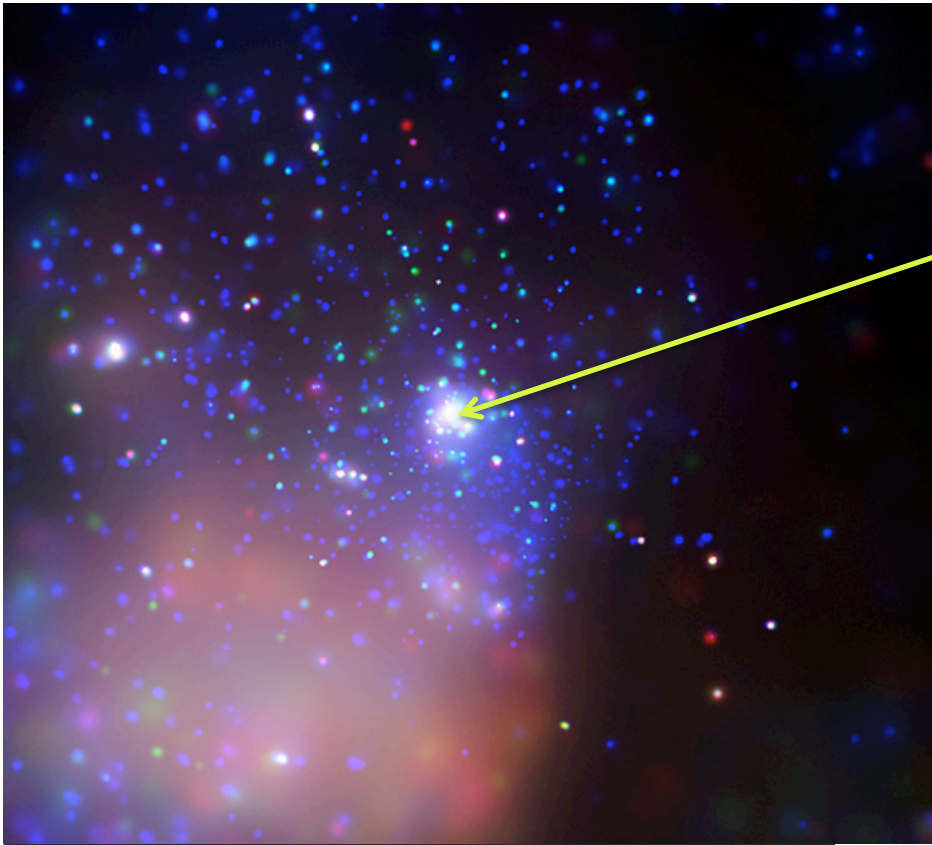
Lagoon Nebula/M8: Barba, Morrell

g Sgr (O₄ V): τ_* values



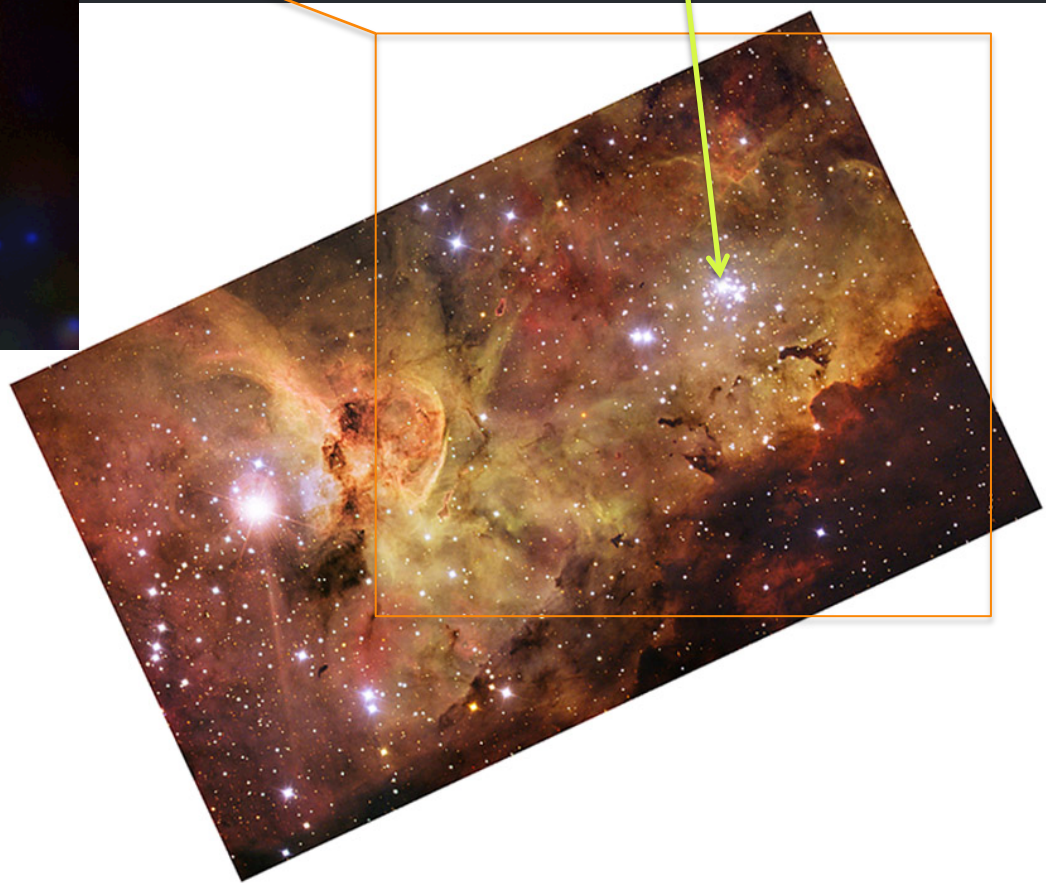
9 Sgr (O₄ V): R_o values





HD 93129A (O2If*)
is the 2nd brightest
X-ray source in Tr 14

Tr 14: Chandra



HD93129A – O2 If*

Extremely massive ($120 M_{\text{sun}}$), luminous O star
($10^{6.1} L_{\text{sun}}$)

Strongest wind of any Galactic O star
($2 \times 10^{-5} M_{\text{sun}}/\text{yr}$; $v_{\text{inf}} = 3200 \text{ km/s}$)

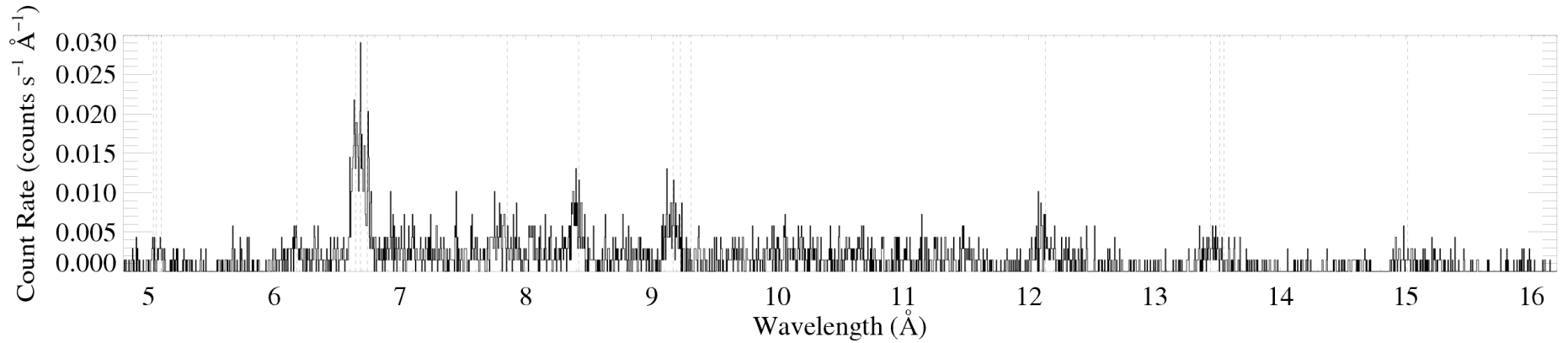
From H-alpha, assuming a
smooth wind



There is an O_{3.5} companion with a
separation of ~100 AU

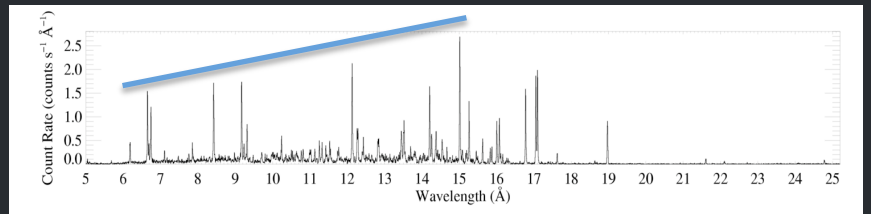
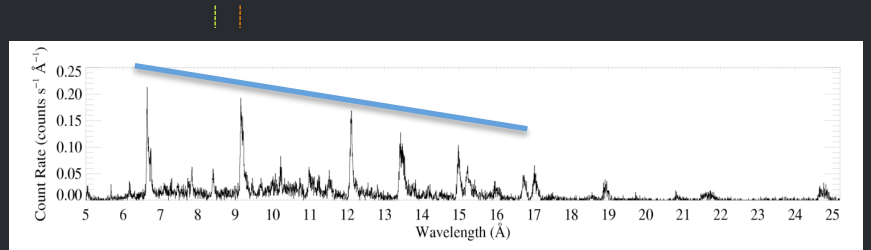
But the vast majority of the X-rays come
from embedded wind shocks in the O₂If*
primary

Its X-ray spectrum is hard



Si XIV Si XIII Mg XII Mg XI

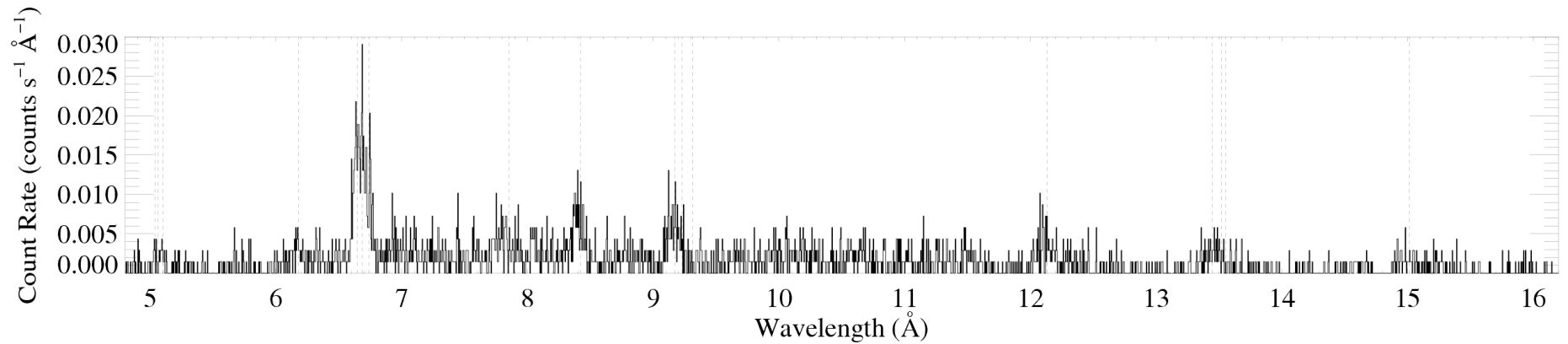
H-like vs. He-like



Its X-ray spectrum is hard

Si

Mg



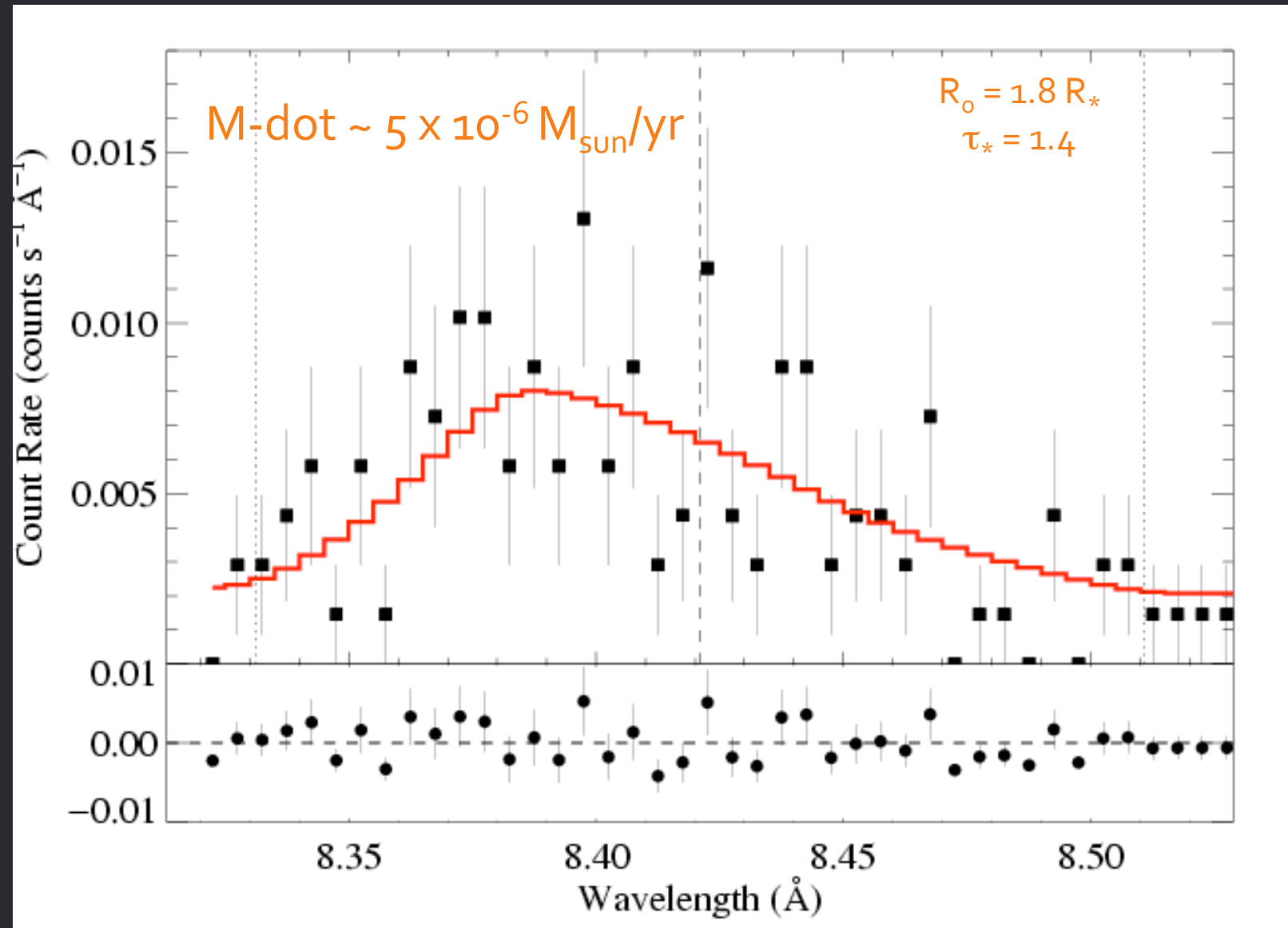
low H/He

But the plasma **temperature is low:**
little plasma with $kT > 8$ million K

$\dot{M} \sim 2 \times 10^{-5} M_{\text{sun}}/\text{yr}$ from unclumped $\text{H}\alpha$

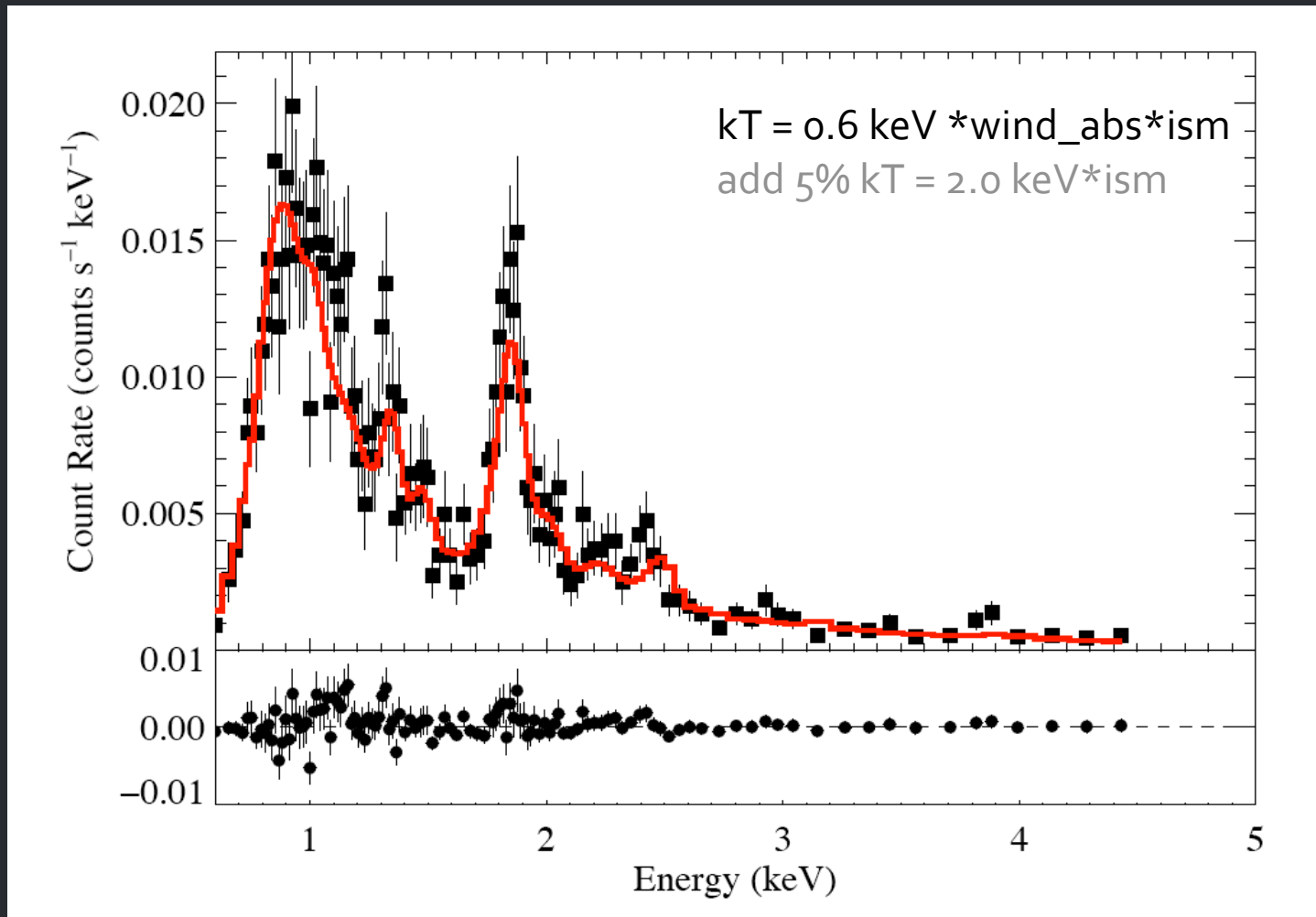
HD 93129A (O₂ If*): Mg XII Ly α 8.42 Å

$V_{\text{inf}} \sim 3200 \text{ km/s}$



Low-resolution *Chandra* CCD spectrum of HD93129A

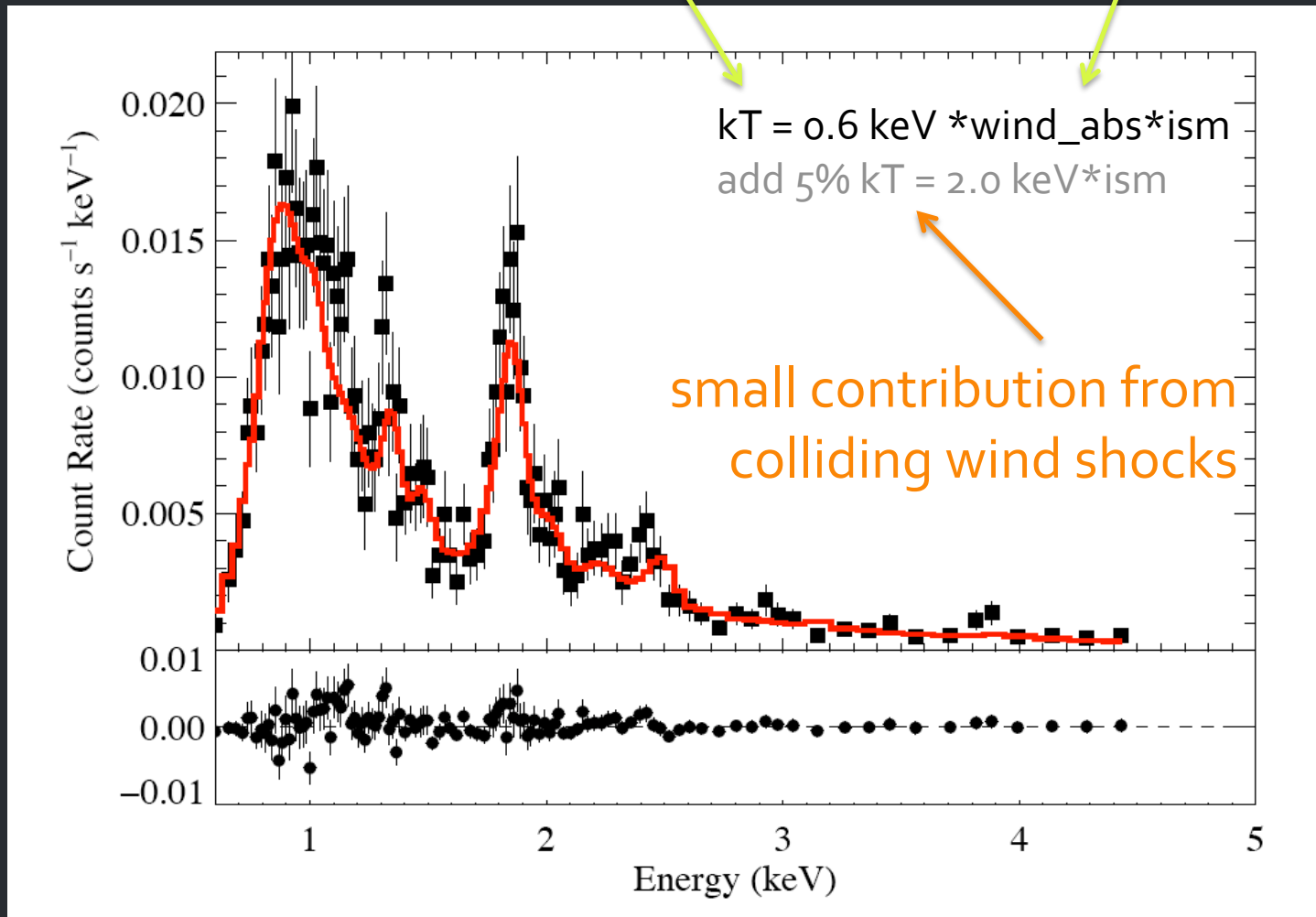
Fit: thermal emission with wind + ISM absorption
plus a second thermal component with just ISM



consistent with result
from line profile fitting

→ $\tau_*/\kappa = 0.03$ (corresp. $\sim 5 \times 10^{-6} M_{\text{sun}}/\text{yr}$)

Typical of O stars like ζ Pup



Approximations and assumptions

Extensively discussed in Cohen et al. 2010

Biggest factors:

β

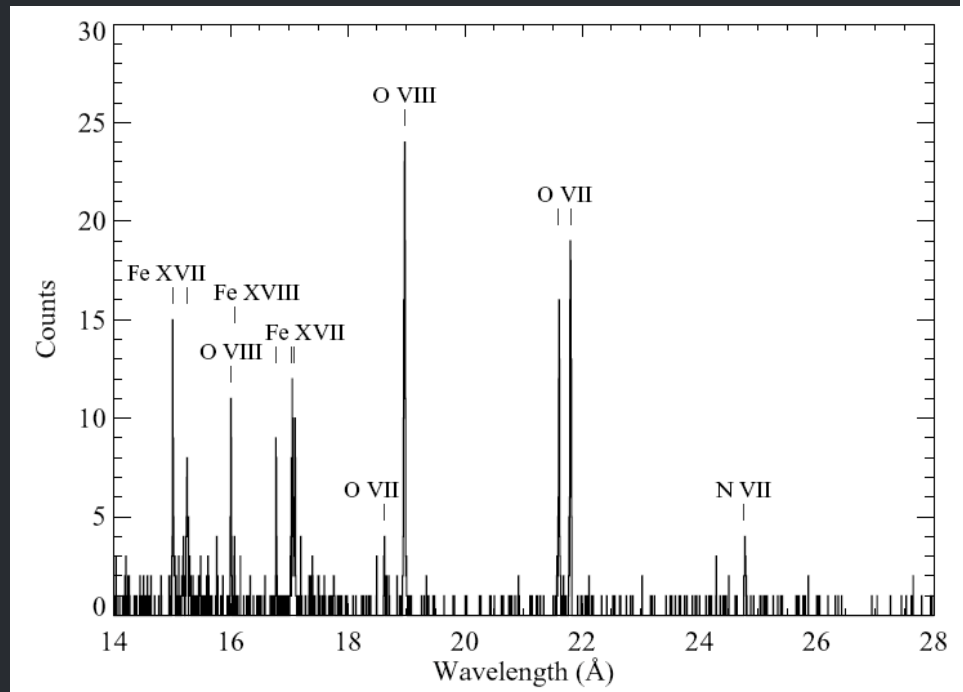
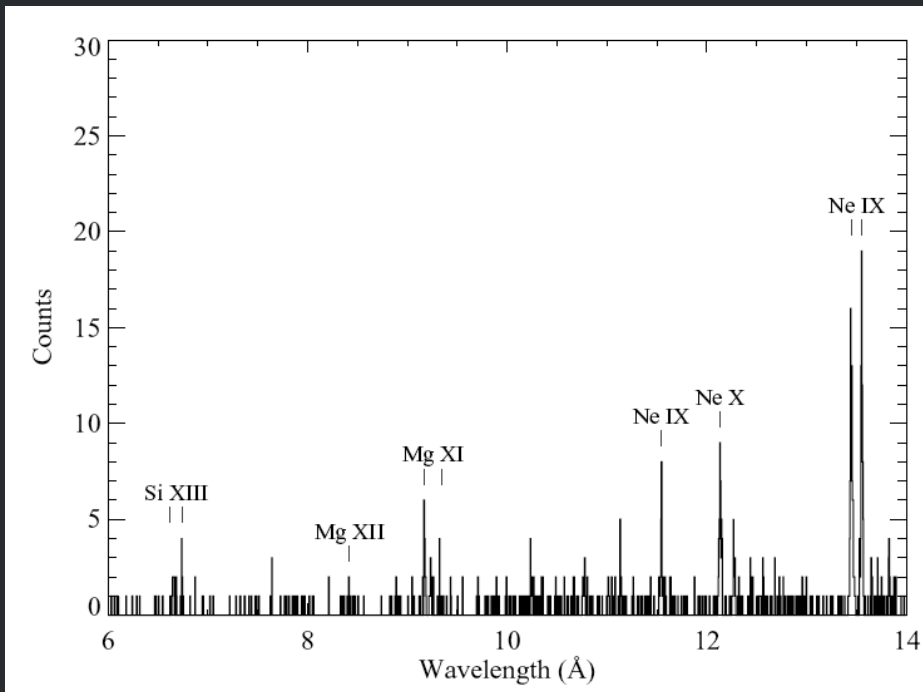
V_{inf}

opacity (due to unc. in metallicity)

Early B (V – III) stars with weak winds

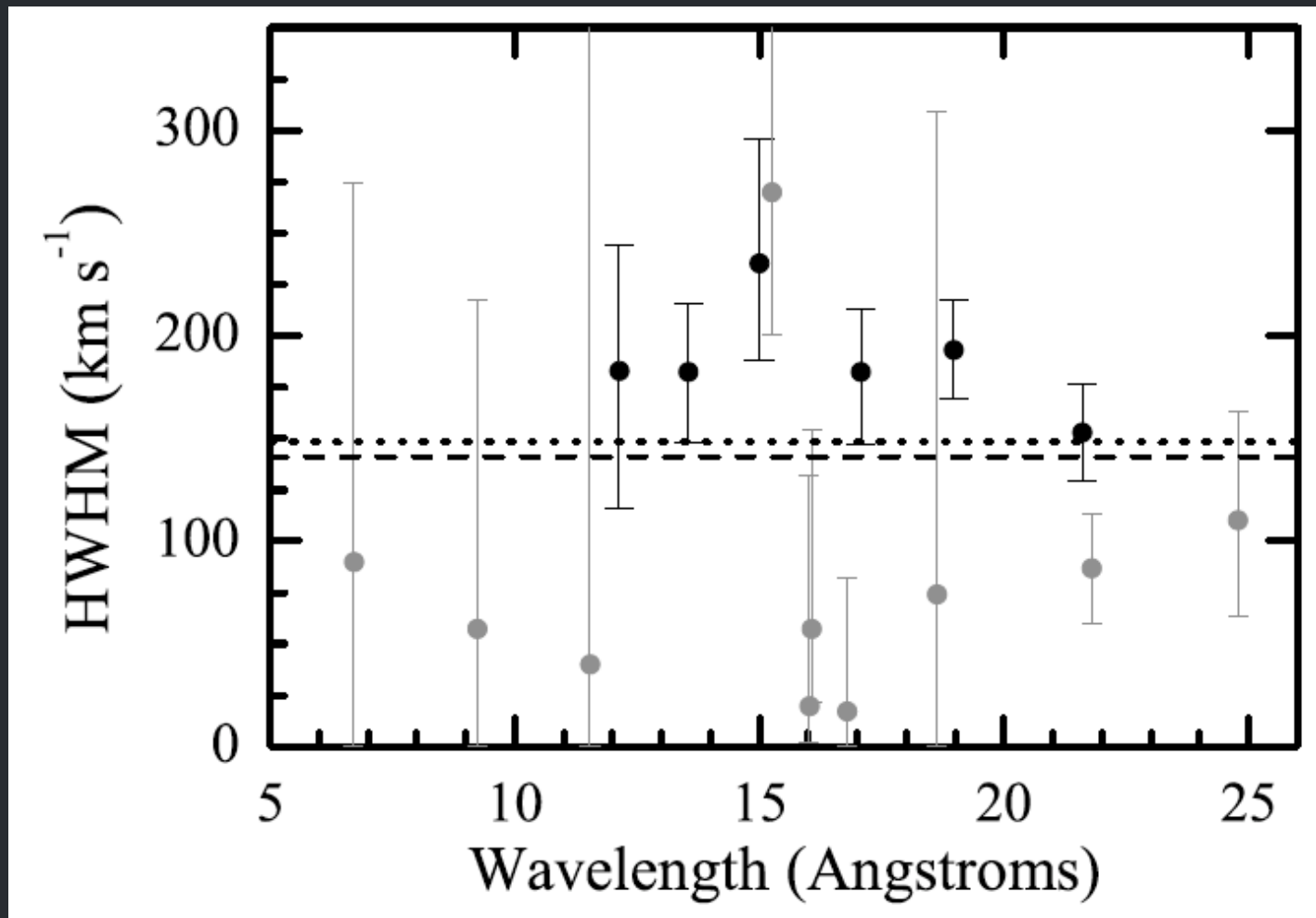
X-ray flux levels in many B star are high considering their low mass-loss rates (known since *ROSAT* in the 1990s)

Chandra spectroscopy of β Cru (B 0.5 III)



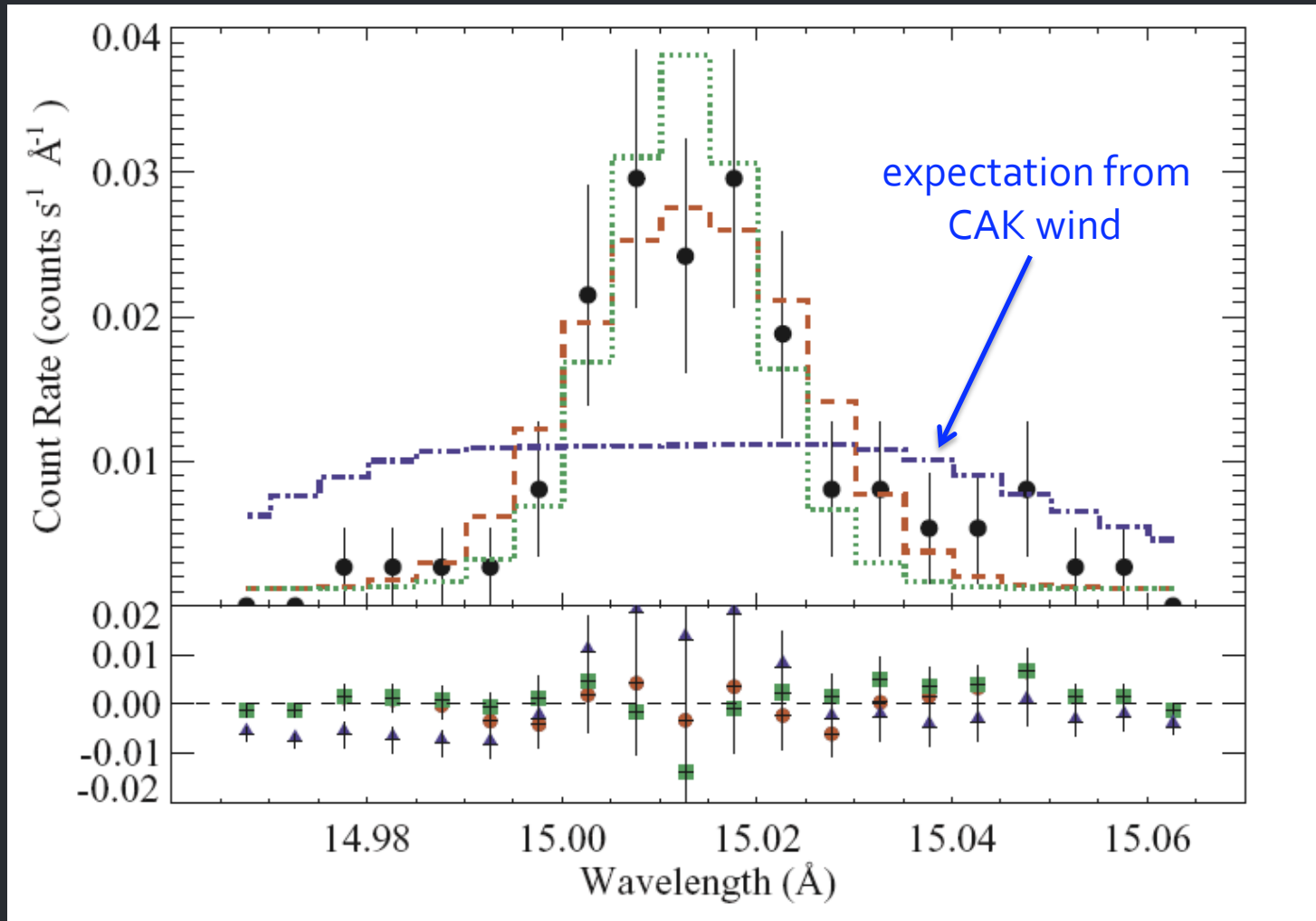
X-ray lines are narrow

HWHM ~ 150 km/s on average



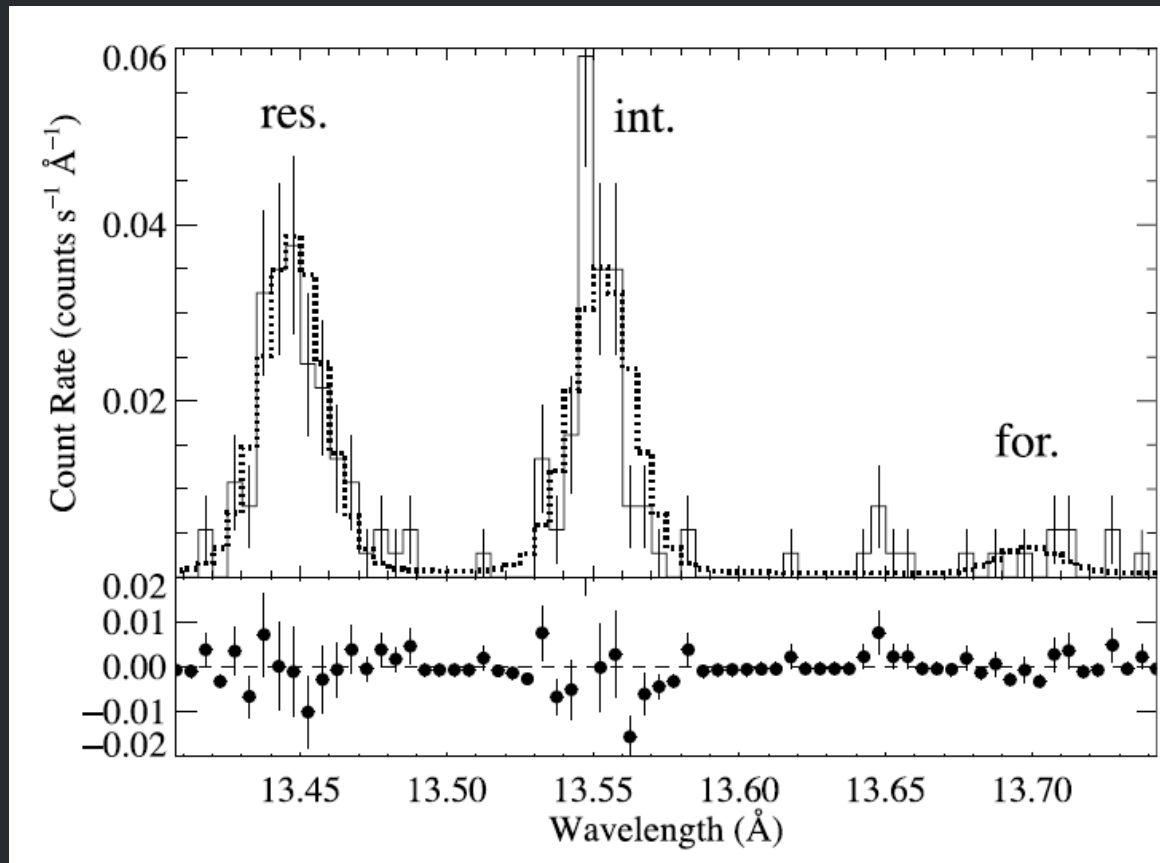
Much narrower than expected...

From the bulk CAK wind

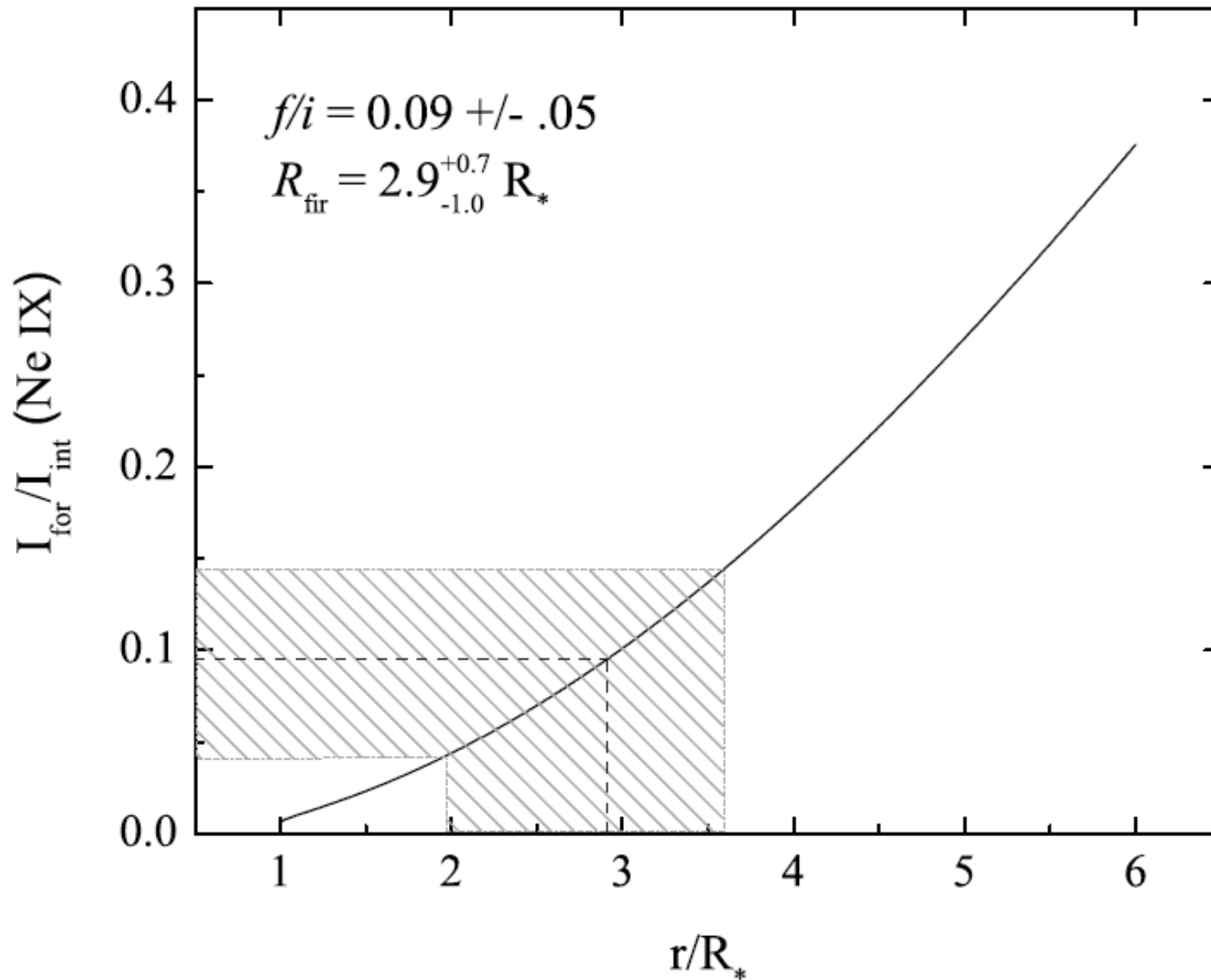


Hot plasma is located in the wind

He-like ions' forbidden-to-intercombination line ratios indicate location



At least $1 R_*$ above the photosphere



B star X-rays are very hard to explain

Lines are not broad

But X-ray plasma is well out in the wind flow

X-ray emission measure requires a substantial fraction of the wind to be hot ($> 10^6$ K)

Conclusions

Single O stars – like ζ Pup – X-ray line shapes are consistent with kinematics from shock models

And profiles can be used as a clumping-independent mass-loss rate diagnostics

Results are consistent with factor of 3 to 6 reduction over $H\alpha$ determinations that assume a smooth wind

Conclusions, pt. 2

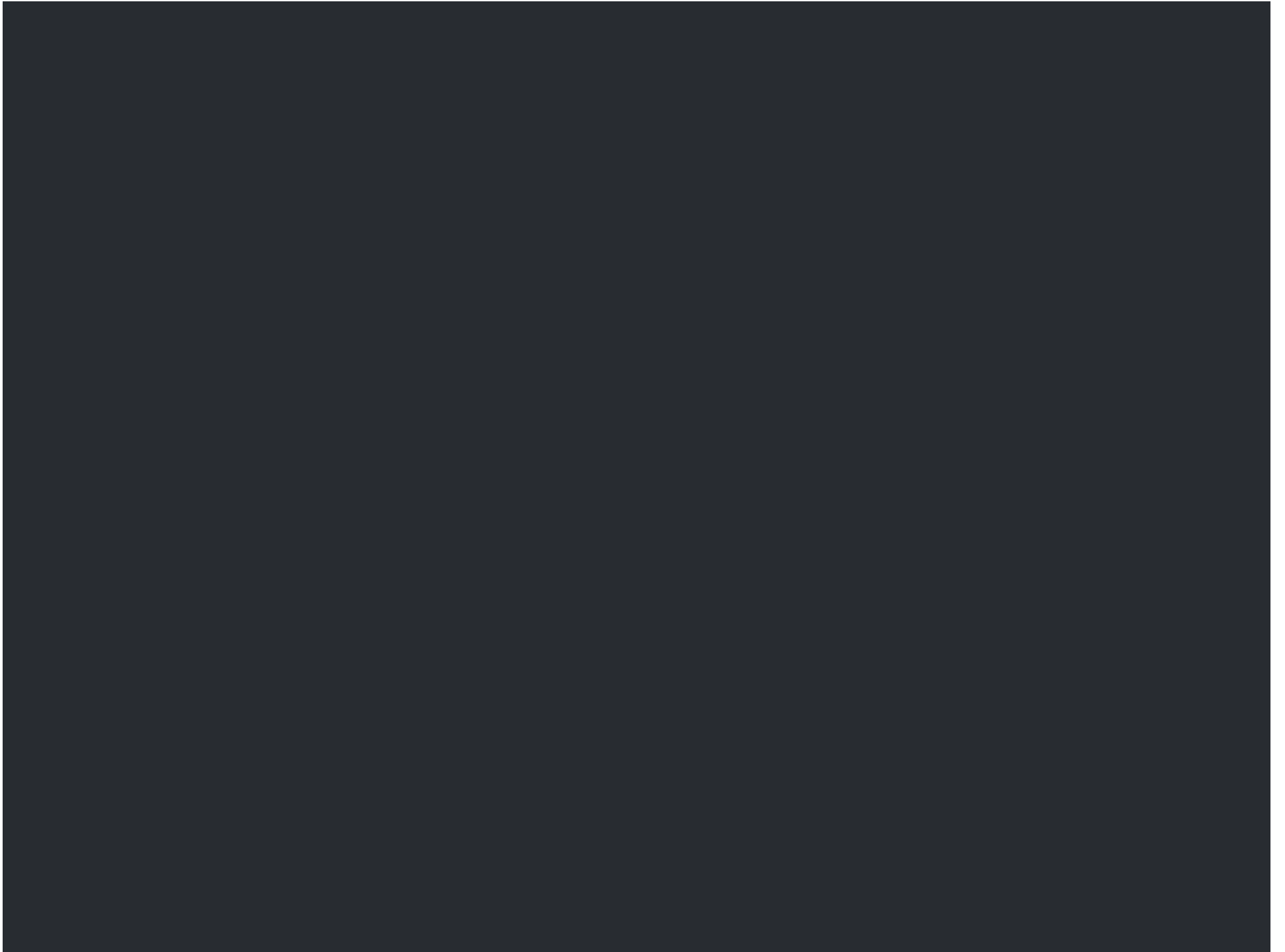
Broadband wind absorption is measurable

It can significantly harden the observed spectra

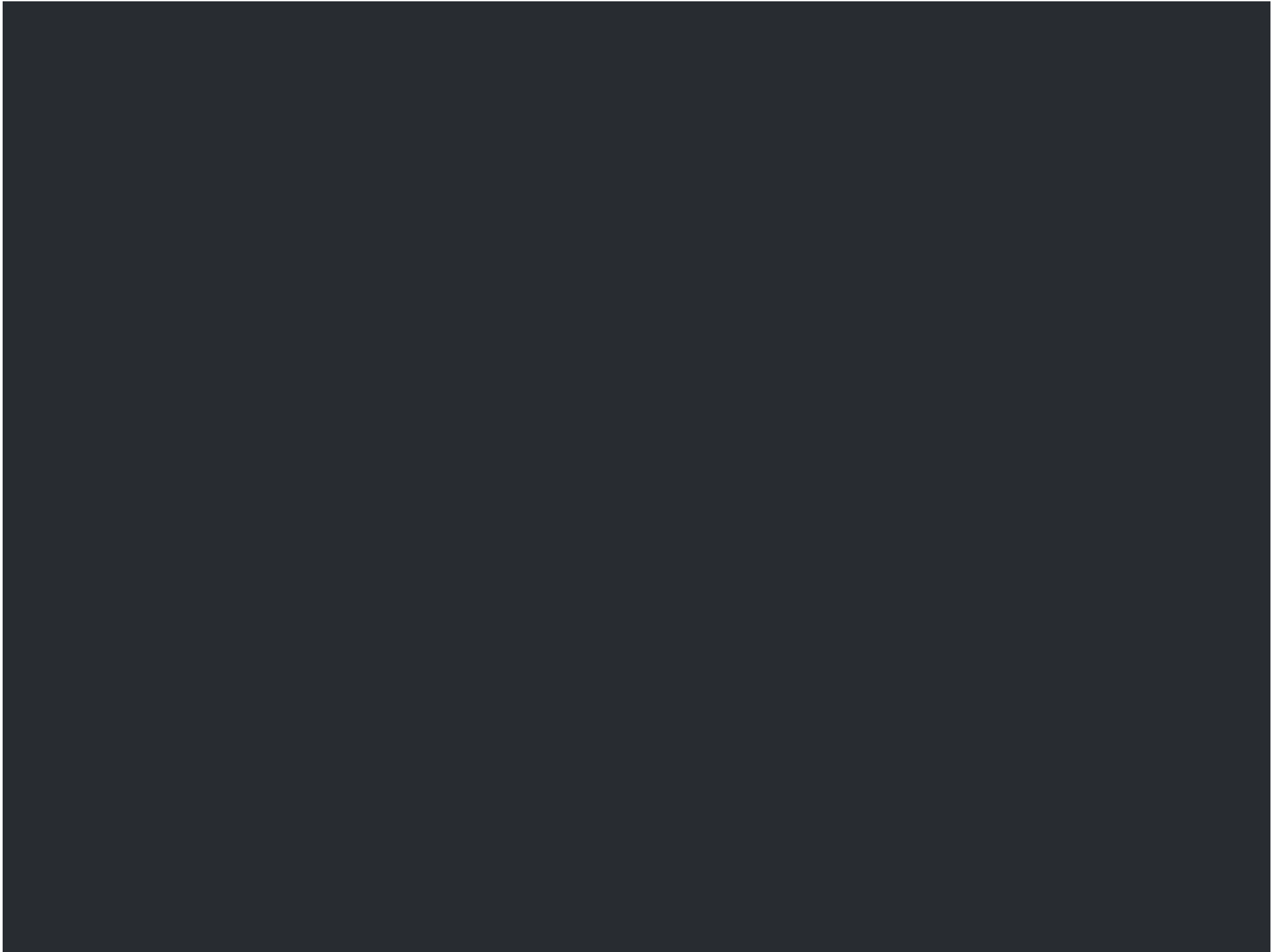
And it, too, is consistent with factor of 3 to 6
reduction over $H\alpha$ determinations that assume a
smooth wind

Even extreme O star winds like HD 93129A's are
consistent with these results

It's the early B star winds that are hard to understand



Extra Slides



Caveats, reflections

Why did it take so long to identify the wavelength trend?

Realistic opacity model

Resonance scattering

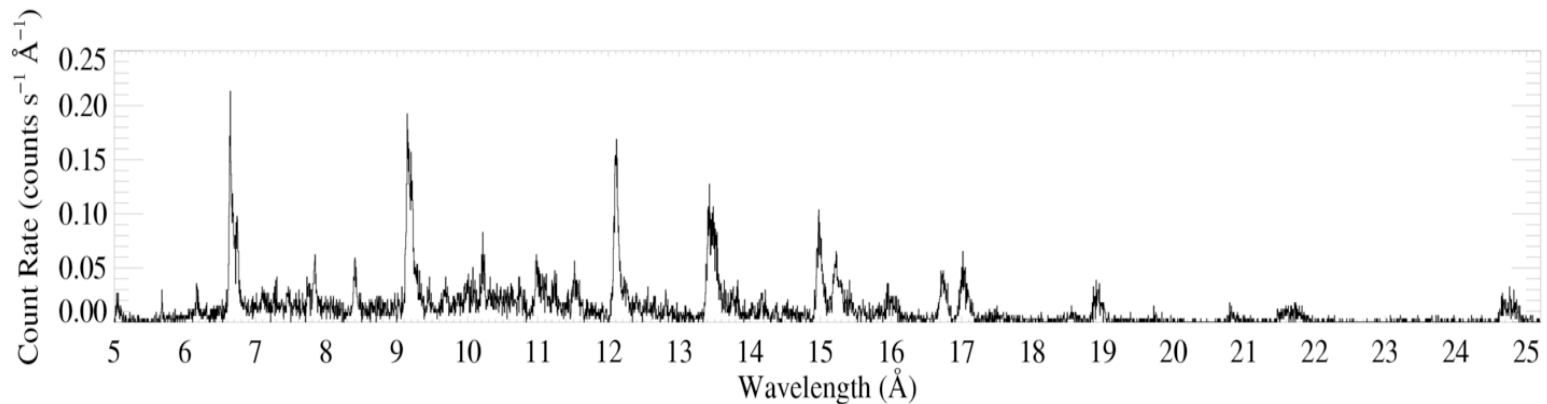
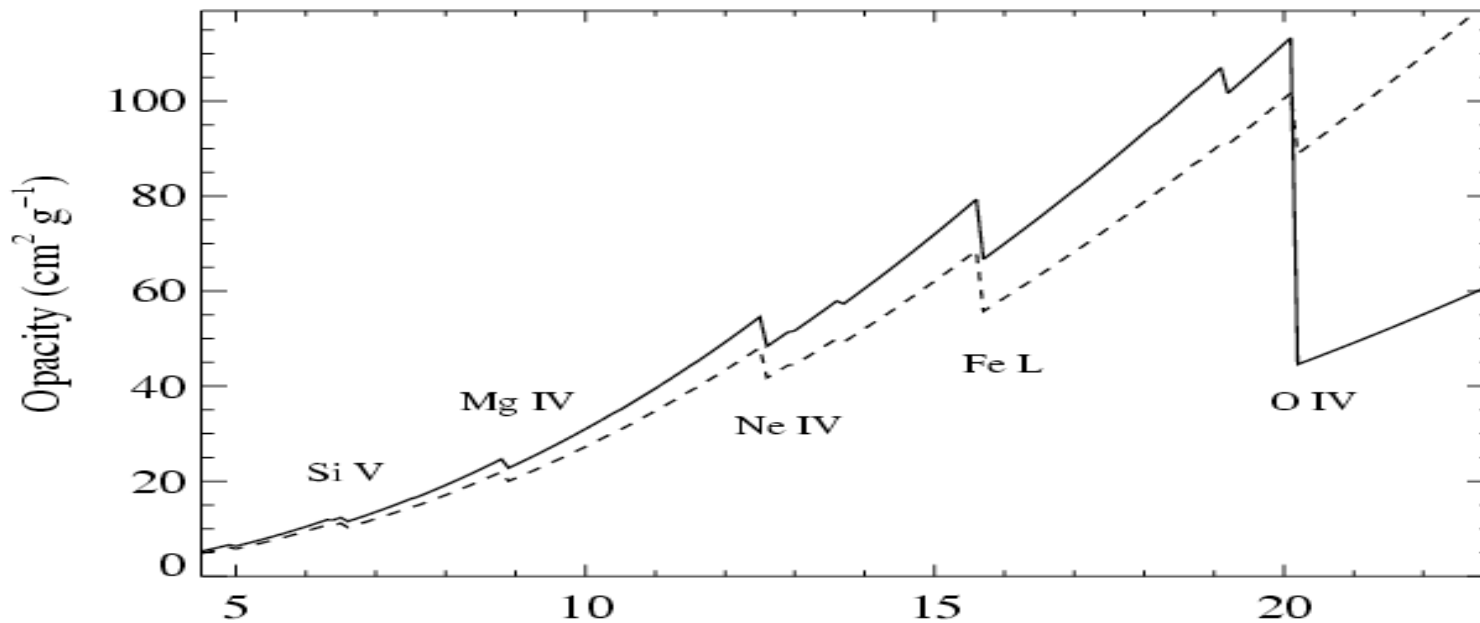
Porosity and clumping

Which lines are analyzed?

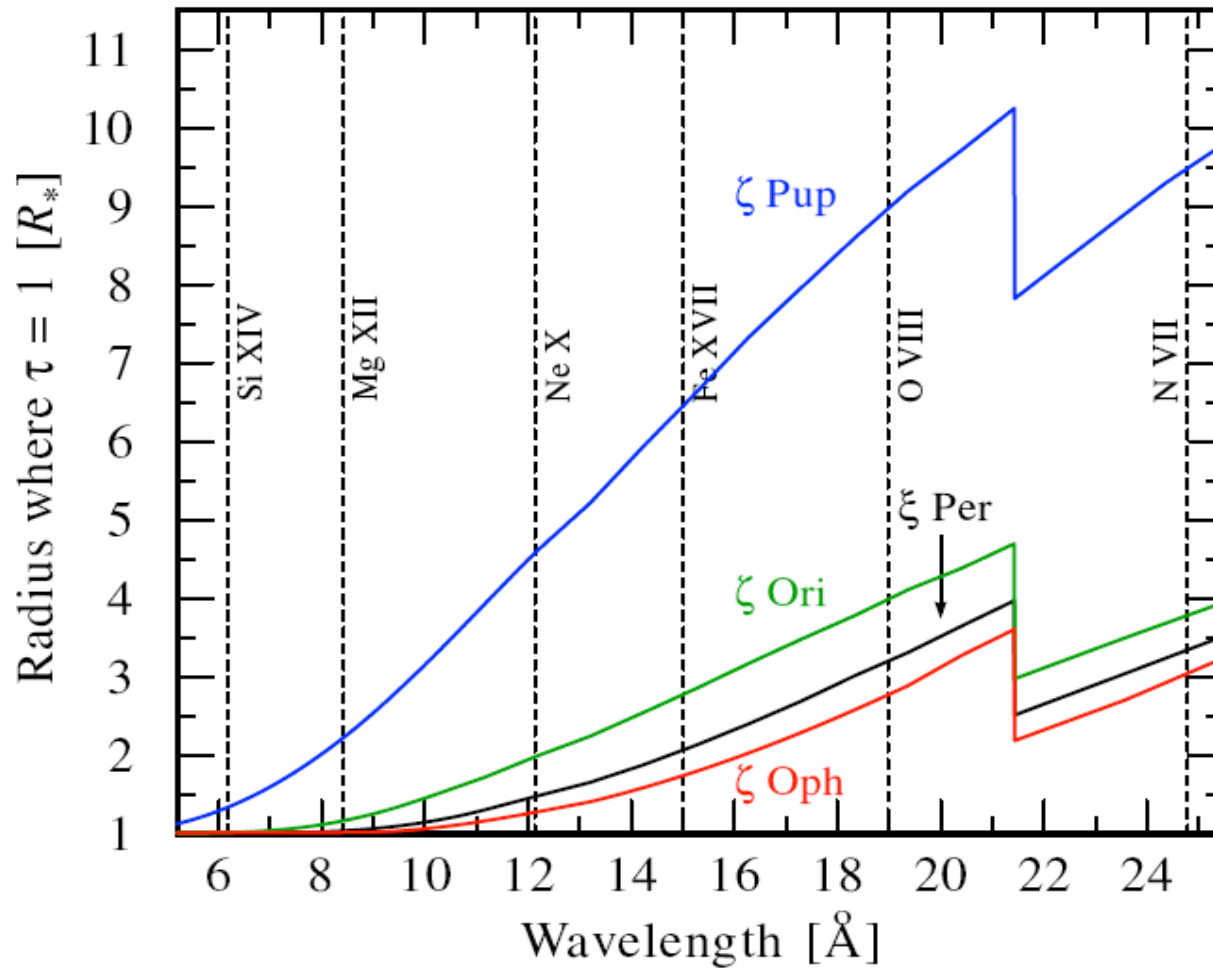
There are 21 complexes in the *Chandra* spectrum;
we had to exclude 5 due to blending

The short wavelength lines have low S/N, but are
very important – leverage on wavelength-
dependence of opacity

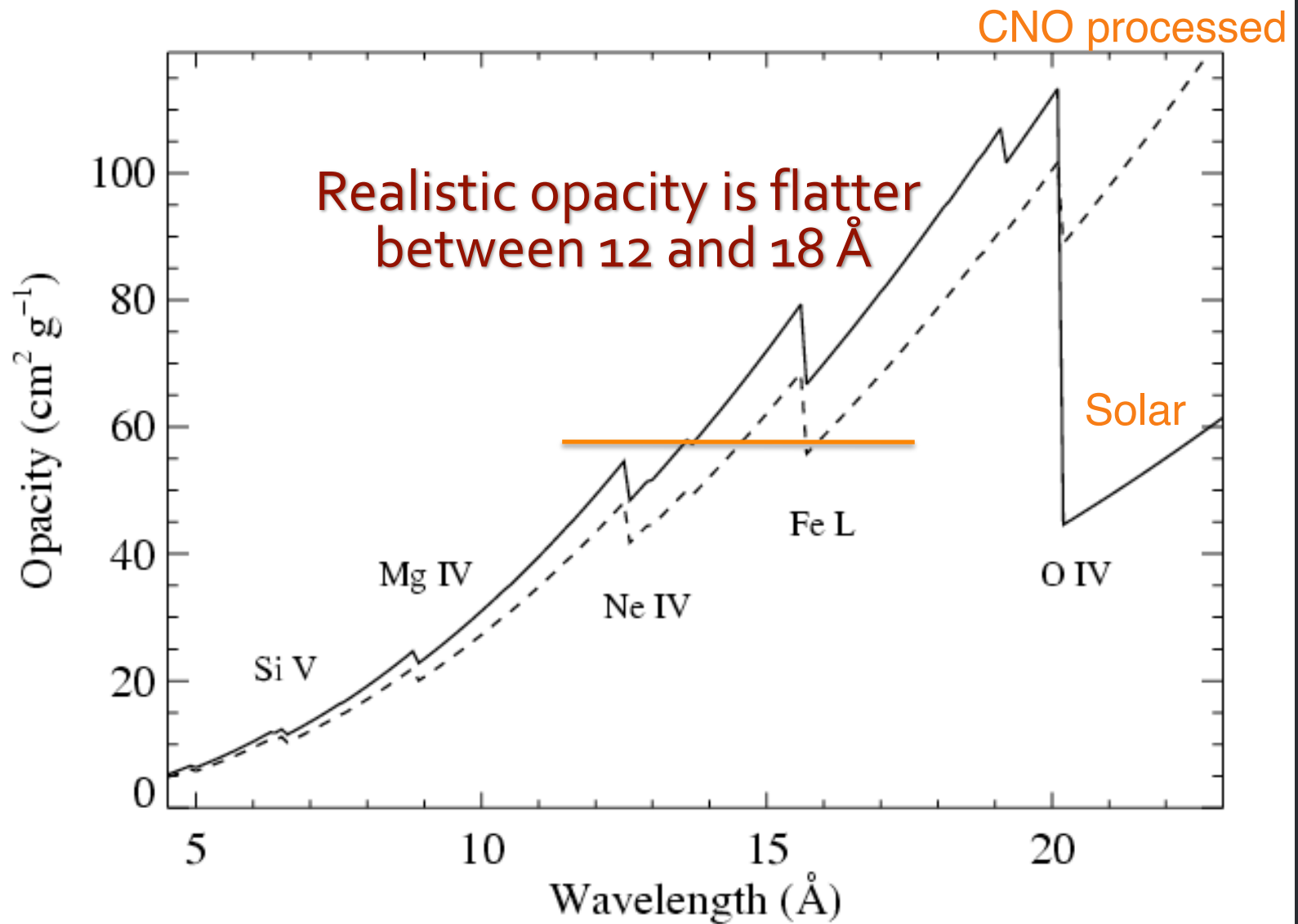
Seven short wavelength lines never before analyzed



Simplified opacity models are too steep



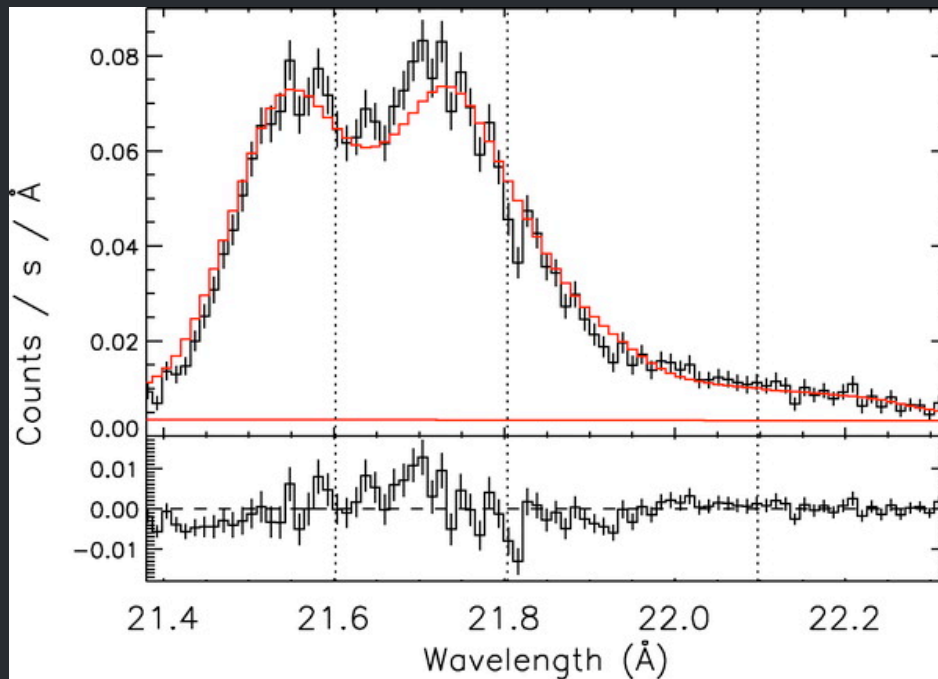
Detailed opacity model is important



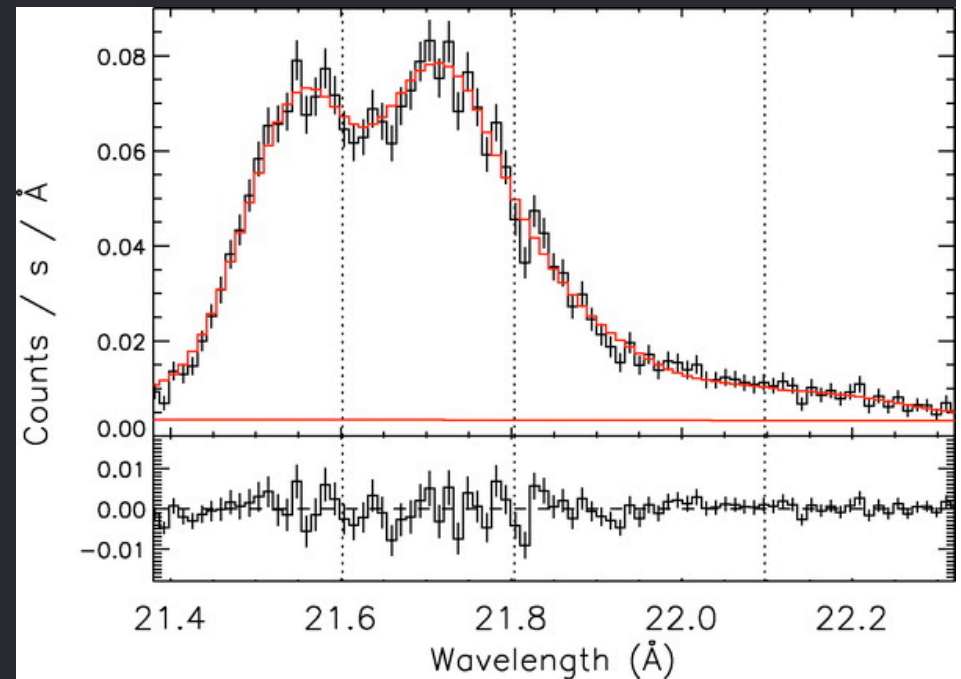
Resonance Scattering

A few lines may be subject to resonance scattering: Evidence in XMM spectrum for O VII:

no res. scatt.

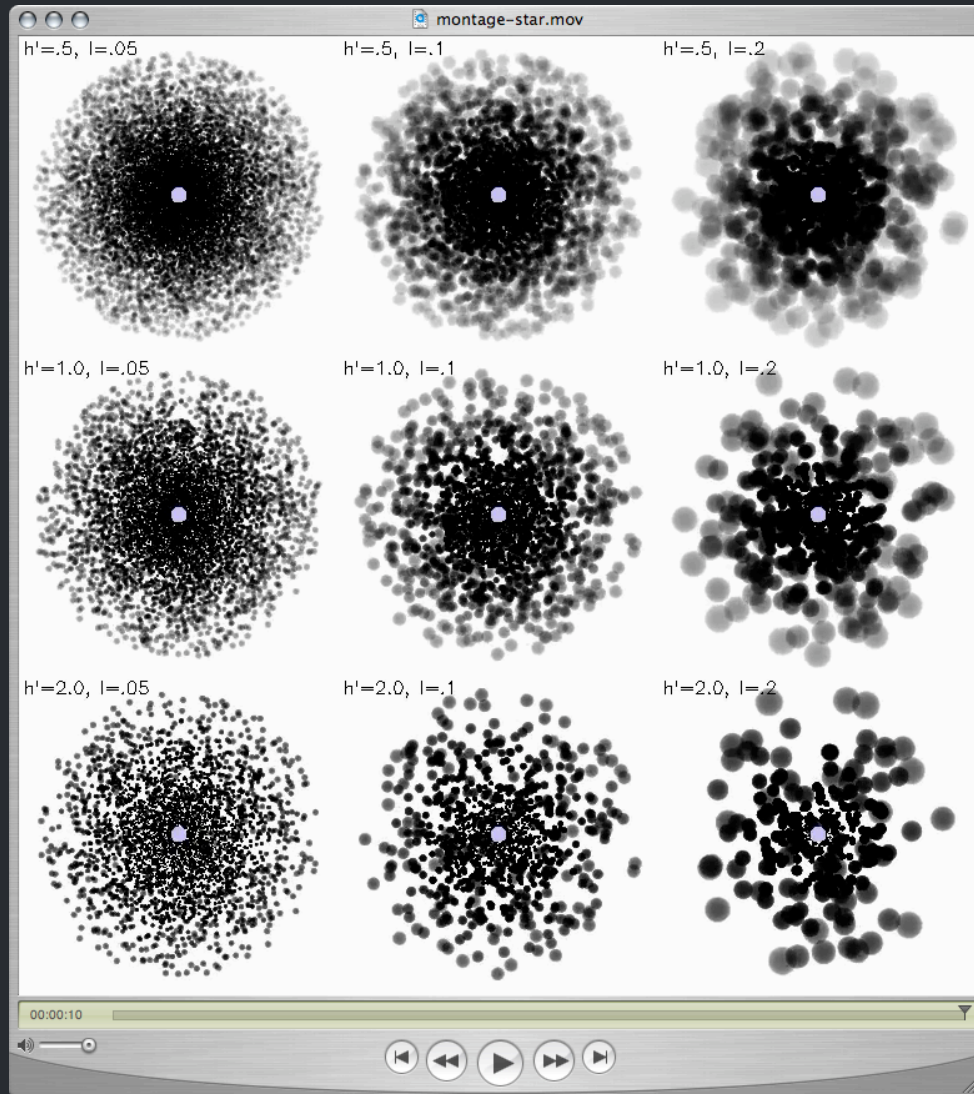


with res. scatt.



What about **porosity**?

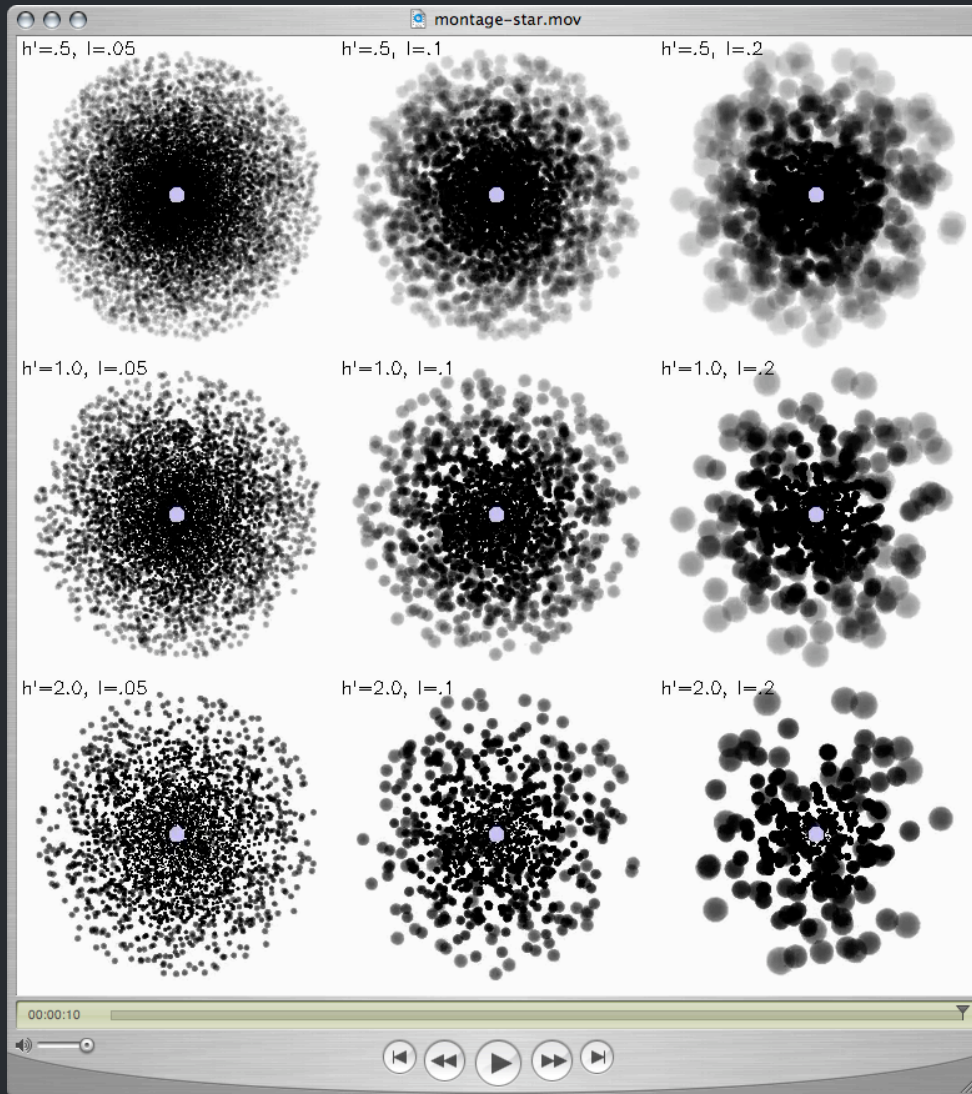
“Clumping” – or micro-clumping: affects density-squared diagnostics; *independent of clump size*, just depends on clump density contrast (or filling factor, f)



visualization: R. Townsend

But **porosity** is associated with optically thick clumps, it acts to reduce the effective opacity of the wind; it *does* depend on the size scale of the clumps

Note: whether clumps meet this criterion depends both on the clump properties and on the atomic process/cross-section under consideration



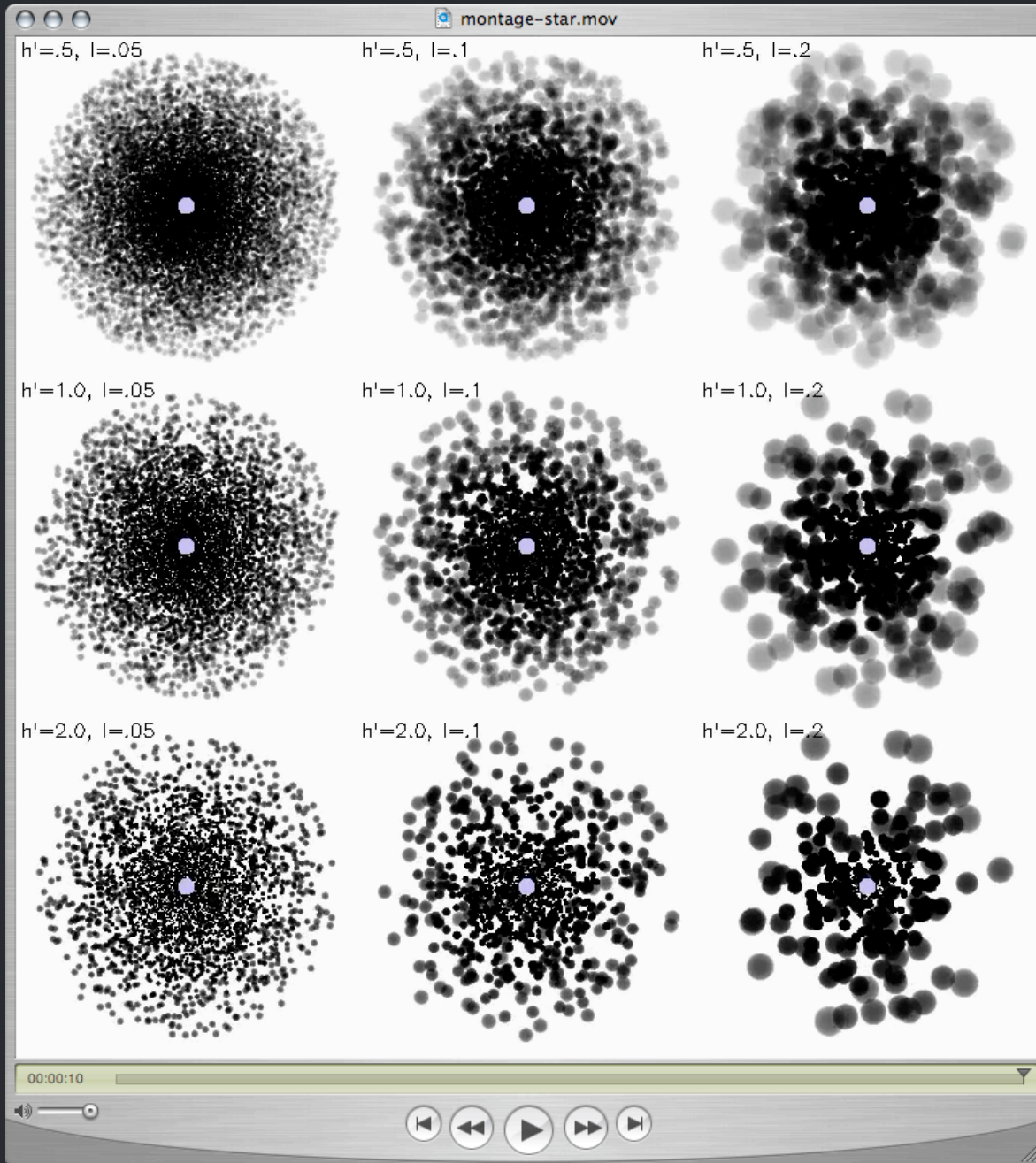
The key parameter is the **porosity length**,
 $h = (L^3/f^2) = \ell/f$



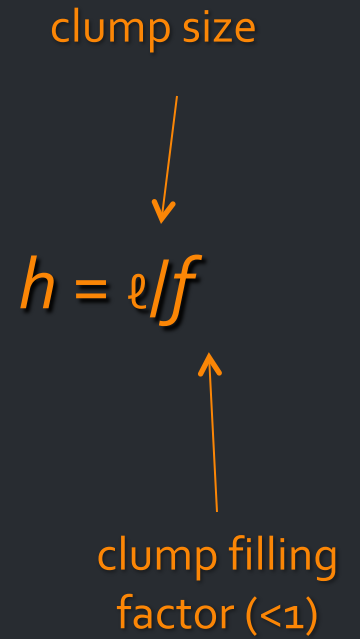
$$f = \ell^3/L^3$$

Clump size increasing →

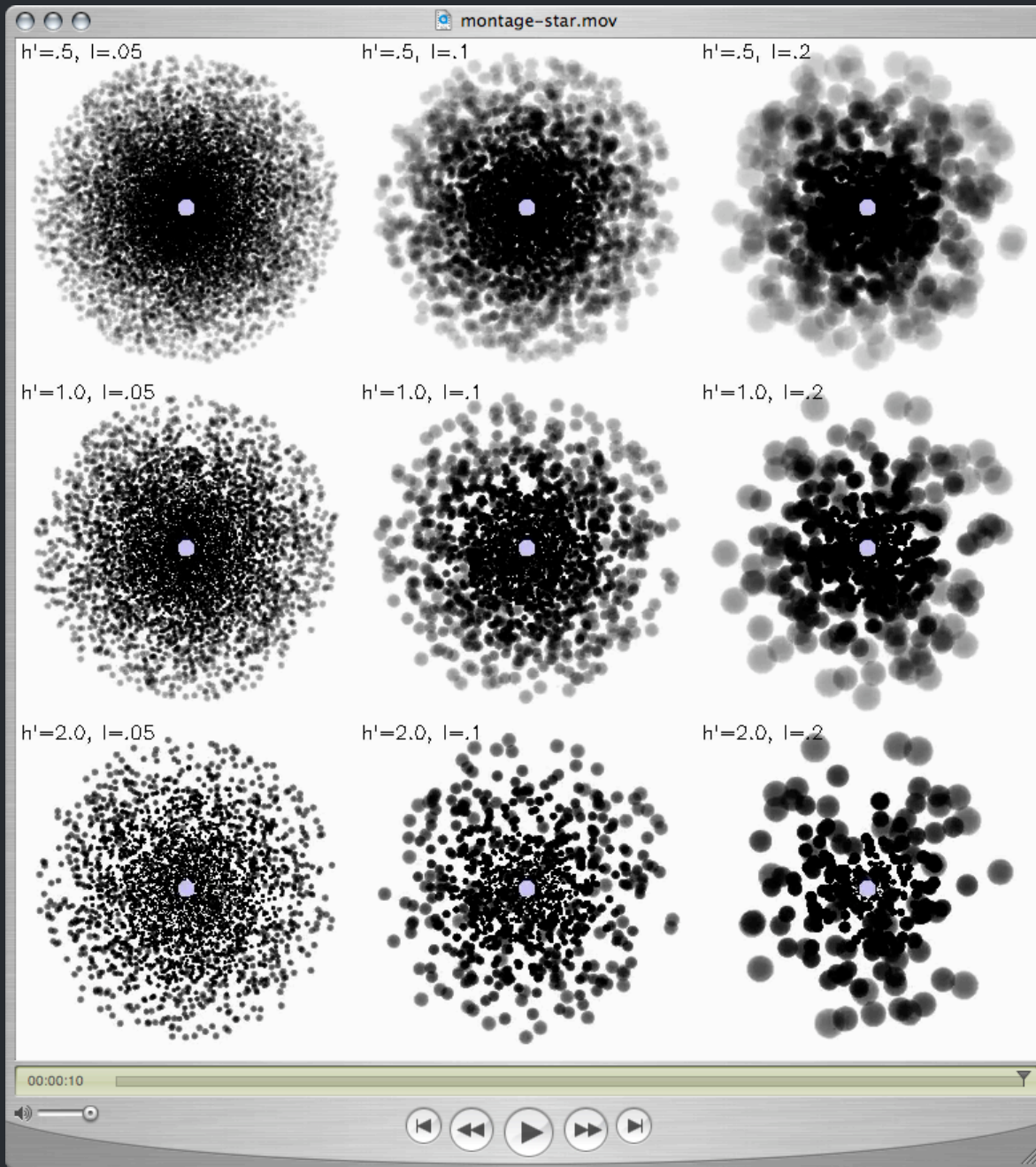
The porosity length, h :



Porosity length increasing →



Clump size increasing →



No Porosity

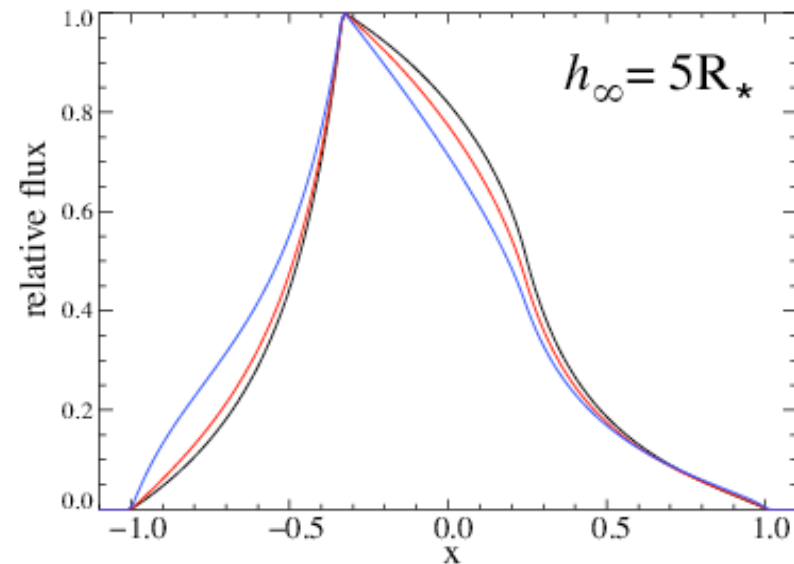
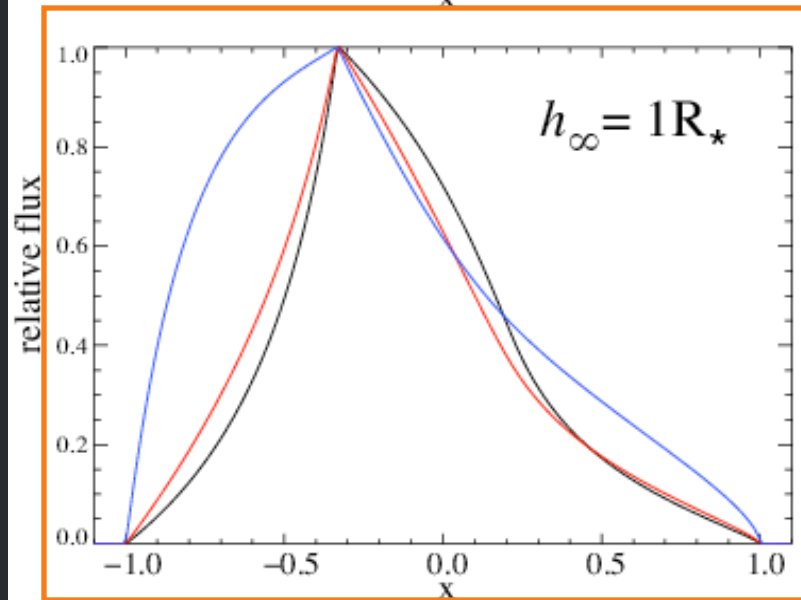
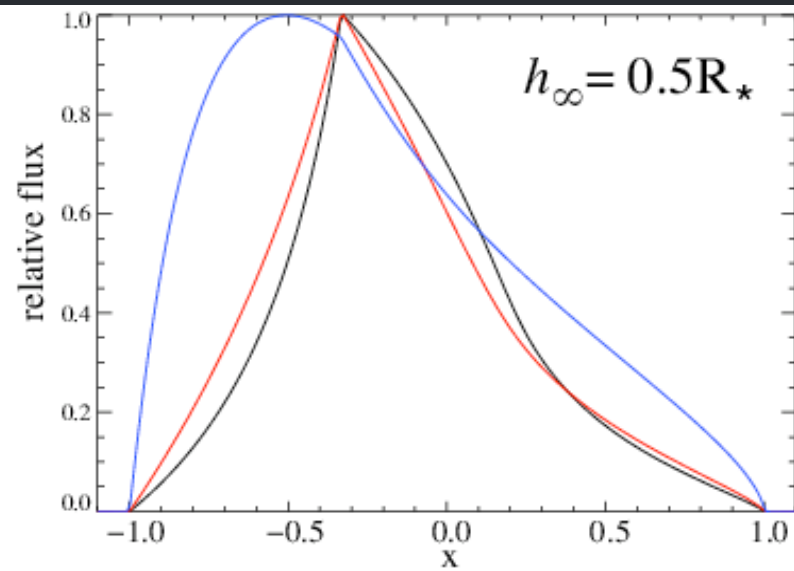
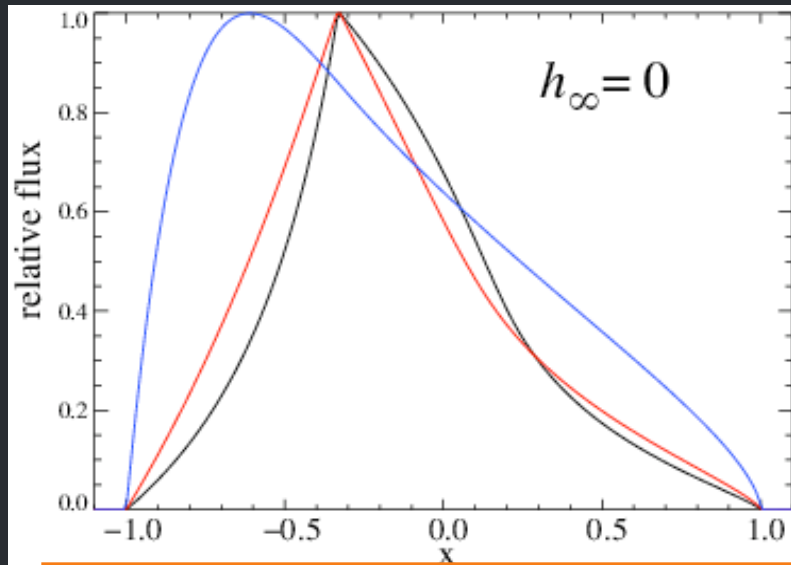


Porosity length increasing →

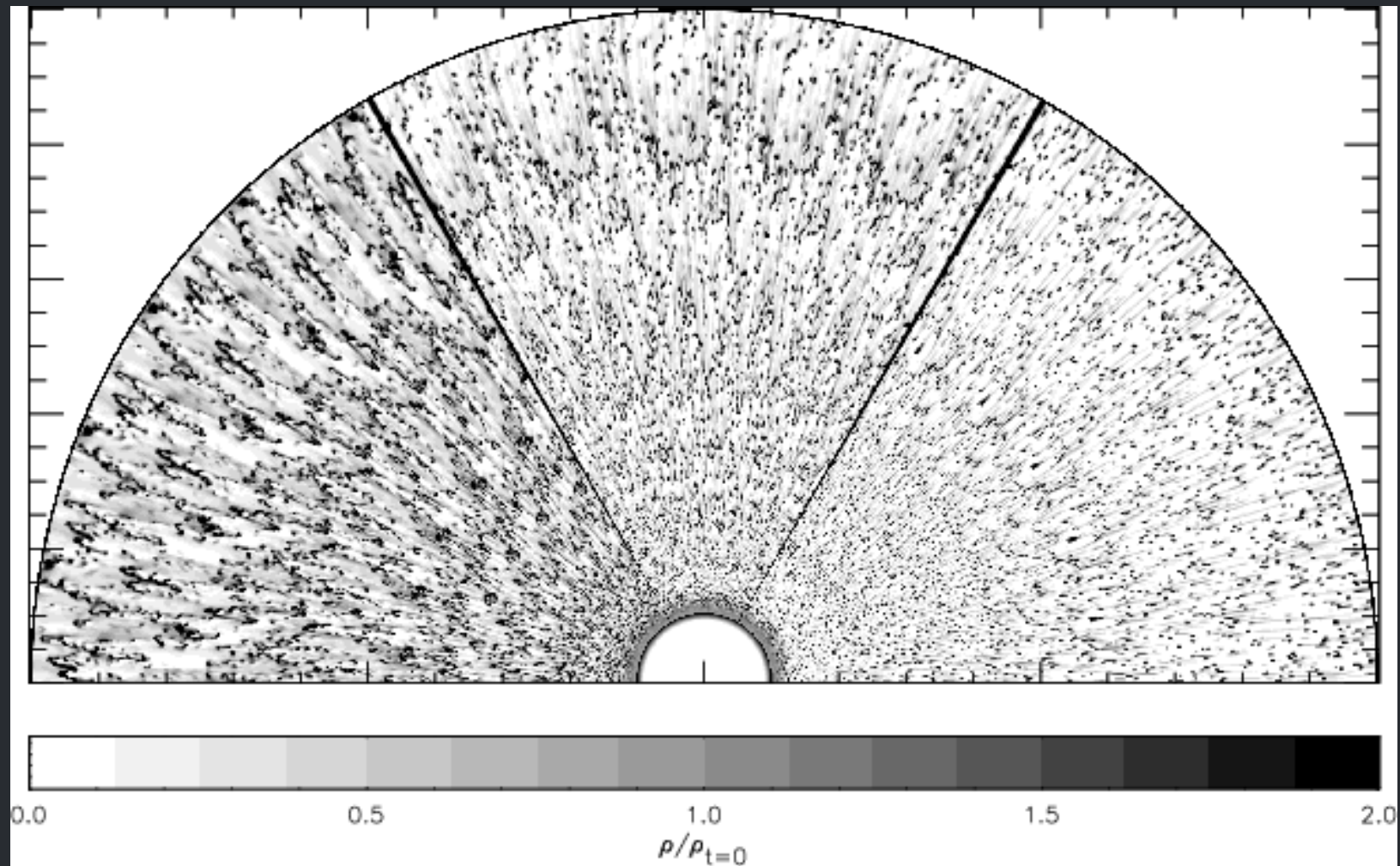
Porous wind



Porosity only affects line profiles if the porosity length (h) exceeds the stellar radius



The clumping in 2-D simulations (density shown below)
is on quite *small scales*



No expectation of porosity from simulations

Natural explanation of line profiles without invoking porosity

Finally, to have porosity, you need clumping in the first place, and once you have clumping... you have your factor ~ 3 reduction in the mass-loss rate

No expectation of porosity from simulations

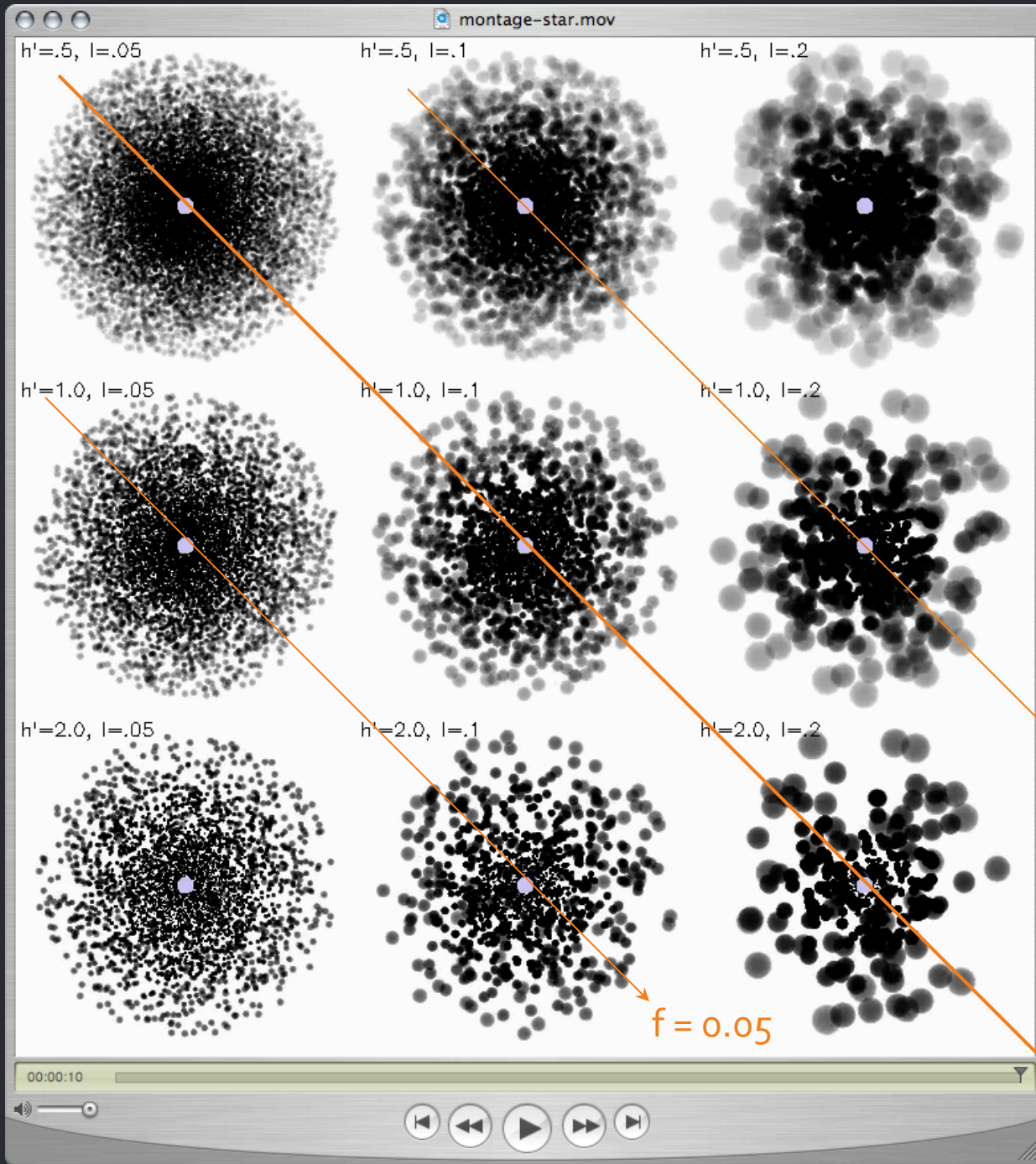
Natural explanation of line profiles without
invoking porosity

Finally, to have porosity, you need clumping in
the first place, and once you have clumping...
you have your factor ~ 3 reduction in the mass-
loss rate

No expectation of porosity from simulations

Natural explanation of line profiles without
invoking porosity

Finally, to have porosity, you need clumping in
the first place, and once you have clumping...
you have your factor ~ 3 reduction in the mass-
loss rate
(for ζ Pup, anyway)

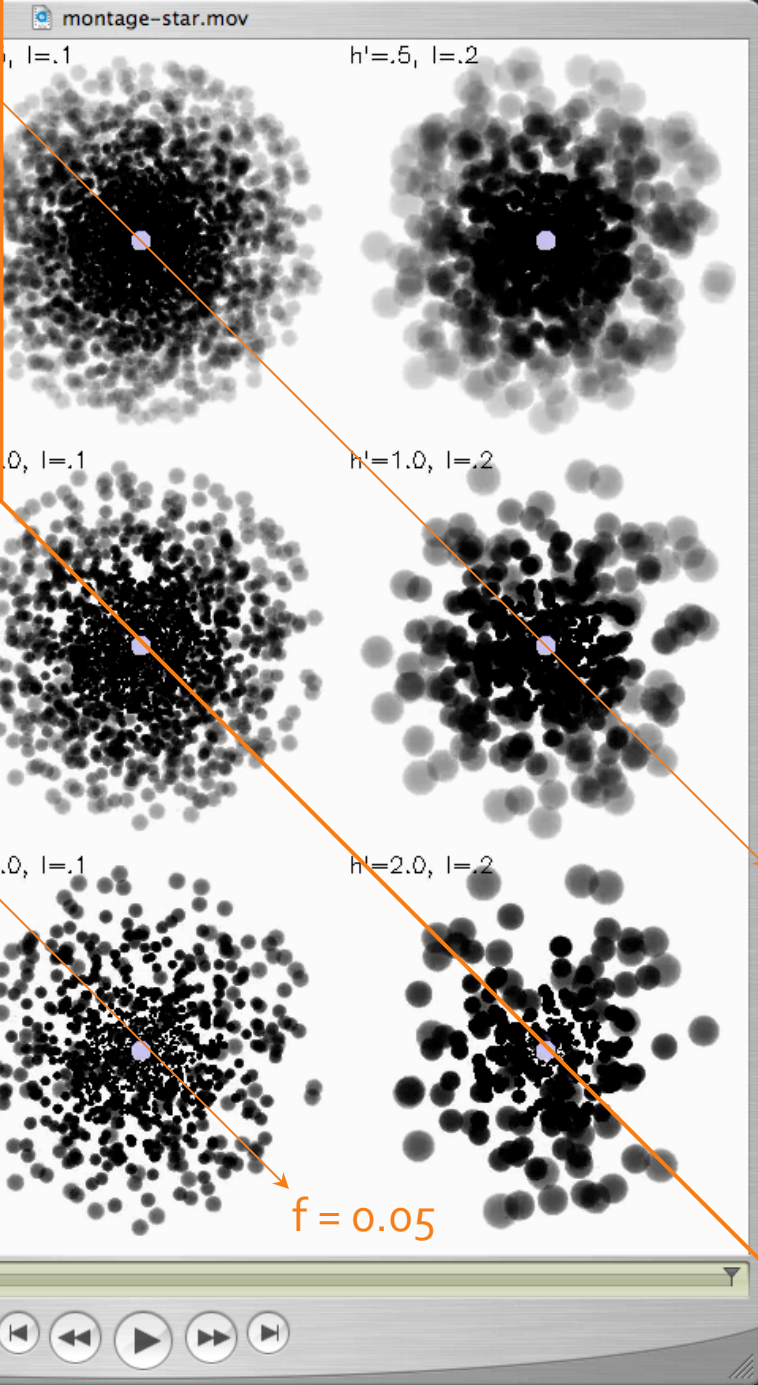
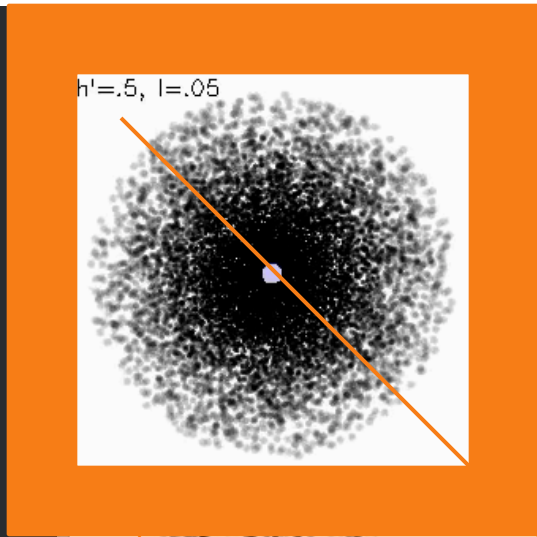


$f \sim 0.1$ is indicated
by $H\alpha$, UV, radio
free-free analysis

$f = 0.2$

$f = 0.05$

$f = 0.1$



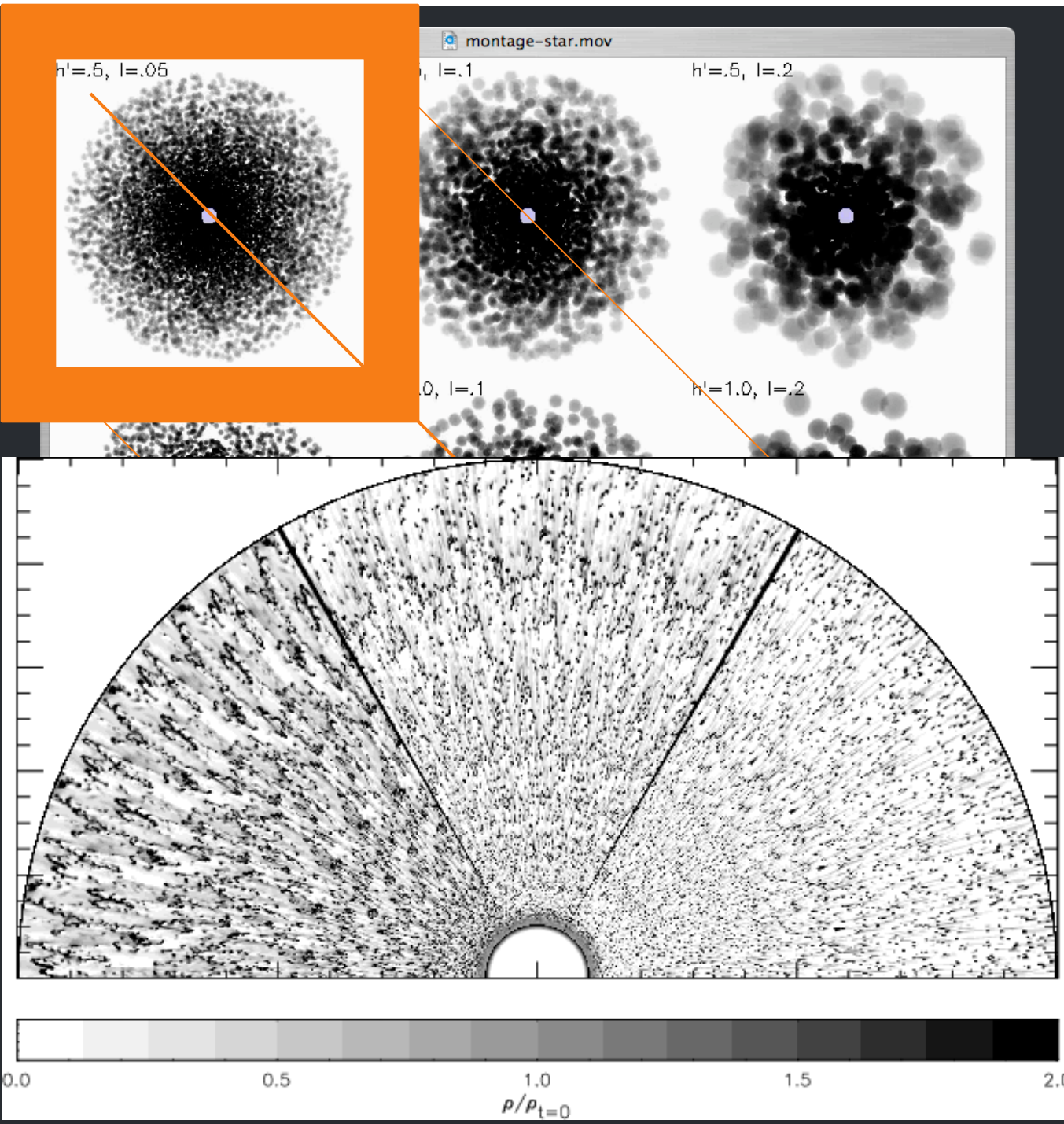
And lack of evidence for porosity... leads us to suggest visualization in upper left is closest to reality

f = 0.2

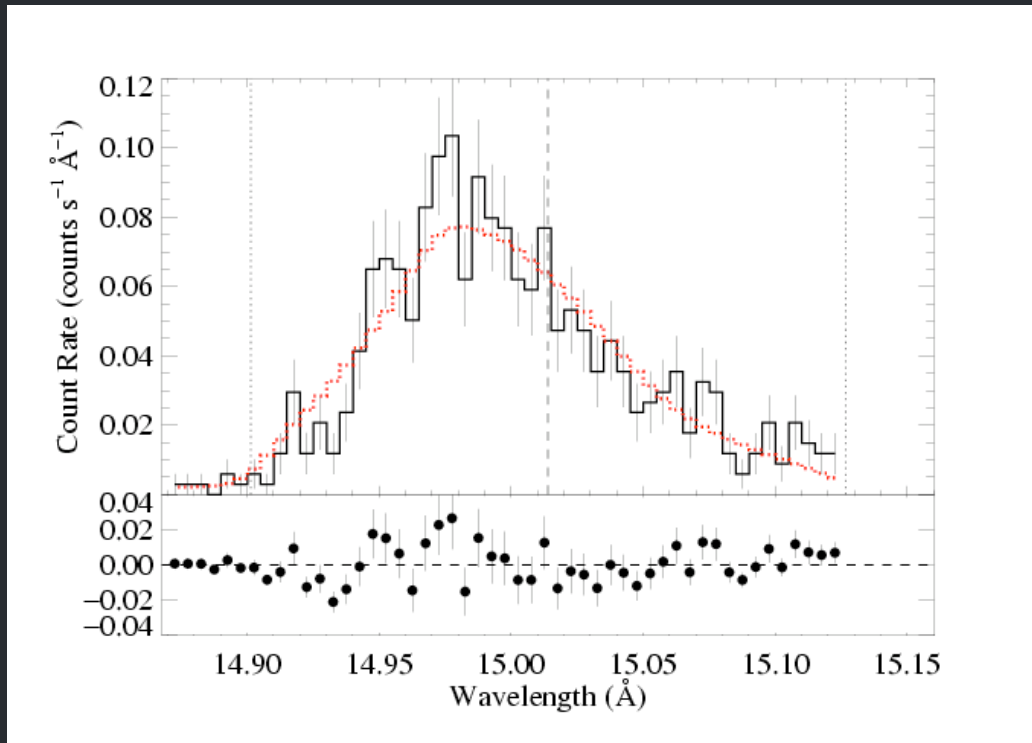
f = 0.05

f = 0.1

Though simulations suggest even smaller-scale clumping



Incidentally, you can fit the *Chandra* line profiles with a porous model



But, the fit isn't as good and it requires a porosity length of $3 R_*$!